Rymp.

UB

NASA TECHNICAL MEMORANDUM

UB
NASA TM X-1309

NASA TM X-1309

AERODYNAMIC CHARACTERISTICS OF A MANEUVERABLE MISSILE WITH CRUCIFORM WINGS AND IN-LINE CANARD SURFACES AT MACH NUMBERS FROM 0.50 TO 4.63

(NASA-TM-X-1309) AERODYNAMIC CHARACTERISTICS OF A MANEUVERABLE MISSILE WITH CRUIFORM WINGS AND IN-LINE CANARD SURFACES AT MACH NUMBERS FROM 0.50 TO (NASA)
N73-70577
Unclas
00/99 51385

by William

Langley Research Center
Langley Station, Hampton, Va.

NATIONAL AERONAUTICS AND SPACE ADMINISTRATION • WASHINGTON, D. C. • NOVEMBER 1966

REPRODUCED BY
NATIONAL TECHNICAL
INFORMATION SERVICE
U. S. DEPARTMENT OF COMMERCE
SPRINGFIELD, VA. 22161

N73 70571

NASA TM X-1309

AERODYNAMIC CHARACTERISTICS OF A MANEUVERABLE MISSILE WITH CRUCIFORM WINGS AND IN-LINE CANARD SURFACES AT MACH NUMBERS FROM 0.50 TO 4.63

By William A. Corlett

Langley Research Center
Langley Station, Hampton, Va.

REPRODUCED BY
NATIONAL TECHNICAL
INFORMATION SERVICE
U.S. DEPARTMENT OF COMMERCE
SPRINGFIELD, VA. 22161

NATIONAL AERONAUTICS AND SPACE ADMINISTRATION

I

95

AERODYNAMIC CHARACTERISTICS OF A MANEUVERABLE MISSILE WITH CRUCIFORM WINGS AND IN-LINE CANARD SURFACES AT MACH NUMBERS FROM 0.50 TO 4.63*

By William A. Corlett
Langley Research Center

SUMMARY

An investigation has been conducted in the Langley 8-foot transonic pressure tunnel at Mach numbers from 0.50 to 1.20 and in the Langley Unitary Plan wind tunnel at Mach numbers from 1.50 to 4.63 to determine the aerodynamic characteristics of a maneuverable missile having cruciform wings and in-line canard surfaces. The angles of attack were varied from about -4° to 30° and the angles of sideslip were varied from about -4° to 8°. The Reynolds number was 2.5×10^6 per foot $(8.2 \times 10^6$ per meter$)$.

Satisfactory longitudinal and directional stability characteristics were obtained throughout the angle-of-attack and Mach number ranges. Deflection of the horizontal canard provided a high degree of longitudinal maneuverability, particularly at the higher Mach numbers. Deflection of trailing-edge flaps on the horizontal wings provided effective roll control with essentially no induced yawing moments. Deflection of the vertical canard provided effective directional control but also induced an adverse rolling moment.

INTRODUCTION

The primary requirement for a ground-to-air or air-to-air missile is a high degree of maneuverability throughout a broad range of Mach numbers. Therefore, a number of missile configurations utilizing various control arrangements have been investigated by the National Aeronautics and Space Administration. (See refs. 1 to 19.)

The present investigation has been conducted to determine the static aerodynamic characteristics of a model which simulated a maneuverable missile configuration. The model had cruciform wings and in-line canard surfaces. The wings in the horizontal plane were equipped with trailing-edge flaps and the canard surfaces were all-movable.

The investigation was conducted at Mach numbers from 0.50 to 4.63 at a constant Reynolds number of 2.5×10^6 per foot $(8.2 \times 10^6$ per meter$)$. The angles of attack were varied from about -4° to 30° and the angles of sideslip were varied from about -4° to 8°.

*Title, Unclassified.

SYMBOLS

The aerodynamic-coefficient data are referred to the body-axis system except for lift and drag which are referred to the stability-axis system. The moment reference was located at 60.2 percent of the body length aft of the model nose.

The units used for the physical quantities defined in this paper are given both in U.S. Customary Units and in the International System of Units (SI).

A maximum cross-sectional area of body 0.068349 sq ft $(63.44\ cm^2)$

d reference diameter (maximum cross section) 3.54 in. (8.99 cm)

C_A axial-force coefficient, $\frac{\text{Axial force}}{qA}$

C_D drag coefficient, $\frac{\text{Drag}}{qA}$

$C_{D,b}$ base drag coefficient

$C_{D,o}$ drag coefficient at $\alpha = 0^o$

C_L lift coefficient, $\frac{\text{Lift}}{qA}$

C_l rolling-moment coefficient, $\frac{\text{Rolling moment}}{qAd}$

C_{l_β} rolling-moment parameter, $\left(\frac{\Delta C_l}{\Delta \beta}\right)_{\beta=0^o,4^o}$, per deg

C_m pitching-moment coefficient, $\frac{\text{Pitching moment}}{qAd}$

C_{m_α} slope of pitching-moment curve measured near zero α

C_{m_δ} pitching-moment coefficient per degree control deflection

C_N normal-force coefficient, $\frac{\text{Normal force}}{qA}$

C_{N_α} slope of normal-force curve measured near zero α

C_n yawing-moment coefficient, $\frac{\text{Yawing moment}}{qAd}$

C_{n_β} directional stability parameter, $\left(\frac{\Delta C_n}{\Delta \beta}\right)_{\beta=0^o,4^o}$, per deg

C_Y side-force coefficient, $\frac{\text{Side force}}{qA}$

C_{Y_β} side-force parameter, $\left(\frac{\Delta C_Y}{\Delta \beta}\right)_{\beta=0^o,4^o}$, per deg

L/D lift-drag ratio, C_L/C_D

M Mach number

q dynamic pressure, lb/sq ft (N/m^2)

α angle of attack, deg

β angle of sideslip, deg

δ_{c_h} horizontal-canard deflection, positive when leading edge is up, deg

δ_{c_v} vertical-canard deflection, positive when leading edge is to right, deg

δ_f horizontal-wing-flap deflection, negative when trailing edge is up, deg (subscript L for left, R for right)

x_{cp}/d location of center of pressure, in reference diameters, from moment center (positive rearward)

APPARATUS AND TESTS

Tunnels

The investigation was conducted in both the Langley 8-foot transonic pressure tunnel and the Langley Unitary Plan wind tunnel. These are both variable-pressure continuous-flow facilities. The 8-foot transonic pressure tunnel has an 8-foot-square test section and a Mach number range from 0.20 to 1.30. The Unitary Plan wind tunnel has two 4-foot-square test sections with asymmetric sliding-block-type nozzles which permit a continuous variation in test-section Mach number from 1.5 to 2.9 in the low Mach number test section and from 2.3 to 4.7 in the high Mach number test section.

Model

Dimensional details of the model are shown in figure 1, and the model mounted in the test section is shown in figure 2. The body had a fineness ratio of about 11.3. The cruciform trapezoidal wings had beveled leading and trailing edges with a maximum thickness of 4 percent chord. The horizontal wing surfaces were equipped with trailing-edge flaps having an overhang balance. The cruciform trapezoidal canard controls also had beveled leading and trailing edges with a maximum thickness of 4 percent chord and were in line with the wings. The model was also provided with removable protuberances which simulated equipment ducts.

Model component designations used are as follows:

W wings

C canards

B body with protuberances

B_o body without protuberances

The complete model configuration is designated BWC.

Tests

The stagnation pressures and temperatures at the test Mach numbers are presented in the following table:

Mach number	Stagnation pressure		Stagnation temperature	
	lb/sq ft abs	kN/m^2	^oF	^oK
0.50	1906	91.3	116	320
.80	1402	67.1	120	322
.90	1331	63.7	120	322
.95	1306	62.5	120	322
1.00	1286	61.6	120	322
1.03	1277	61.1	120	322
1.20	1256	60.1	120	322
1.50	1390	66.6	150	339
1.90	1585	75.9	150	339
2.30	1910	91.5	150	339
2.96	2700	129.3	150	339
3.95	4800	229.8	175	353
4.63	6575	314.8	175	353

The Reynolds number was 2.5×10^6 per foot $(8.2 \times 10^6$ per meter). The dewpoint, measured at stagnation pressure, was maintained low enough to assure negligible condensation effects. For the tests conducted in the Langley Unitary Plan wind tunnel, the angle of attack was varied from approximately -4° to 30° at angles of sideslip of 0° and 4°, and the sideslip angle was varied from about -4° to 8° at angles of attack of 0°, 10°, and 21°. In order to assure boundary-layer transition to turbulent conditions, 1/16-inch-wide (0.159-cm) strips of No. 60 carborundum grit were placed on the wings 0.4 inch (1.016 cm) behind the leading edge, on the canards at 15 percent chord (measured streamwise), and on the body 1.6 inches (4.064 cm) aft of the nose. For the tests conducted in the Langley 8-foot transonic pressure tunnel, the angle of attack was varied from approximately -4° to 12° at a sideslip angle of 0°, and No. 120 carborundum grit was used for the transition strip.

Measurements

Aerodynamic forces and moments on the model were measured by means of a six-component electrical strain-gage balance which was housed within the model. The balance was attached to a sting which was rigidly fastened to the tunnel support system. Base pressure was measured by means of a single static-pressure orifice located in the vicinity of the balance.

CORRECTIONS AND ACCURACY

The angles of attack and sideslip have been corrected for deflection of the balance and sting due to aerodynamic loads; angles of attack have also been corrected for tunnel airflow misalinement. The results have been adjusted to correspond to free-stream static pressure acting over the model base. (See fig. 3.)

Based on balance calibration and data repeatability, the data presented herein are estimated to be accurate to within the following limits:

C_A or C_D	±0.015
C_N or C_L	±0.076
C_m	±0.057
C_n or C_Y	±0.029
C_l	±0.010
M	
For M = 0.50 to 1.20	±0.005
For M = 1.50 to 2.96	±0.015
For M = 3.95 to 4.63	±0.050
α or β, deg	±0.1

PRESENTATION OF RESULTS

A table of the figures presenting the results is given as follows:

Data in the Mach number range from 0.50 to 1.20 are presented in figures 4 and 7 only.

DISCUSSION

Longitudinal Aerodynamic Characteristics

The longitudinal stability and control characteristics of the model are presented in figures 4 to 6 and are summarized in figure 7. Deflection of the horizontal-canard surface (fig. 4) provides effective pitch control throughout the angle-of-attack and Mach number ranges with little effect on the lift but with a measurable increase in drag. The pitching-moment increments provided by canard deflection decrease with increasing angle of attack at the lower Mach numbers, presumably because of a loss in lift effectiveness of the canard surface. (See figs. 4(a) to 4(h).) At the higher Mach numbers, however, the effectiveness of the canard surfaces increases considerably with increasing angle of attack, and a high degree of longitudinal maneuverability is indicated. (See fig. 4(l), for example.)

The effect of horizontal-wing-flap deflection and horizontal-canard deflection is presented in figure 5 for the Mach number range from 1.50 to 4.63. Deflection of only

the wing flap provides a relatively effective means of pitch control at Mach number 1.50. The pitching effectiveness of the wing flap decreases rapidly with increasing Mach number, however. Deflection of the canard in addition to deflection of the wing flap results in a substantial increase in maneuvering capability.

The longitudinal aerodynamic characteristics determined for various combinations of component parts throughout the Mach number range from 1.50 to 4.63 are shown in figure 6 and indicate that the addition of the canard surfaces provides a small increase in lift and a destabilizing increment in pitching moment. The pitch characteristics indicate little effect of the canard flow field on the wing inasmuch as the increments provided by the canard are essentially the same for the model both with and without the wing. The variations of pitching moment with angle of attack for the complete model are reasonably linear and, at the higher angles of attack and Mach numbers (fig. 6(f), for example), exhibit a slight pitch-down tendency that appears to be inherent in the body-wing combination. The axial-force increment due to the protuberances may be determined by comparing the results for the smooth body (B_0) with those for the body with protuberances (B) and is found to be approximately 5 percent of the total drag of the complete vehicle near $\alpha = 0^o$.

The effectiveness of the canards in providing pitching moment near $\alpha = 0^o$ and the parameters C_{N_α} and C_{m_α} are shown in figure 7(a). These parameters show the expected trend with variation in Mach number. The variation with Mach number of center of pressure and drag coefficient at $\alpha = 0^o$ are presented in figure 7(b). The center of pressure is shown to move rearward throughout the transonic range to about Mach number 1.2; however, with further increase in Mach number, the center of pressure moves forward.

Sideslip Derivatives

The sideslip derivatives for various combinations of model components (fig. 8) indicate satisfactory directional stability for the complete configuration throughout the angle-of-attack and Mach number ranges. This stability is maintained even though the presence of the canard surfaces causes a destabilizing increment of yawing moment. Some interference effects of the canard flow field on the wing are indicated at the lower Mach numbers by the fact that the decrement in C_{n_β} caused by the addition of the canards is greater with the wing on than with the wing off. In addition, a substantial increment in C_{l_β} occurs at the lower Mach numbers for the complete model as an indication of the asymmetric flow field effects of the canard on the wing.

Deflection of the horizontal canard for pitch control has little effect on the directional stability characteristics of the complete configuration but does cause a generally negative increment of rolling moment due to sideslip (fig. 9).

Lateral Control Characteristics

Differential deflection of the wing flaps provides an effective means of obtaining roll control with essentially no induced yawing moment throughout the angle-of-attack and Mach number ranges (fig. 10). With increasing Mach number, the roll effectiveness of the flaps decreases at the lower angles of attack; however, the roll effectiveness increases with increasing angle of attack at the higher Mach numbers. The roll control characteristics are essentially the same with the horizontal canard deflected 20° (fig. 11).

Deflection of the vertical canard provides an effective means of obtaining directional control throughout the angle-of-attack and Mach number ranges (fig. 12); however, deflection of the vertical canard also produces a flow field at the wing that induces an adverse rolling moment. In some instances the induced roll caused by $\delta_{C_V} = 20^{\circ}$ is in excess of the rolling moment that could be controlled by a wing-flap deflection of $\pm 20^{\circ}$. (Compare figs. 12(b) and 11(b) at $\alpha = 10^{\circ}$, for example.)

CONCLUDING REMARKS

An investigation has been conducted in both the Langley 8-foot transonic pressure tunnel and the Langley Unitary Plan wind tunnel at Mach numbers from 0.50 to 4.63 to determine the aerodynamic characteristics of a maneuverable missile having cruciform wings and in-line canard surfaces.

The results indicated satisfactory longitudinal and directional stability characteristics throughout the angle-of-attack and Mach number ranges. Deflection of the horizontal canard provided a high degree of longitudinal maneuverability, particularly at the higher Mach numbers. Deflection of trailing-edge flaps on the horizontal wings provided effective roll control with essentially no induced yawing moments. Deflection of the vertical canard provided effective directional control but also induced an adverse rolling moment.

Langley Research Center,
National Aeronautics and Space Administration,
Langley Station, Hampton, Va., June 22, 1966,
126-13-02-01-23.

REFERENCES

1. Spearman, M. Leroy: Aerodynamic Characteristics in Pitch of a Series of Cruciform-Wing Missiles With Canard Controls at a Mach Number of 2.01. NASA TN D-839, 1961. (Supersedes NACA RM L53I14.)

2. Spearman, M. Leroy: Component Tests To Determine the Aerodynamic Characteristics of an All-Movable 70° Delta Canard-Type Control in the Presence of a Body at a Mach Number of 1.61. NACA RM L53I03, 1953.

3. Spearman, M. Leroy: Effect of Large Deflections of a Canard Control and Deflections of a Wing-Tip Control on the Static-Stability and Induced-Roll Characteristics of a Cruciform Canard Missile at a Mach Number of 2.01. NACA RM L53K03, 1953.

4. Spearman, M. Leroy; and Robinson, Ross B.: Aerodynamic Characteristics of a Cruciform-Wing Missile With Canard Control Surfaces and of Some Very Small Span Wing-Body Missiles at a Mach Number of 1.41. NACA RM L54B11, 1954.

5. Spearman, M. Leroy; and Driver, Cornelius: Wind-Tunnel Investigation at a Mach Number of 2.01 of the Aerodynamic Characteristics in Combined Pitch and Sideslip of Some Canard-Type Missiles Having Cruciform Wings and Canard Surfaces With 70° Delta Plan Forms. NACA RM L54F09, 1954.

6. Robinson, Ross B.: Aerodynamic Characteristics of Missile Configurations With Wings of Low Aspect Ratio for Various Combinations of Forebodies, Afterbodies, and Nose Shapes for Combined Angles of Attack and Sideslip at a Mach Number of 2.01. NACA RM L57D19, 1957.

7. Robinson, Ross B.: Wind-Tunnel Investigation at a Mach Number of 2.01 of the Aerodynamic Characteristics in Combined Angles of Attack and Sideslip of Several Hypersonic Missile Configurations With Various Canard Controls. NACA RM L58A21, 1958.

8. Katzen, Elliott D.; and Jorgensen, Leland H.: Aerodynamics of Missiles Employing Wings of Very Low Aspect Ratio. NACA RM A55L13b, 1956.

9. Foster, Gerald V.: Sideslip Characteristics at Various Angles of Attack for Several Hypersonic Missile Configurations With Canard Controls at a Mach Number of 2.01. NASA TM X-134, 1959.

10. Stone, David G.: Maneuver Performance of Interceptor Missiles. NACA RM L58E02, 1958.

11. Spearman, M. Leroy; and Robinson, Ross B.: Longitudinal Stability and Control Characteristics at Mach Numbers of 2.01, 4.65, and 6.8 of Two Hypersonic Missile Configurations, One Having Low-Aspect-Ratio Cruciform Wings With Trailing-Edge Flaps and One Having a Flared Afterbody and All-Movable Controls. NASA TM X-46, 1959.

12. Robinson, Ross B.; and Bernot, Peter T.: Aerodynamic Characteristics at a Mach Number of 6.8 of Two Hypersonic Missile Configurations, One With Low-Aspect-Ratio Cruciform Fins and Trailing-Edge Flaps and One With a Flared Afterbody and All-Movable Controls. NACA RM L58D24, 1958.

13. Church, James D.; and Kirkland, Ida M.: Static Aerodynamic Characteristics of Several Hypersonic Missile-and-Control Configurations at a Mach Number of 4.65. NASA TM X-187, 1960.

14. Robinson, Ross B.; and Spearman, M. Leroy: Aerodynamic Characteristics for Combined Angles of Attack and Sideslip of a Low-Aspect-Ratio Cruciform-Wing Missile Configuration Employing Various Canard and Trailing-Edge Flap Controls at a Mach Number of 2.01. NASA MEMO 10-2-58L, 1958.

15. Robinson, Ross B.; and Foster, Gerald V.: Static Longitudinal Stability and Control Characteristics at a Mach Number of 2.01 of a Hypersonic Missile Configuration Having All-Movable Wing and Tail Surfaces. NASA TM X-516, 1961.

16. Spearman, M. Leroy; and Robinson, Ross B.: Longitudinal Stability and Control Characteristics of a Winged and a Flared Hypersonic Missile Configuration With Various Nose Shapes and Flare Modifications at a Mach Number of 2.01. NASA TM X-693, 1962.

17. Fuller, Dennis E.; and Corlett, William A.: Supersonic Aerodynamic Characteristics of a Cruciform Missile Configuration With Low-Aspect-Ratio Wings and In-Line Tail Controls. NASA TM X-1025, 1964.

18. Corlett, William A.; and Fuller, Dennis E.: Aerodynamic Characteristics at Mach 1.60, 2.00, and 2.50 of a Cruciform Missile Configuration With In-Line Tail Controls. NASA TM X-1112, 1965.

19. Foster, Gerald V.; and Corlett, William A.: Aerodynamic Characteristics at Mach Numbers From 0.40 to 2.86 of a Missile Model Having All-Movable Wings and Interdigitated Tails. NASA TM X-1184, 1965.

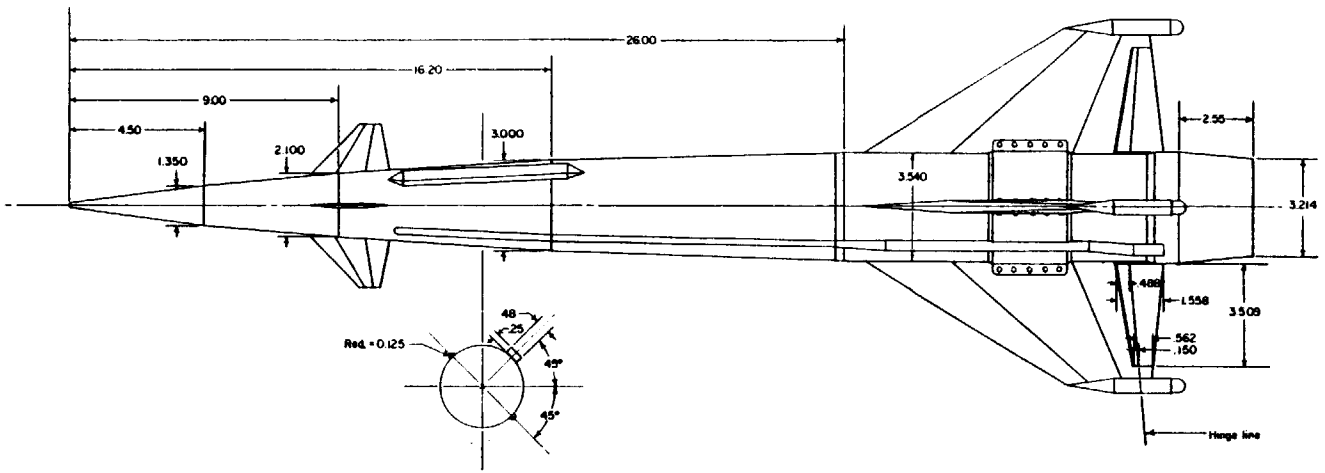

(a) Top view.

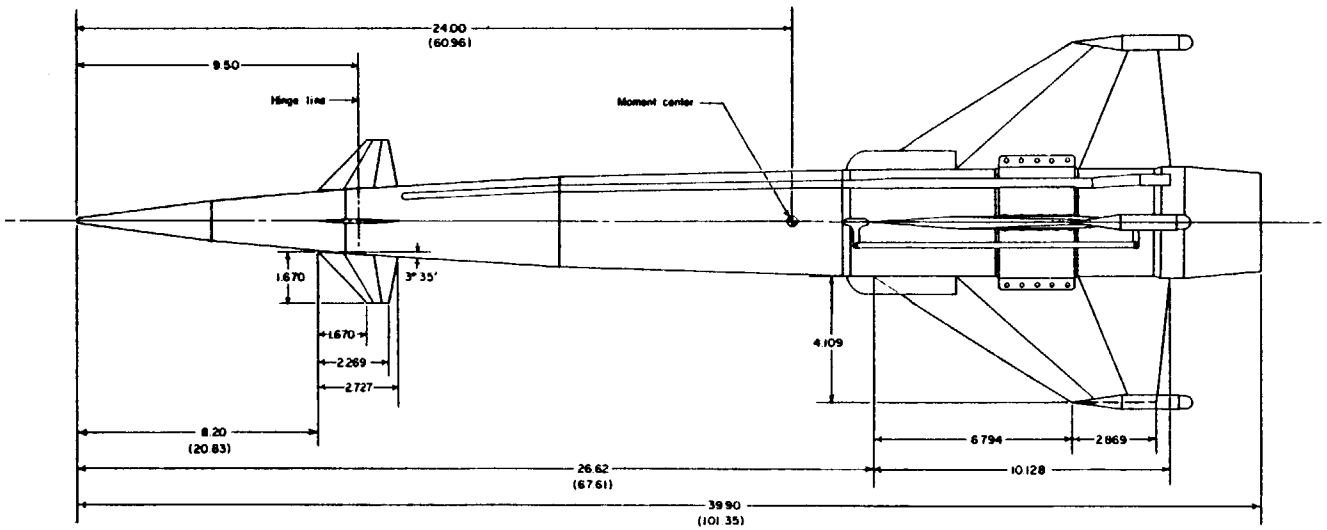

(b) Side view.

Figure 1.- Details of model. Dimensions are given in inches and conversions to the International System of Units are presented for only a few representative dimensions (given in centimeters in parentheses).

Reproduced from
best available copy.

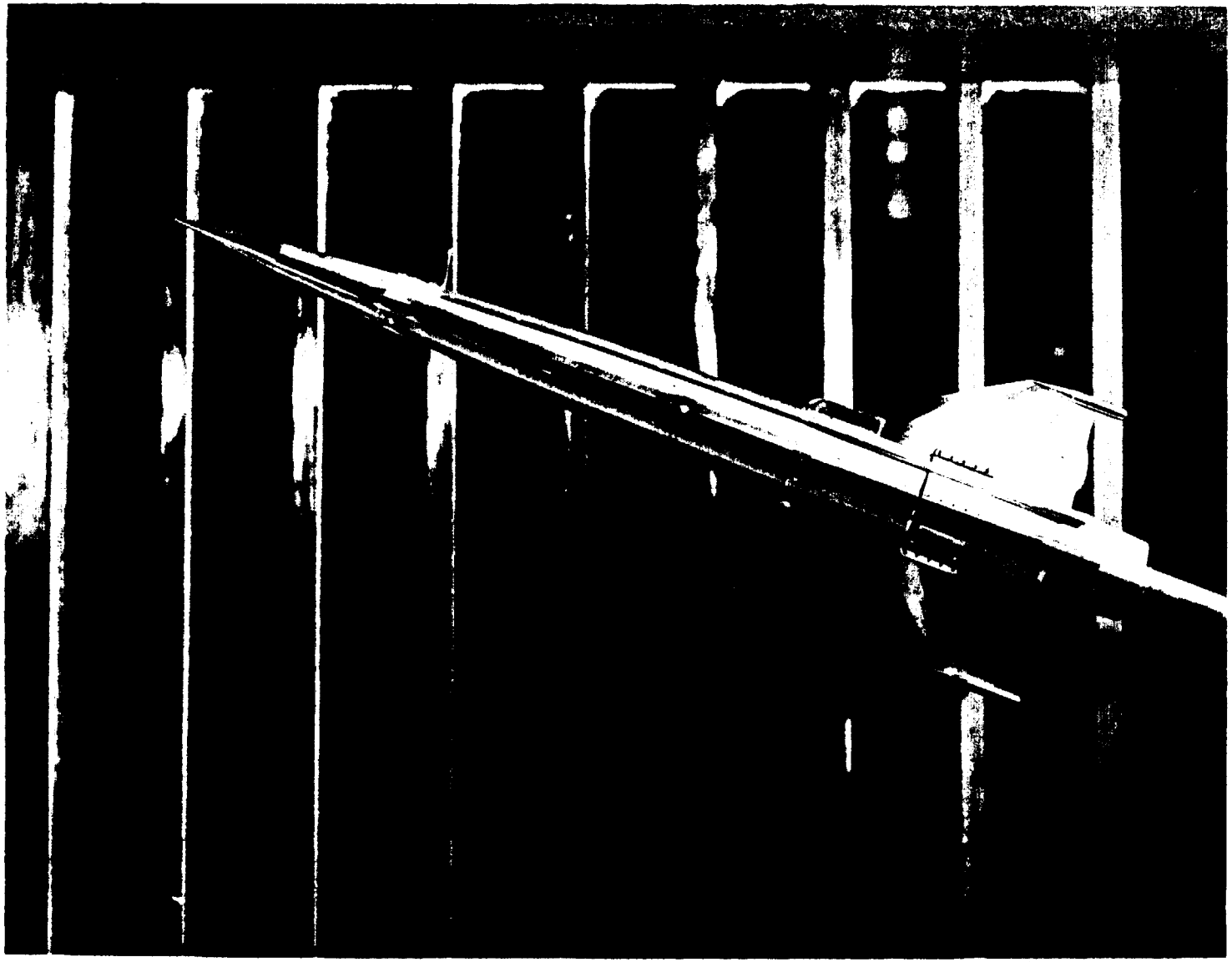

Figure 2.- Model mounted in Langley Unitary Plan wind tunnel. L-65-2685

N O T I C E

THIS DOCUMENT HAS BEEN REPRODUCED FROM THE BEST COPY FURNISHED US BY THE SPONSORING AGENCY. ALTHOUGH IT IS RECOGNIZED THAT CERTAIN PORTIONS ARE ILLEGIBLE, IT IS BEING RELEASED IN THE INTEREST OF MAKING AVAILABLE AS MUCH INFORMATION AS POSSIBLE.

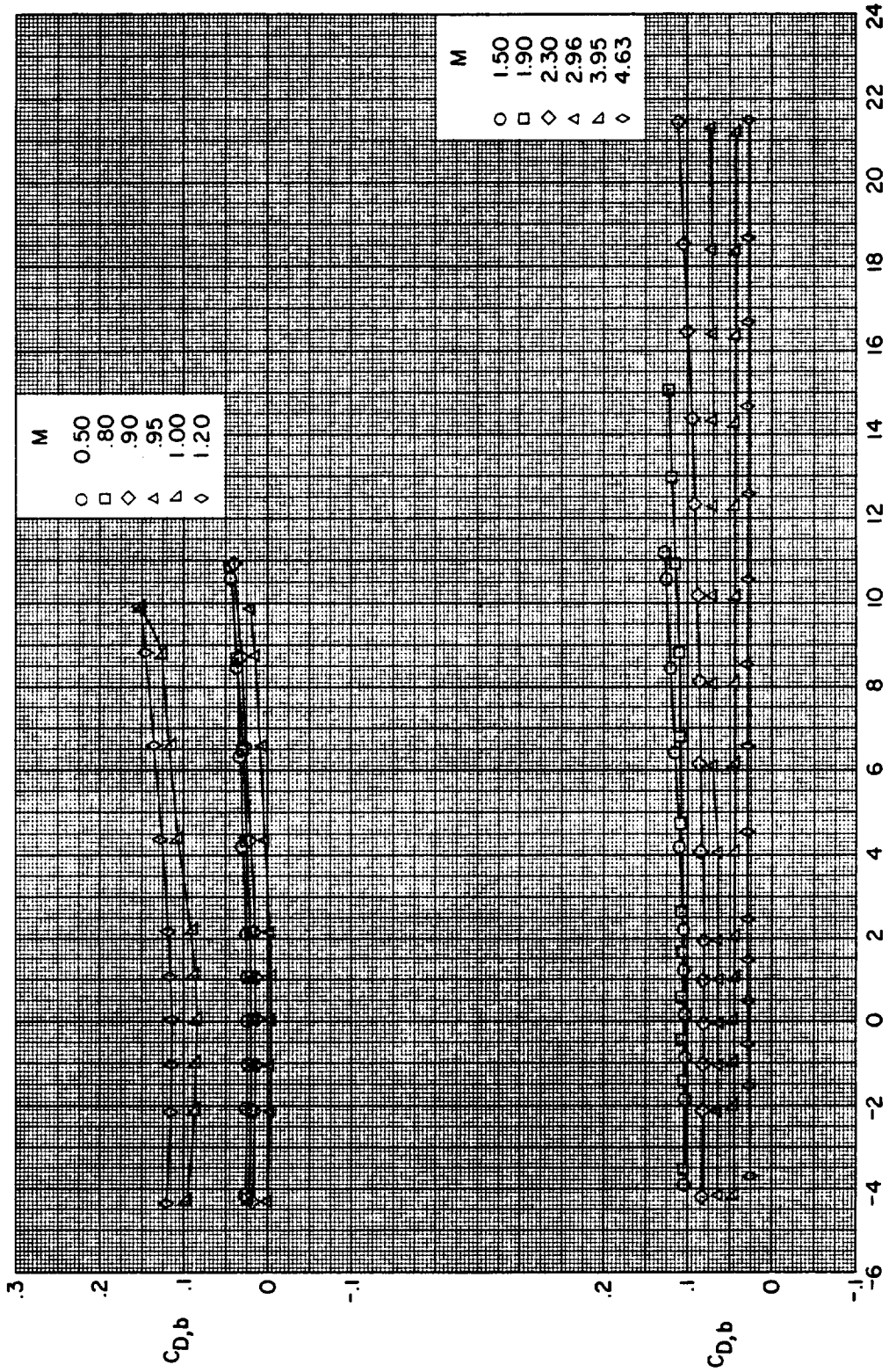

Figure 3.- Variation of base drag coefficients with angle of attack.

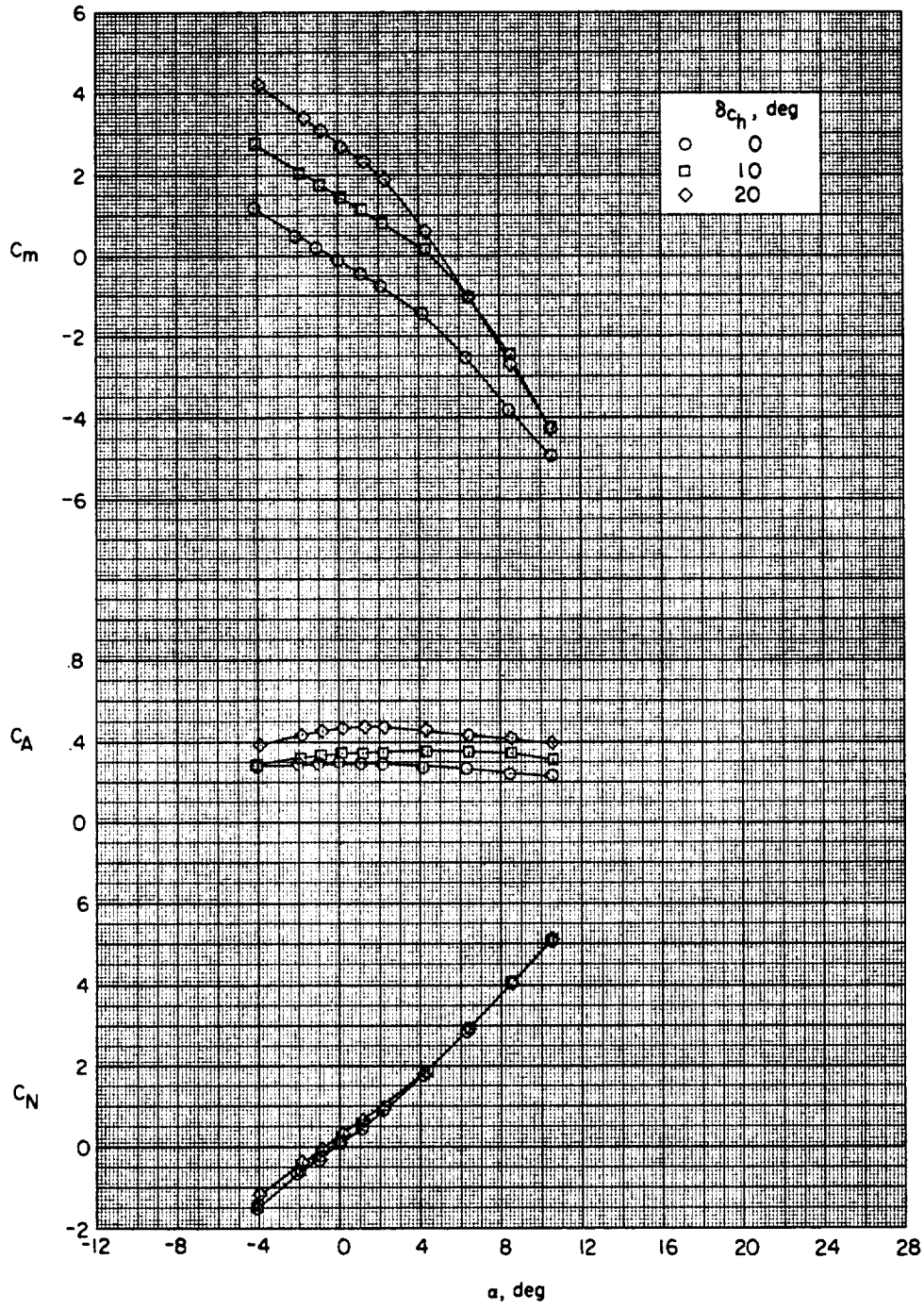

(a) M = 0.50.

Figure 4.- Effect of horizontal-canard deflection on the longitudinal aerodynamic characteristics of configuration BWC. $\delta_f = 0^0$; $\delta_{c_v} = 0^0$.

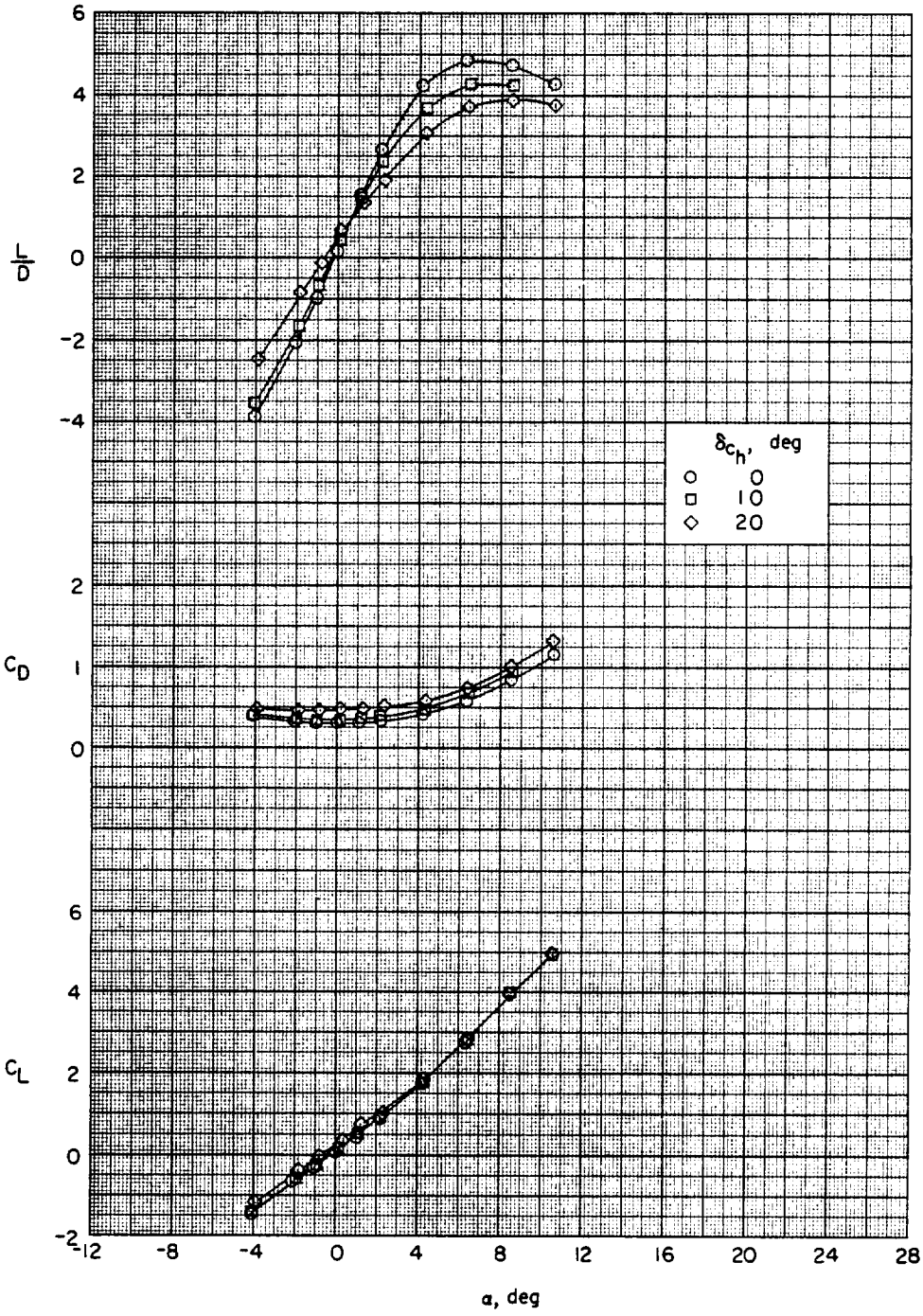

(a) Concluded.

Figure 4.- Continued.

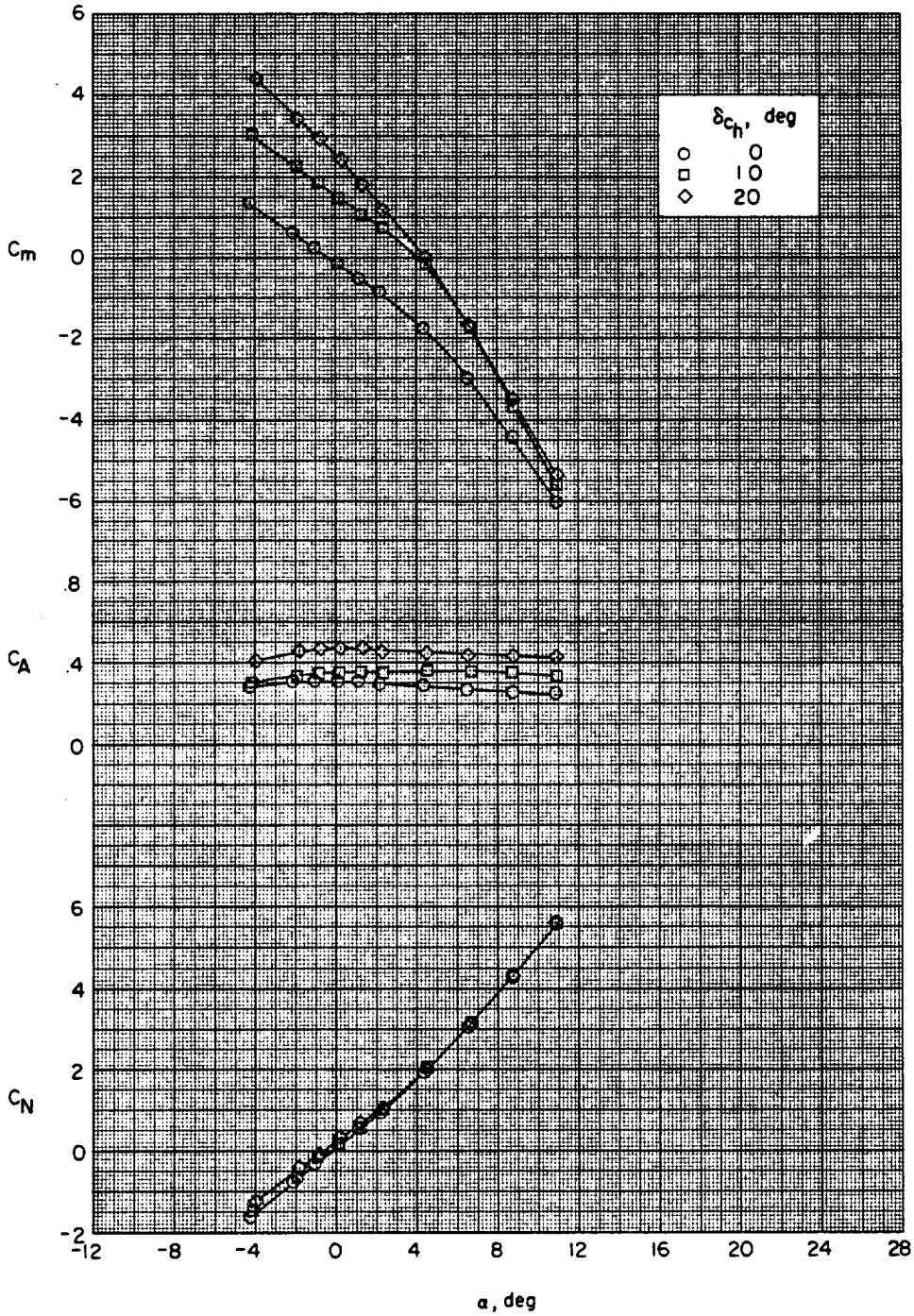

(b) M = 0.80.

Figure 4.- Continued.

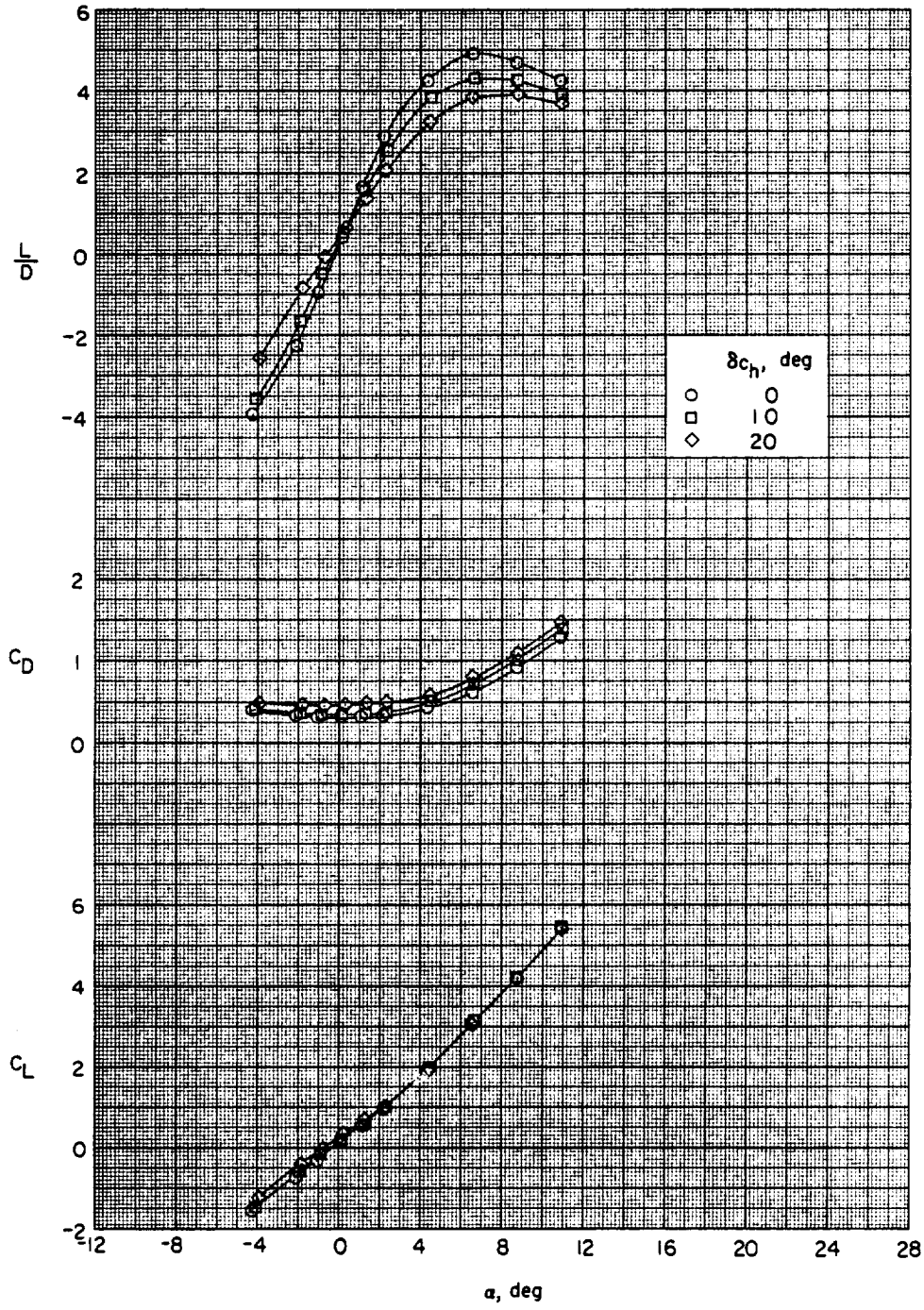

(b) Concluded.

Figure 4.- Continued.

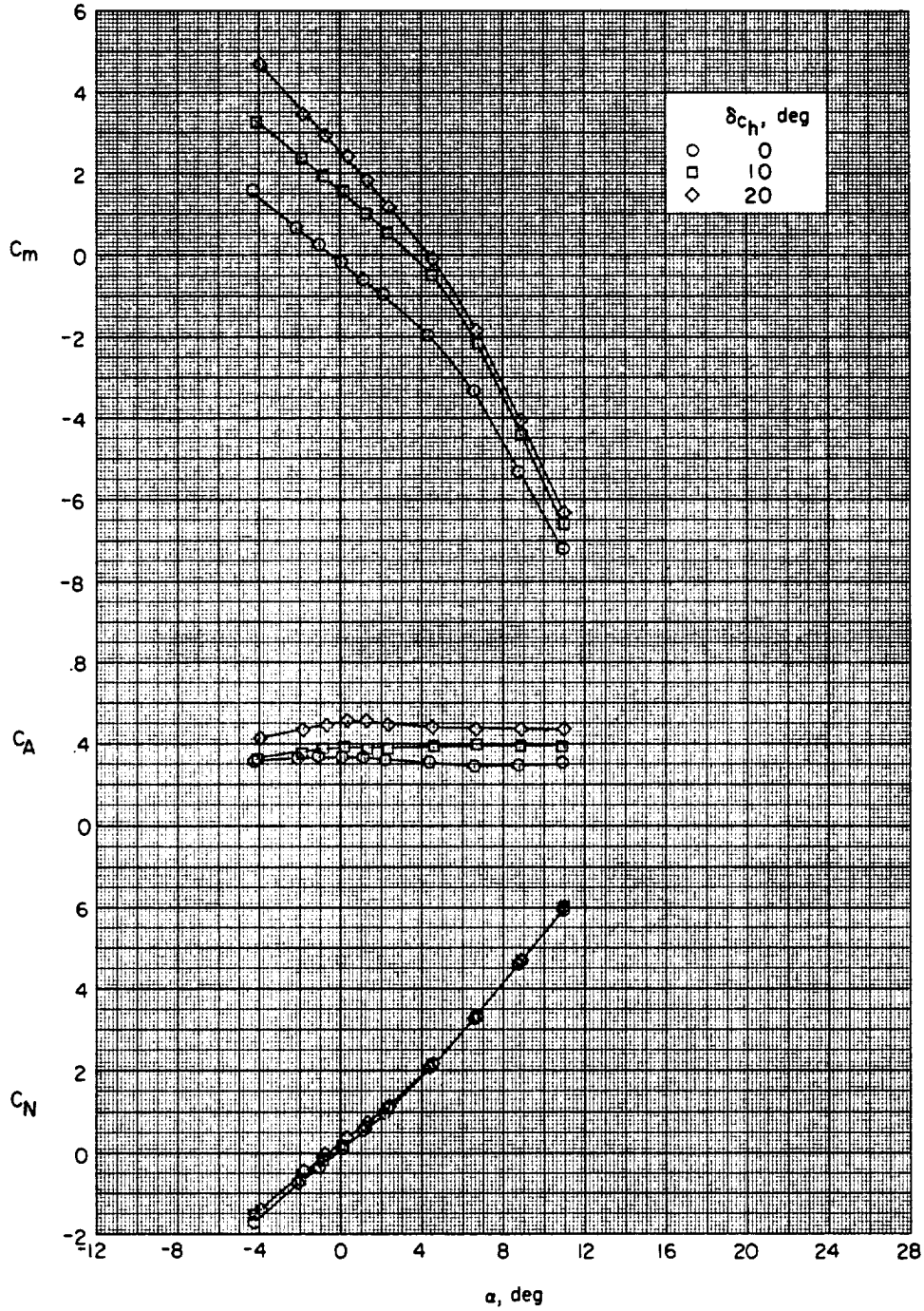

(c) M = 0.90.

Figure 4.- Continued.

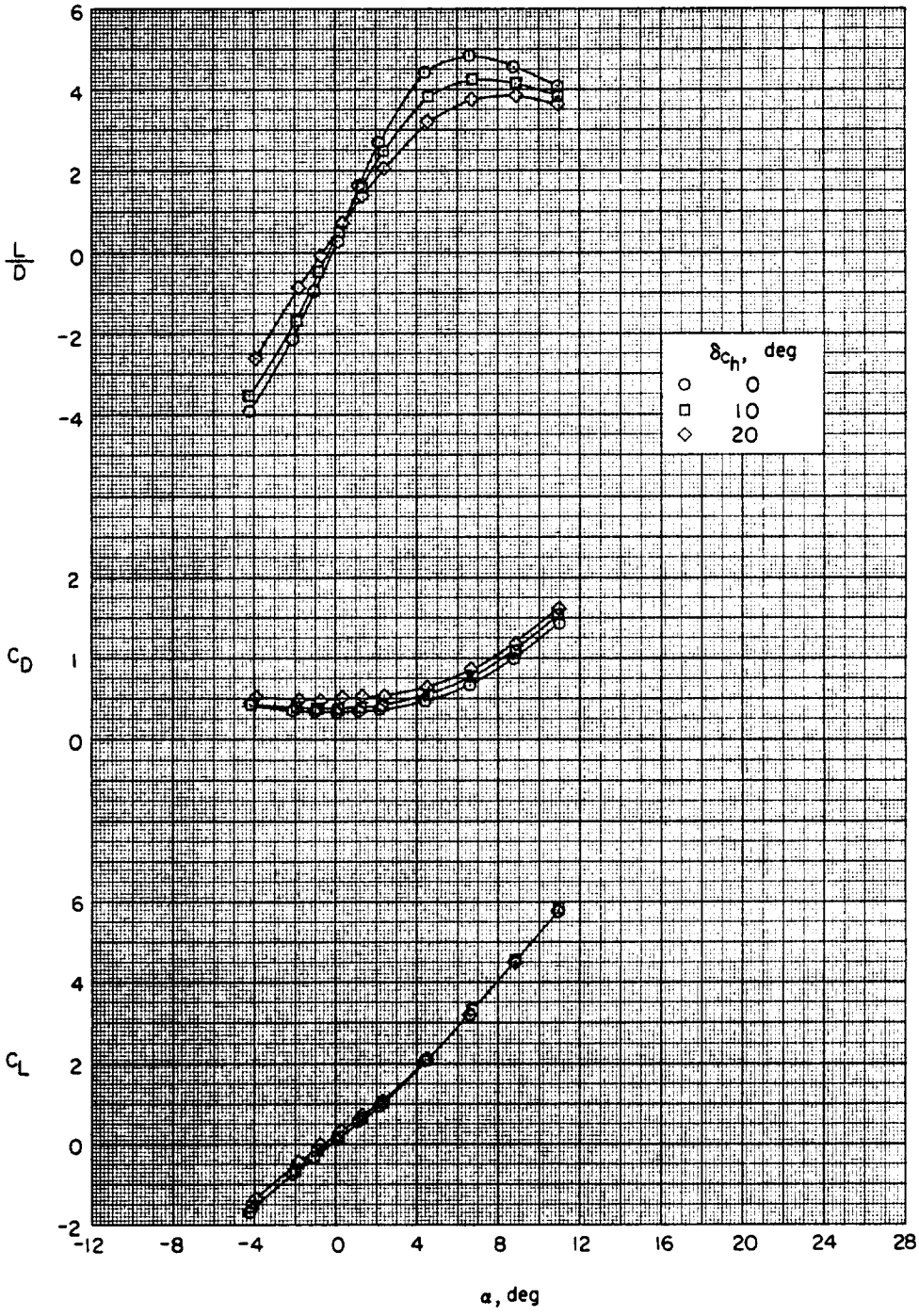

(c) Concluded.

Figure 4.- Continued.

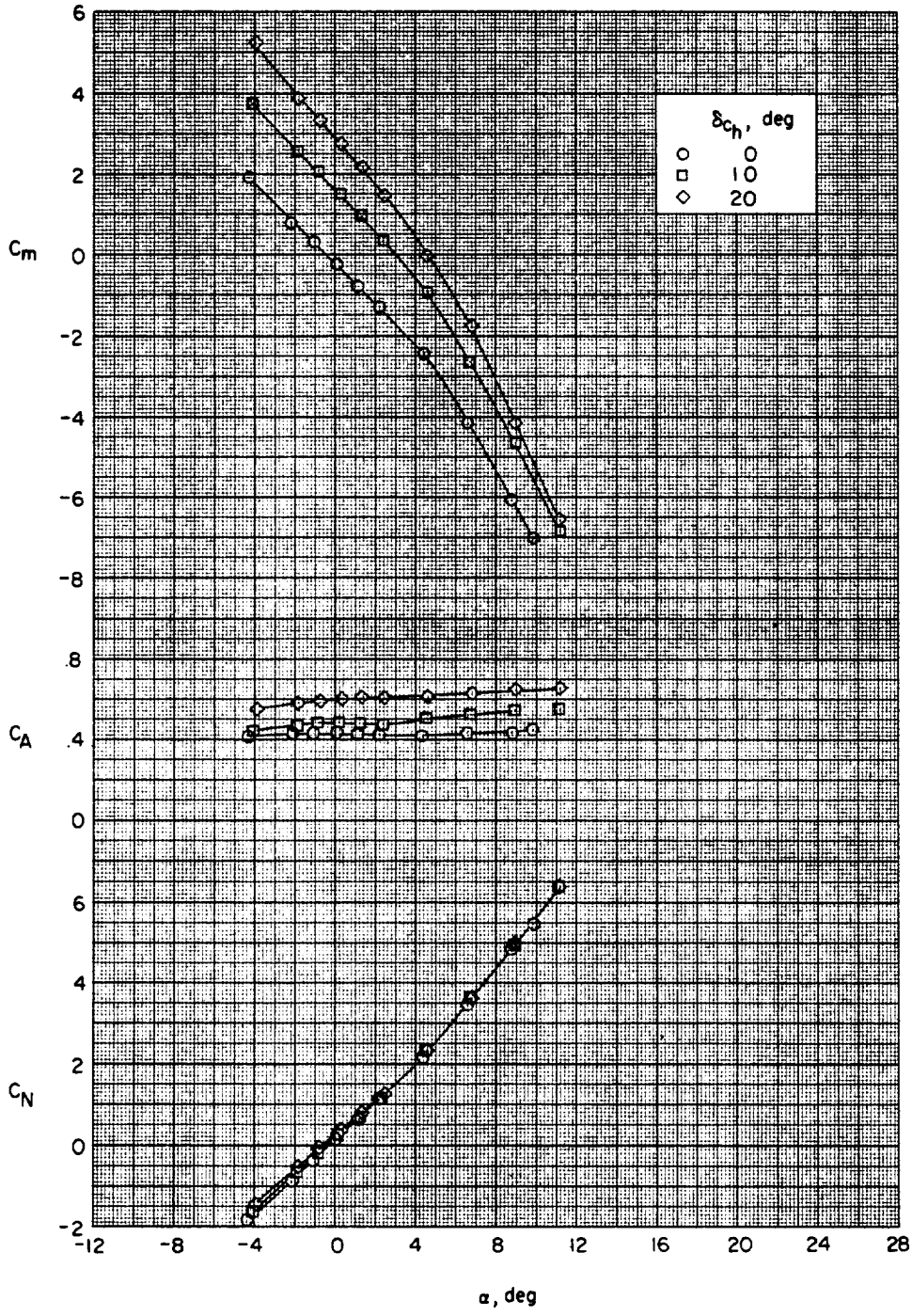

(d) M = 0.95.

Figure 4.- Continued.

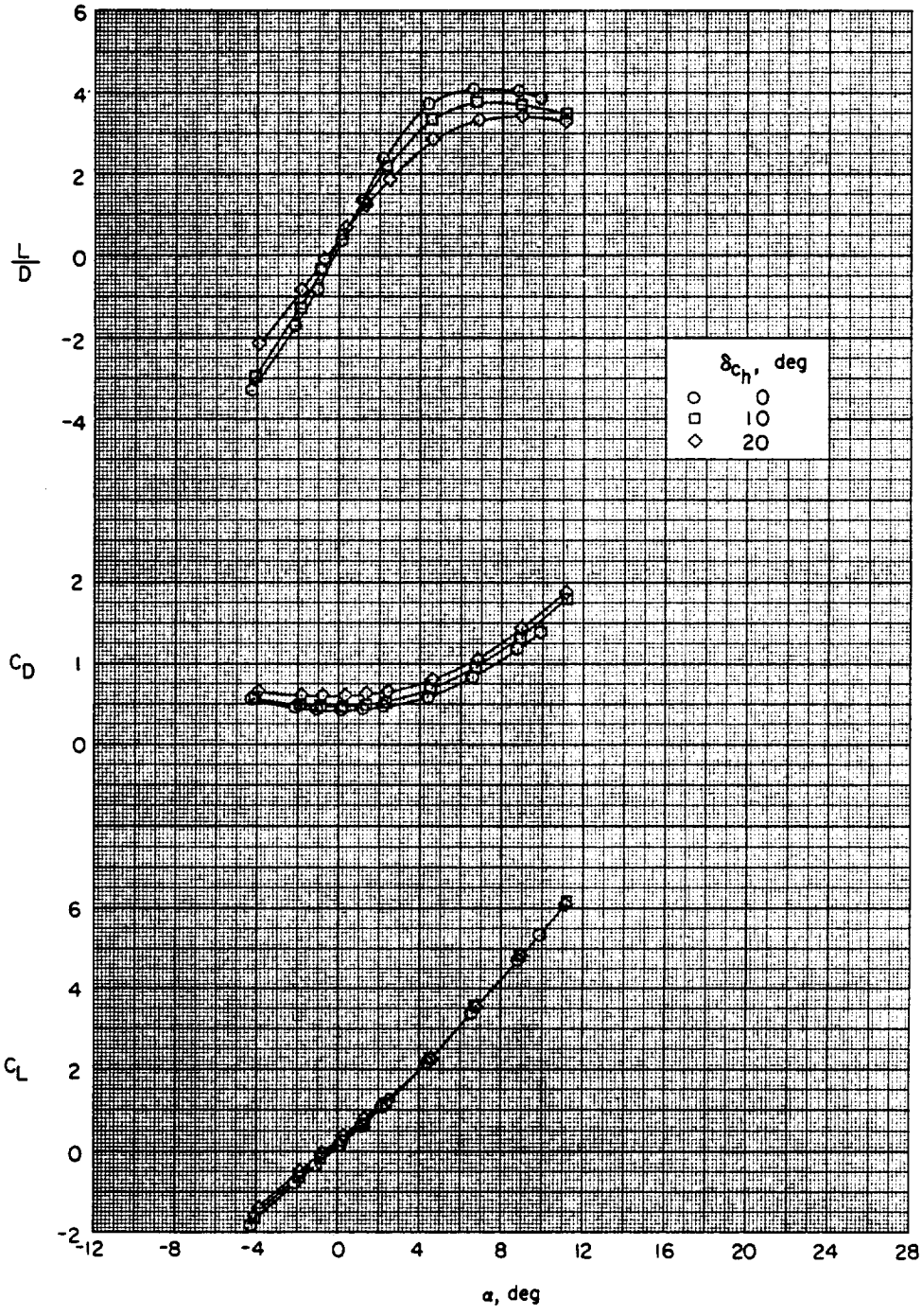

(d) Concluded.

Figure 4.- Continued.

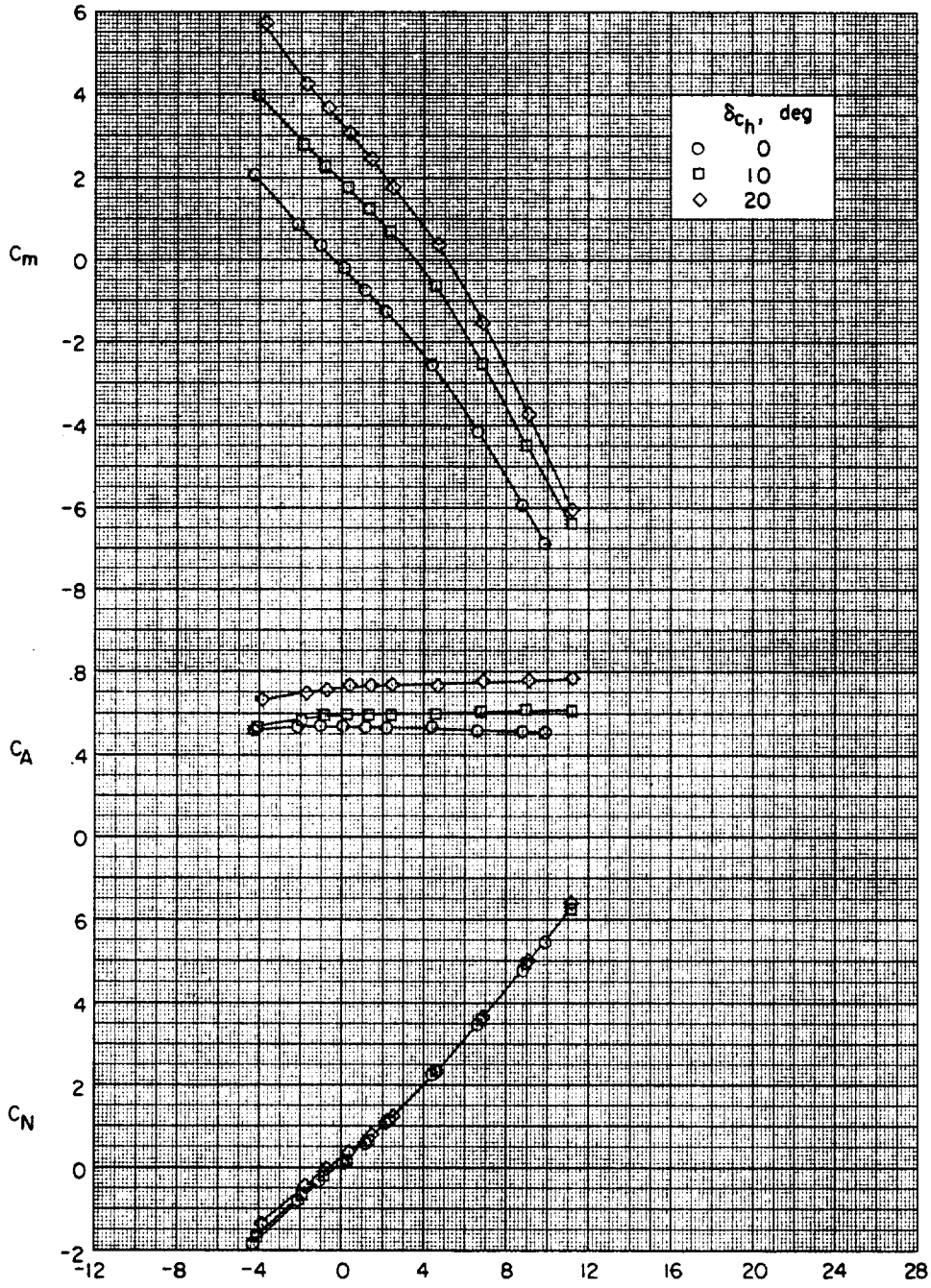

(e) M = 1.00.

Figure 4.- Continued.

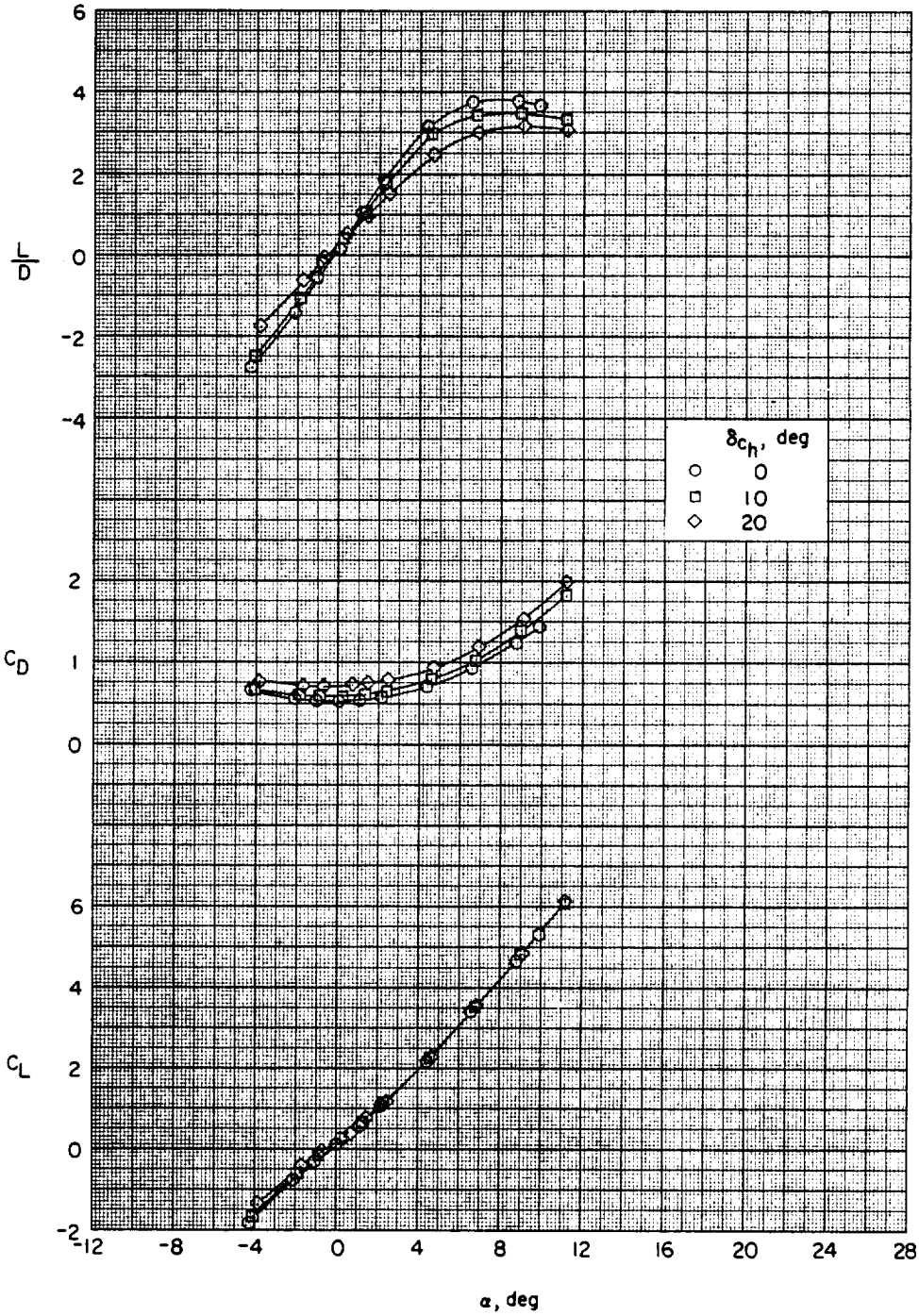

(e) Concluded.

Figure 4.- Continued.

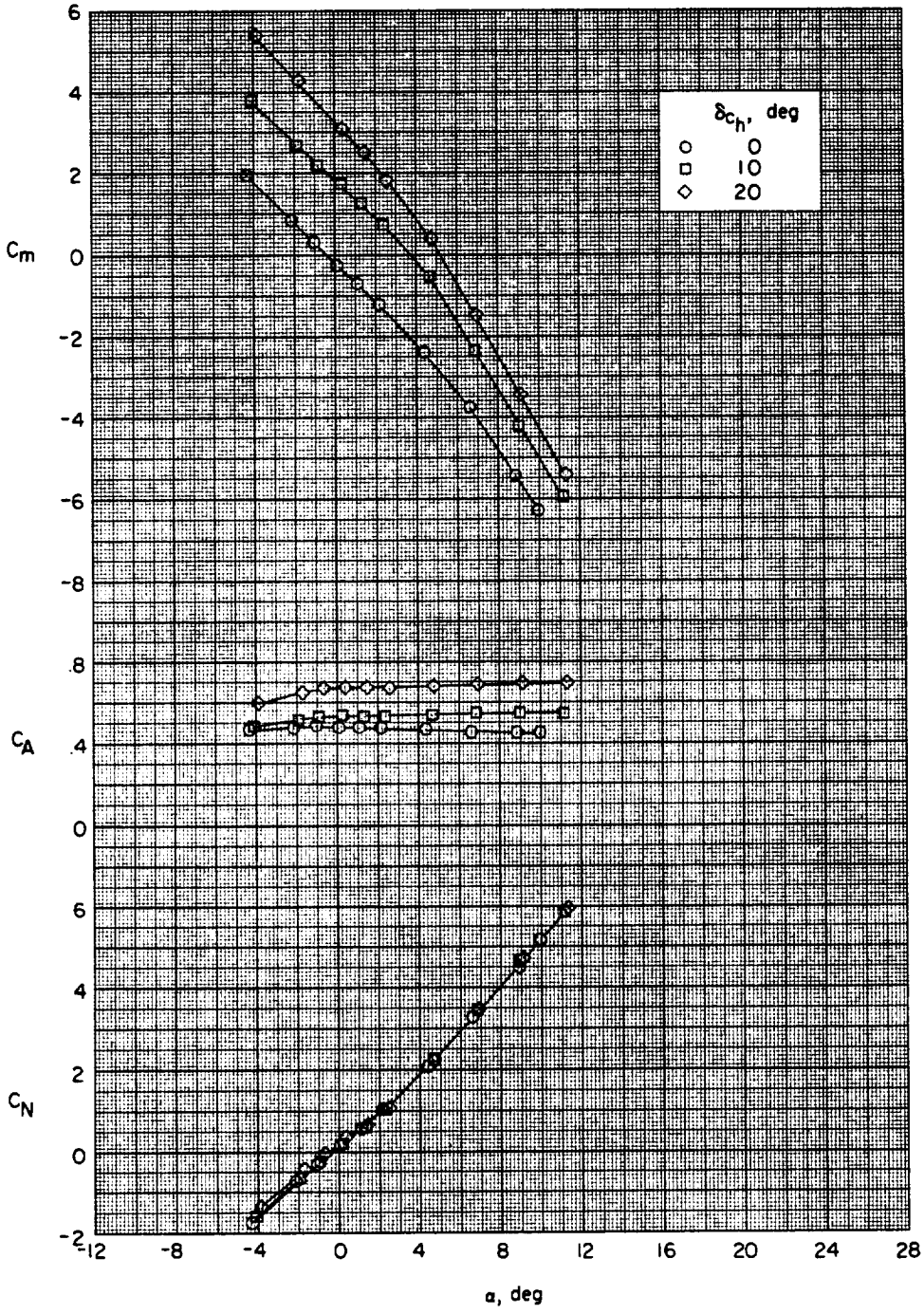

(f) M = 1.20.

Figure 4.- Continued.

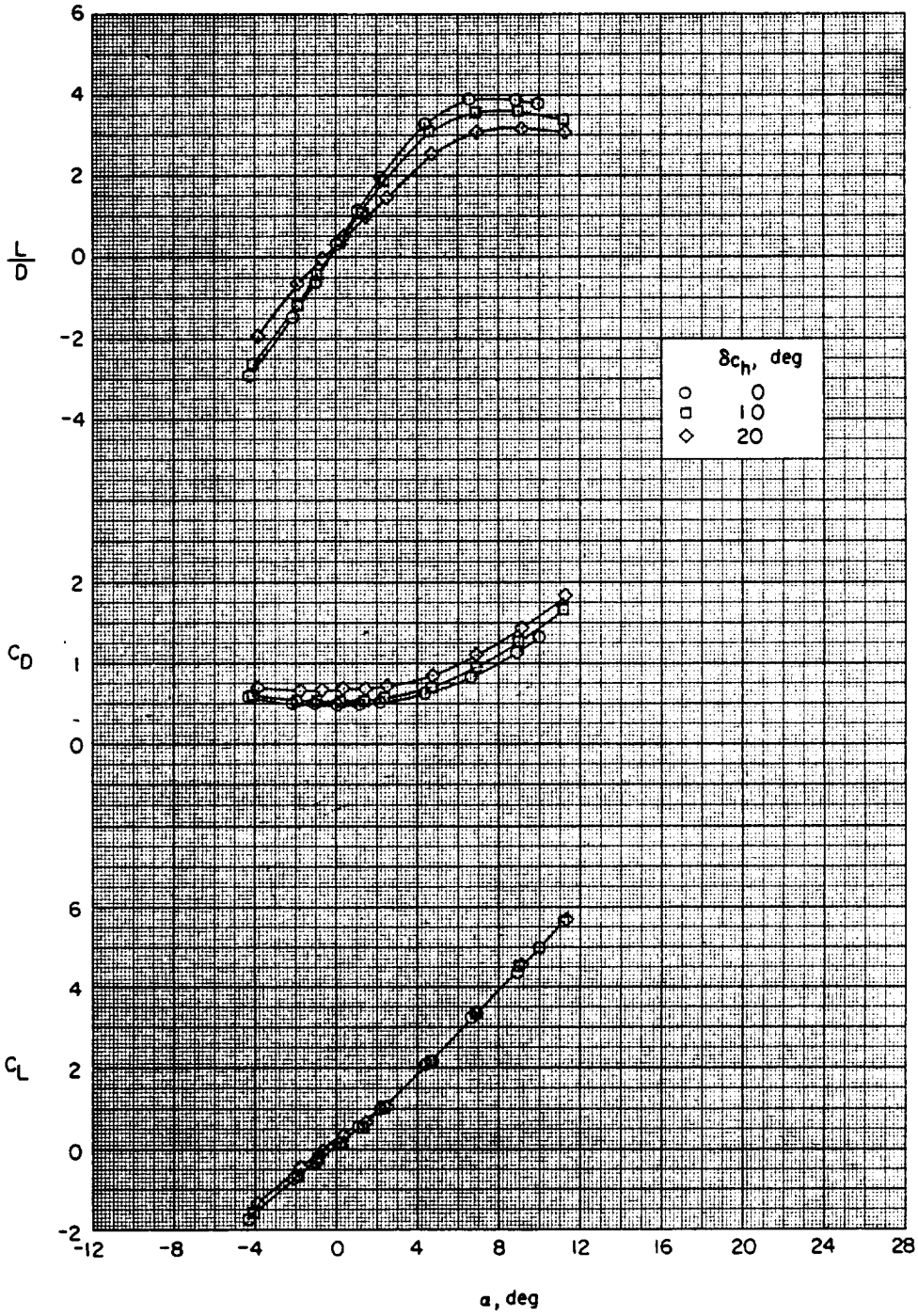

(f) Concluded.

Figure 4.- Continued.

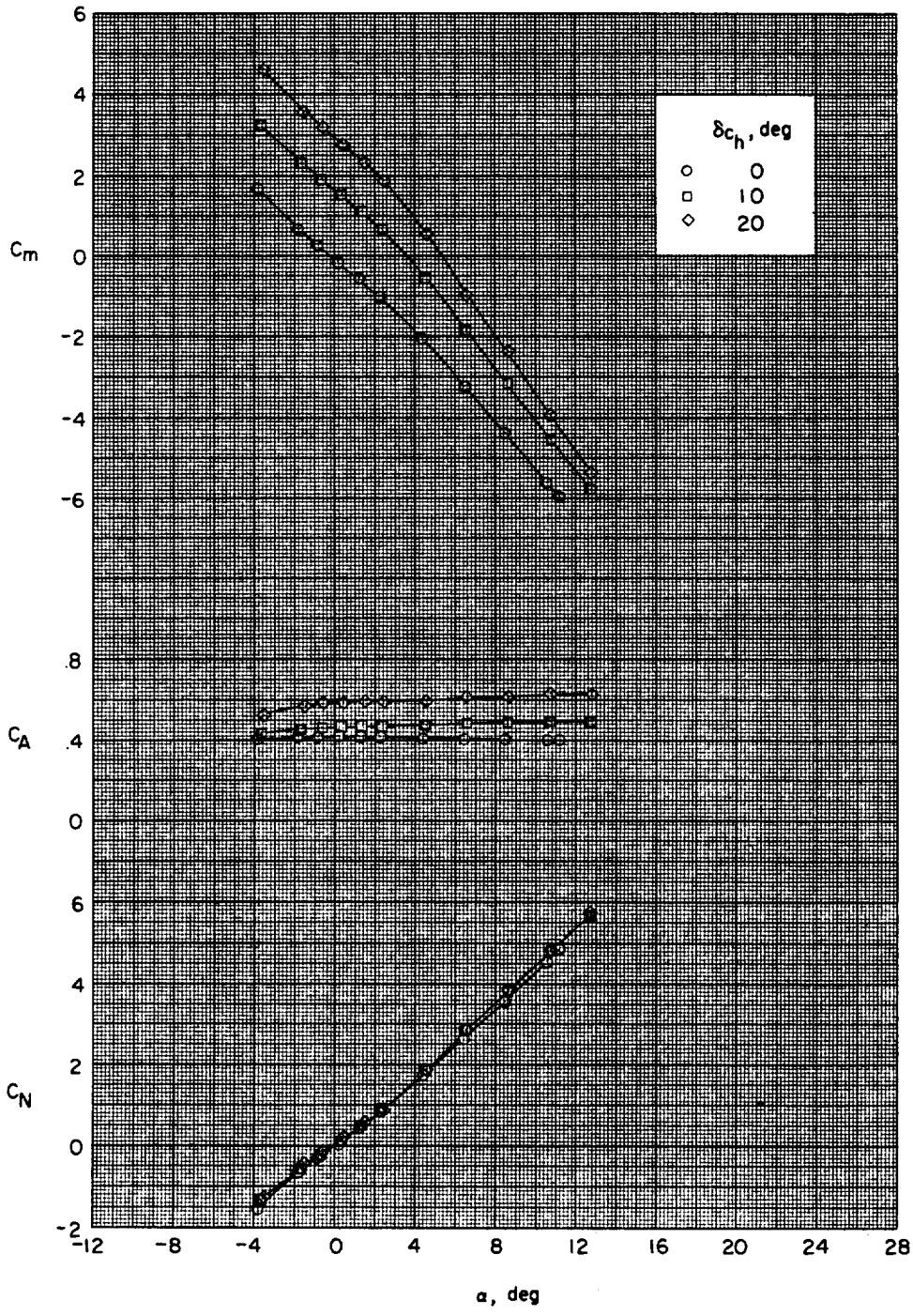

(g) M = 1.50.

Figure 4.- Continued.

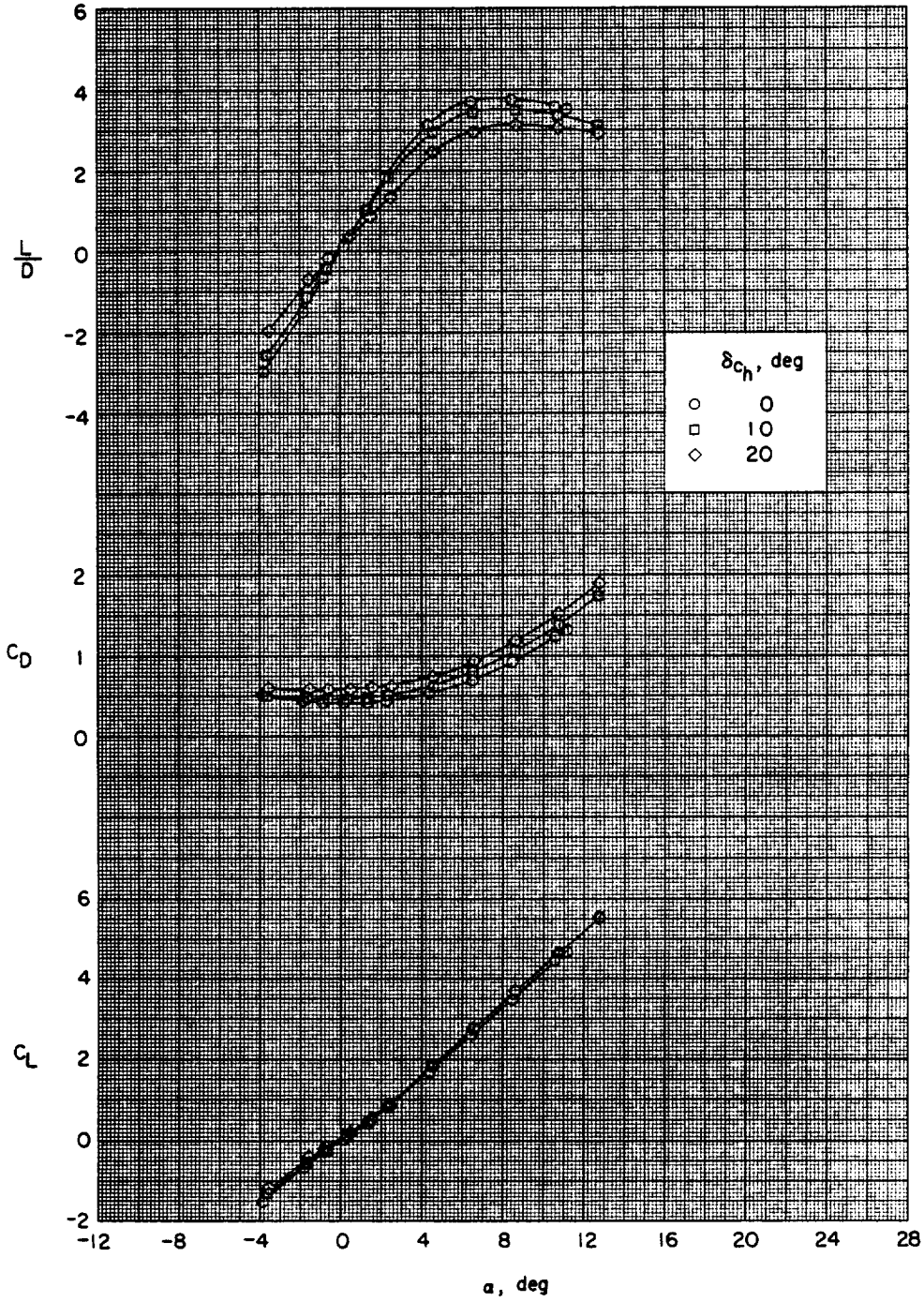

(g) Concluded.

Figure 4.- Continued.

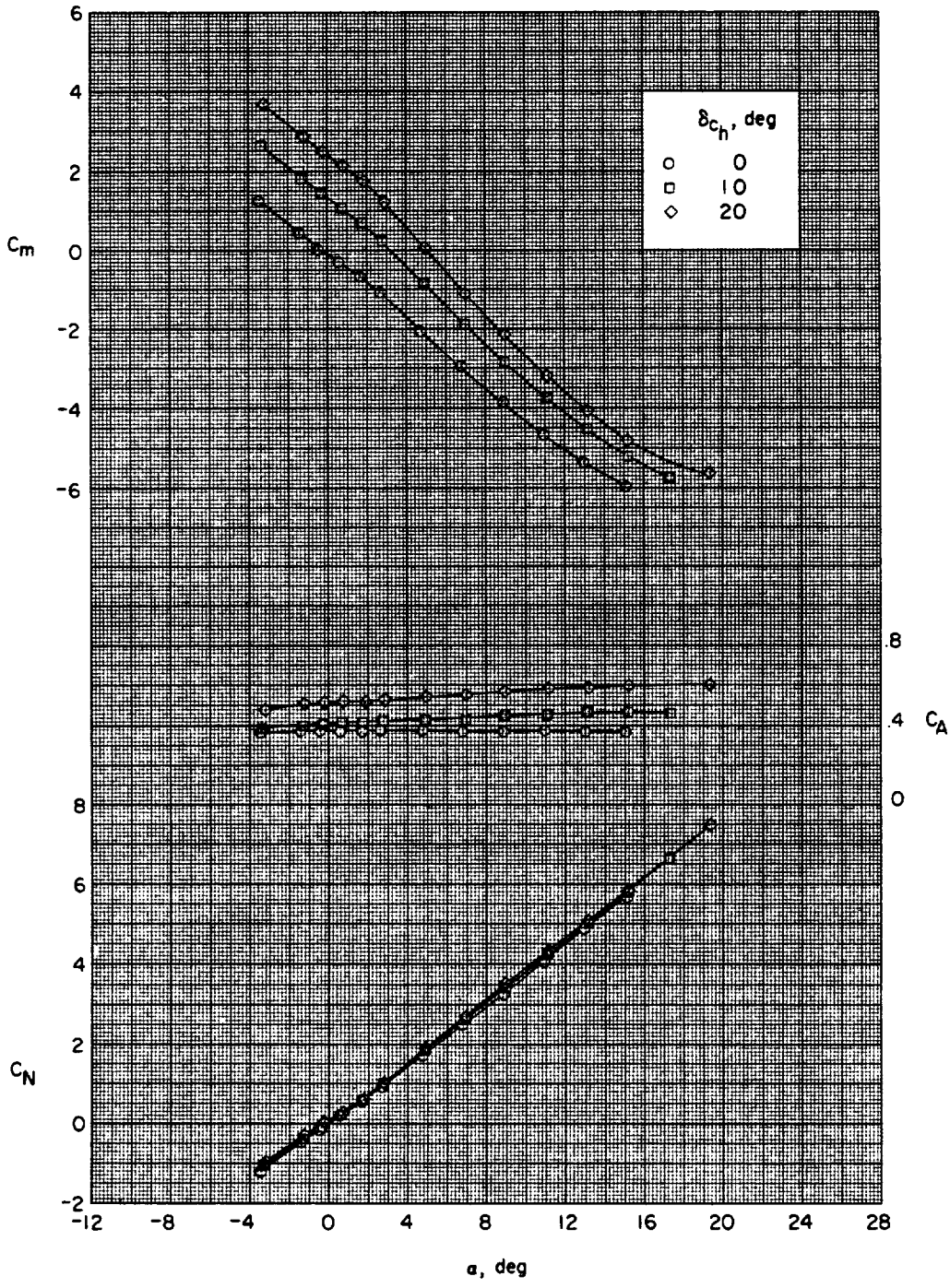

(h) M = 1.90.

Figure 4.- Continued.

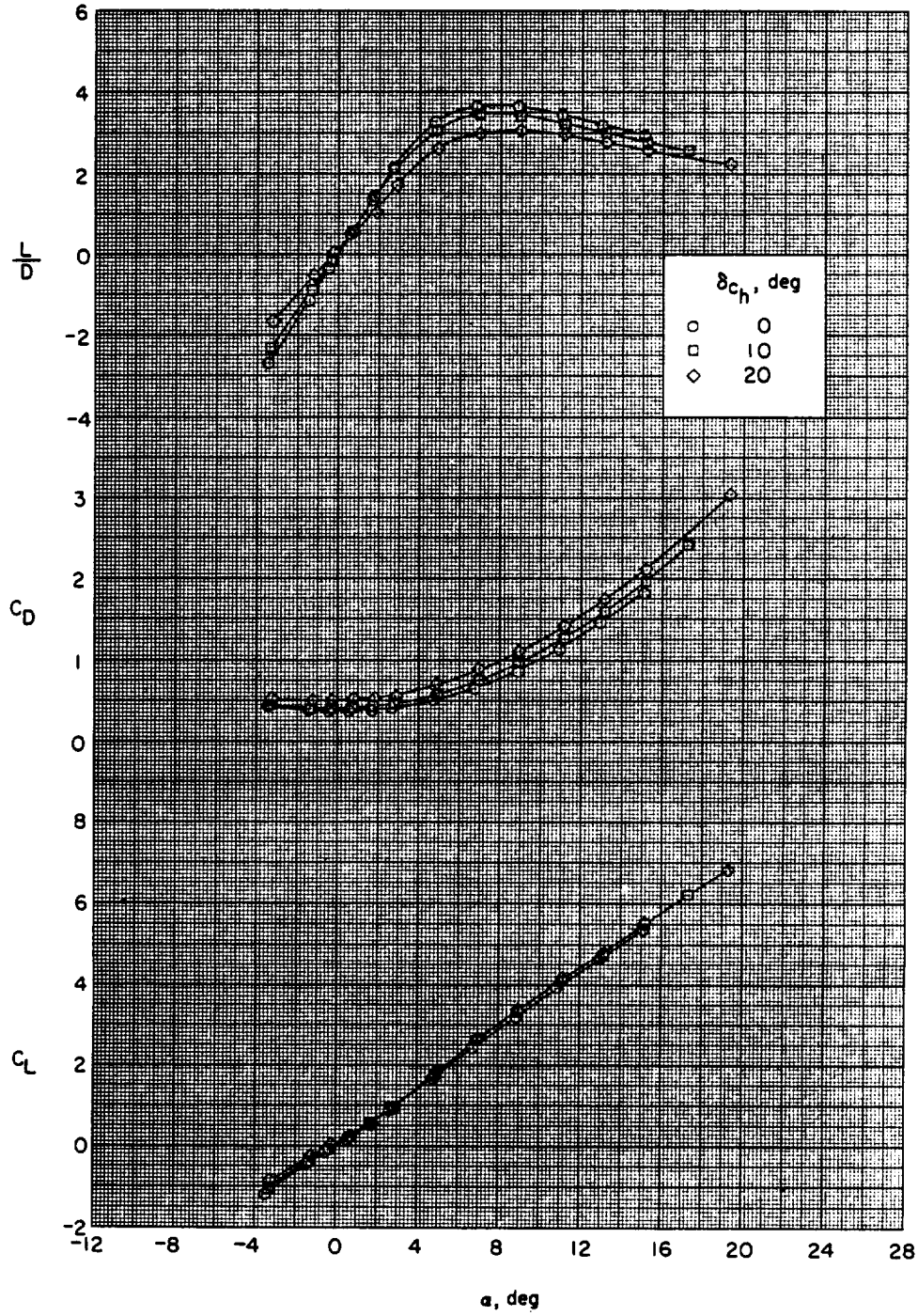

(h) Concluded.

Figure 4.- Continued.

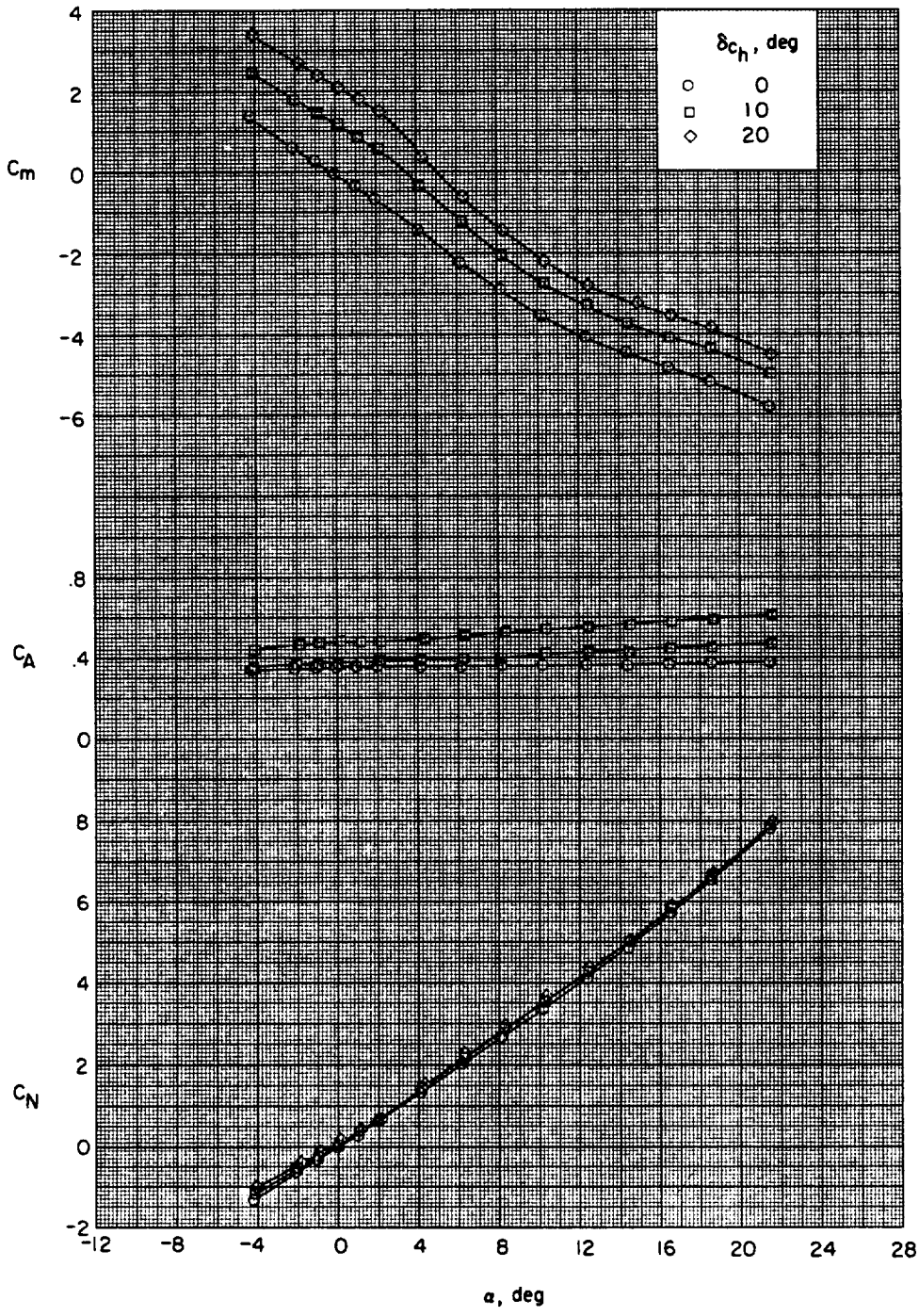

(i) M = 2.30.

Figure 4.- Continued.

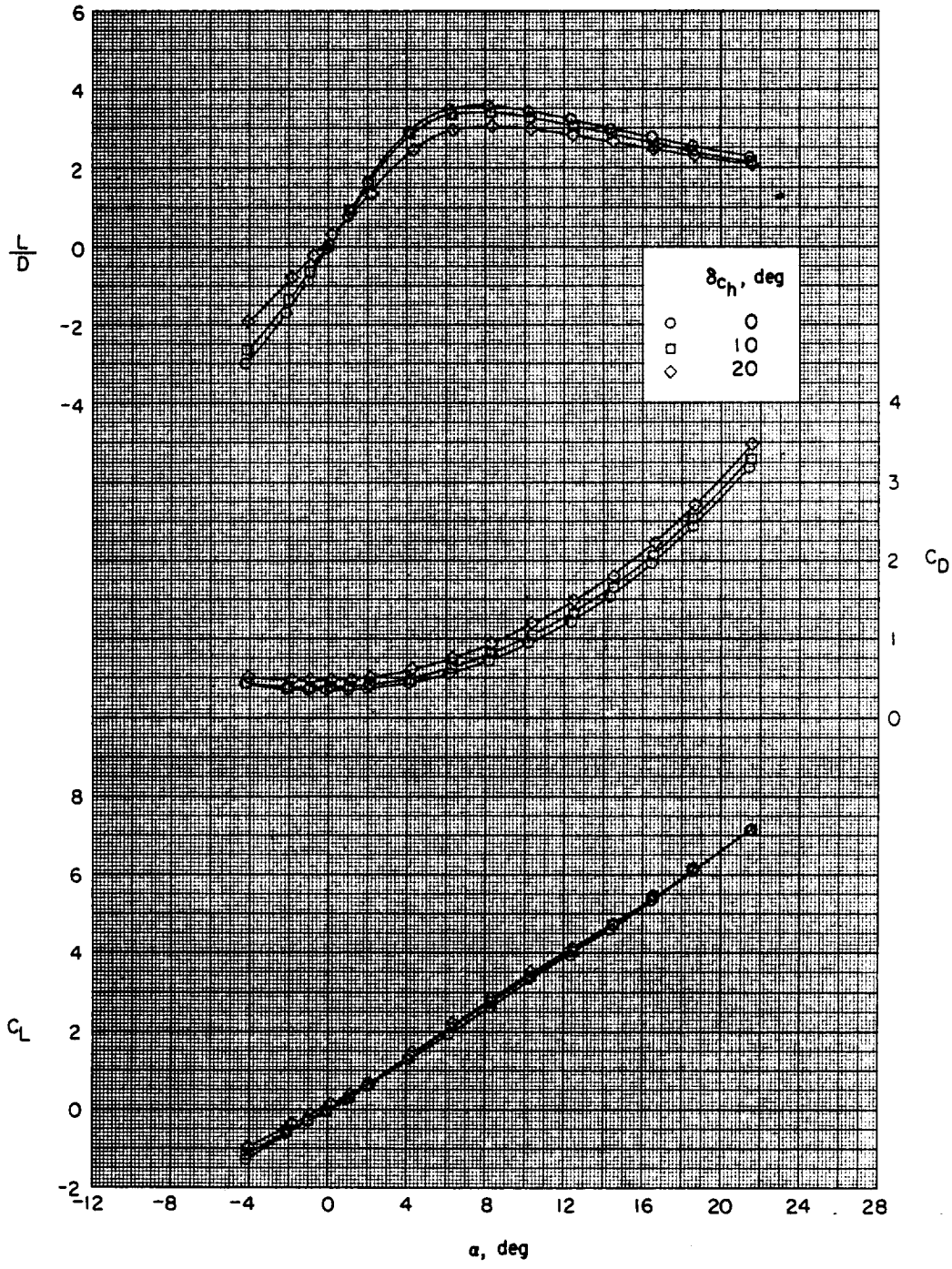

(i) Concluded.

Figure 4.- Continued.

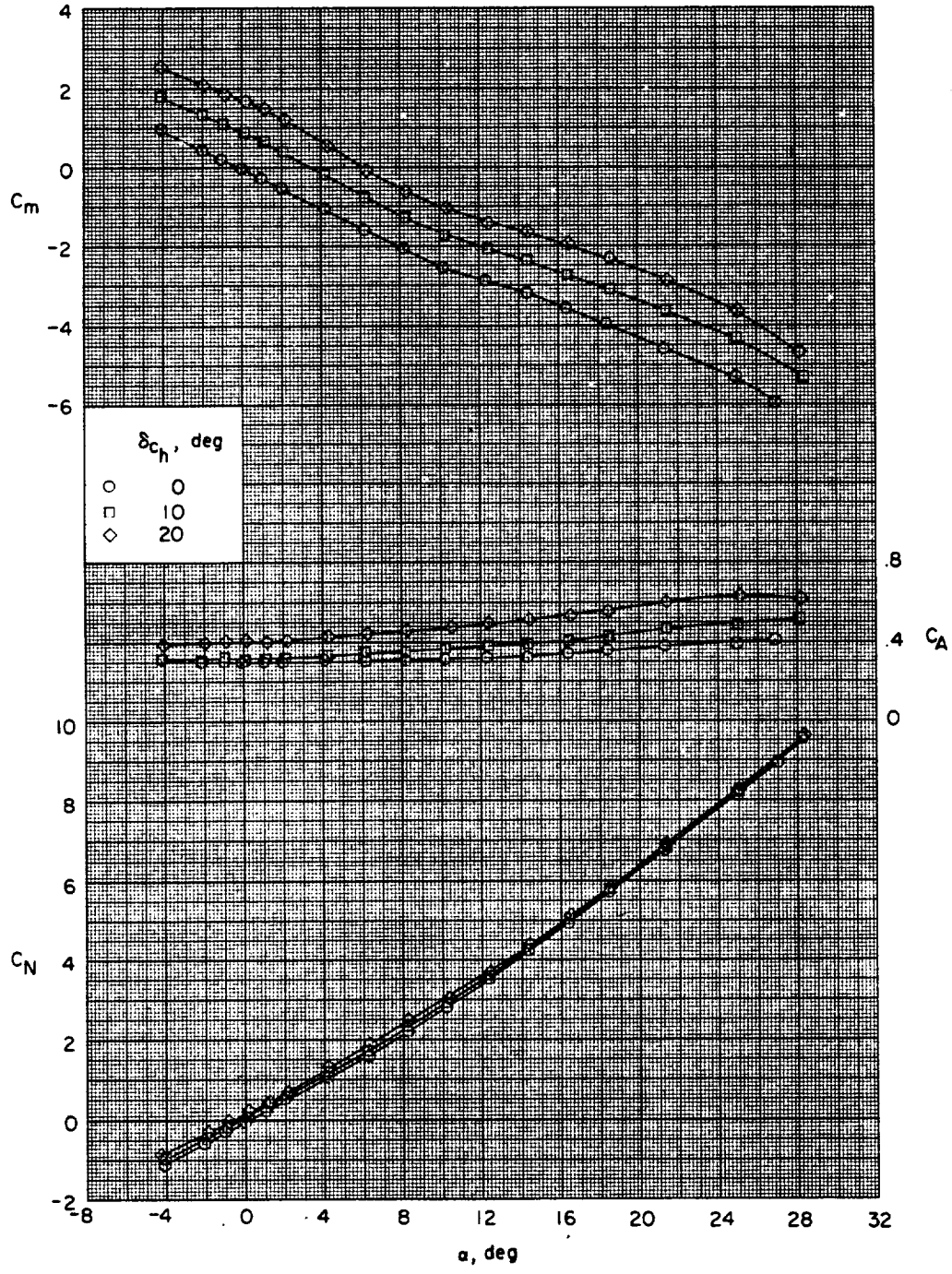

(j) M = 2.96.

Figure 4.- Continued.

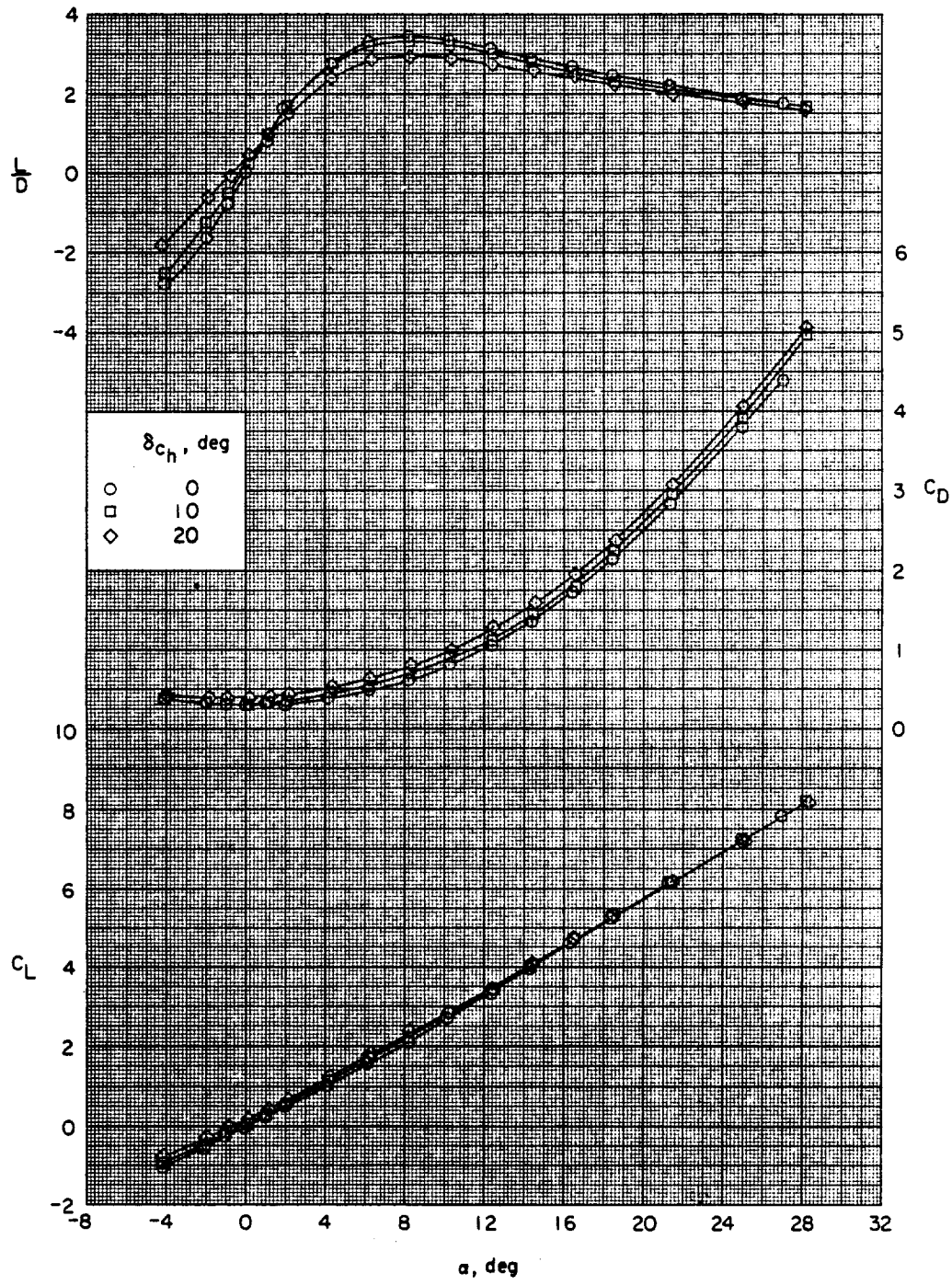

(j) Concluded.

Figure 4.- Continued.

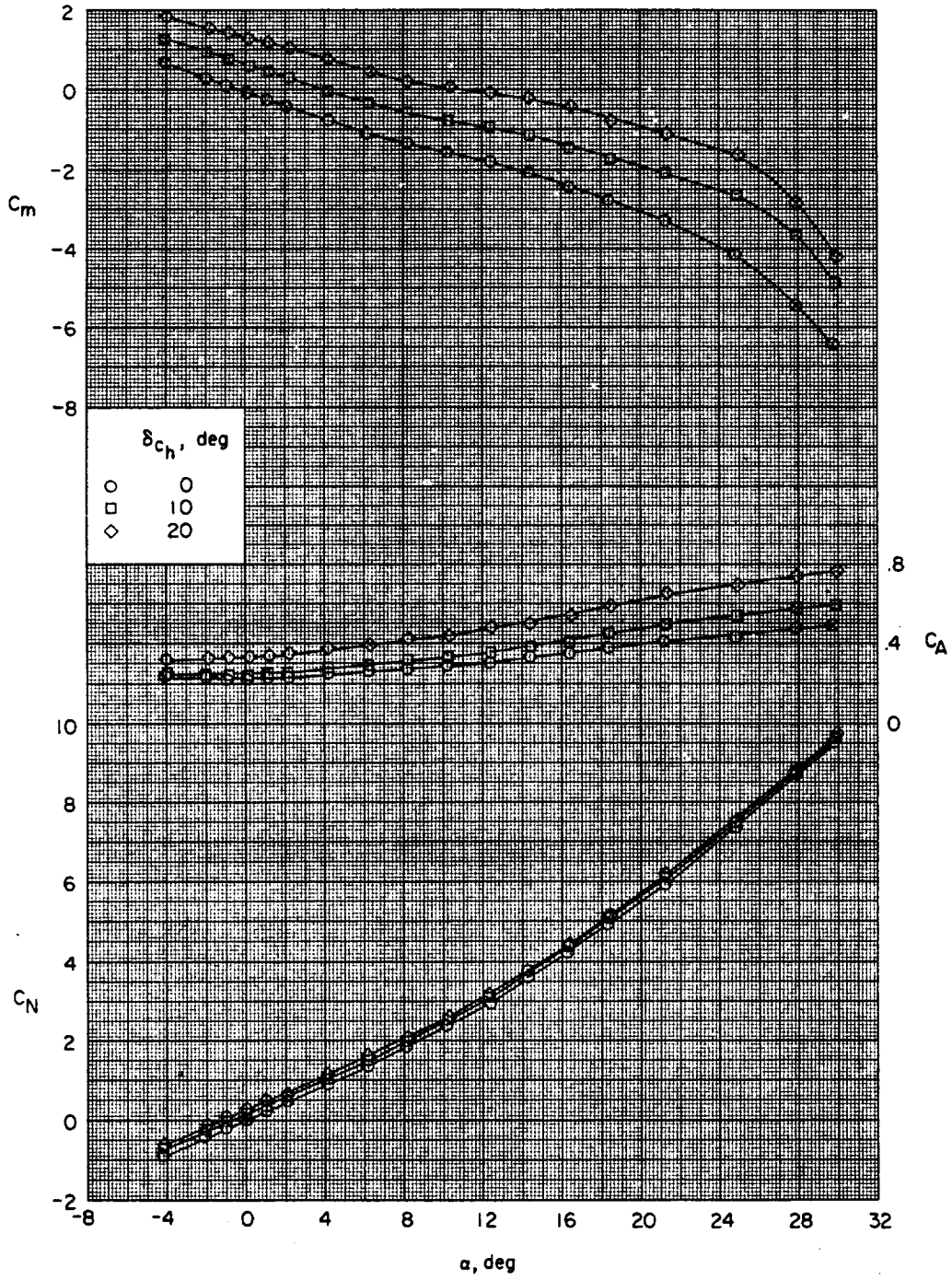

(k) M = 3.95.

Figure 4.- Continued.

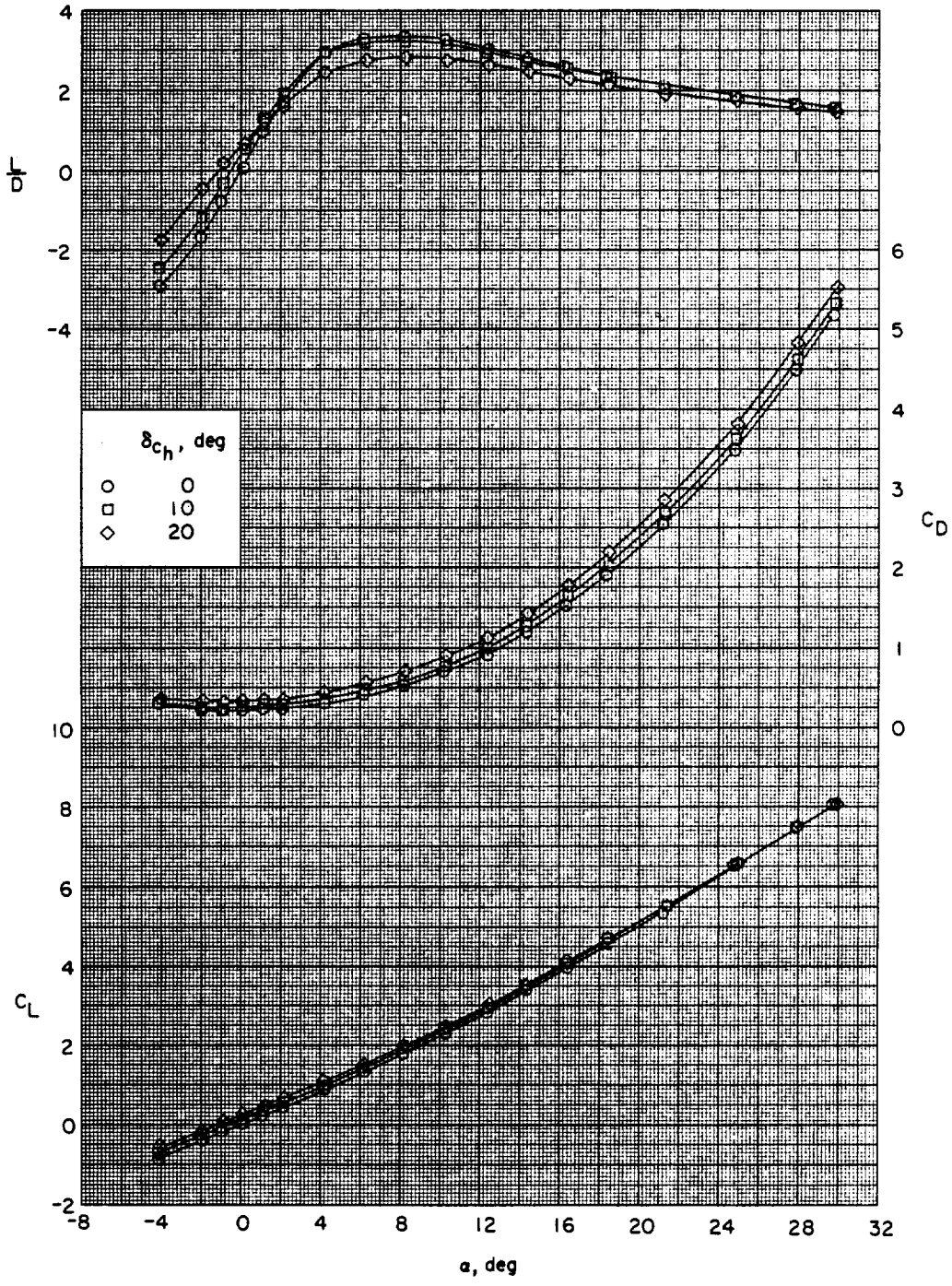

(k) Concluded.

Figure 4.- Continued.

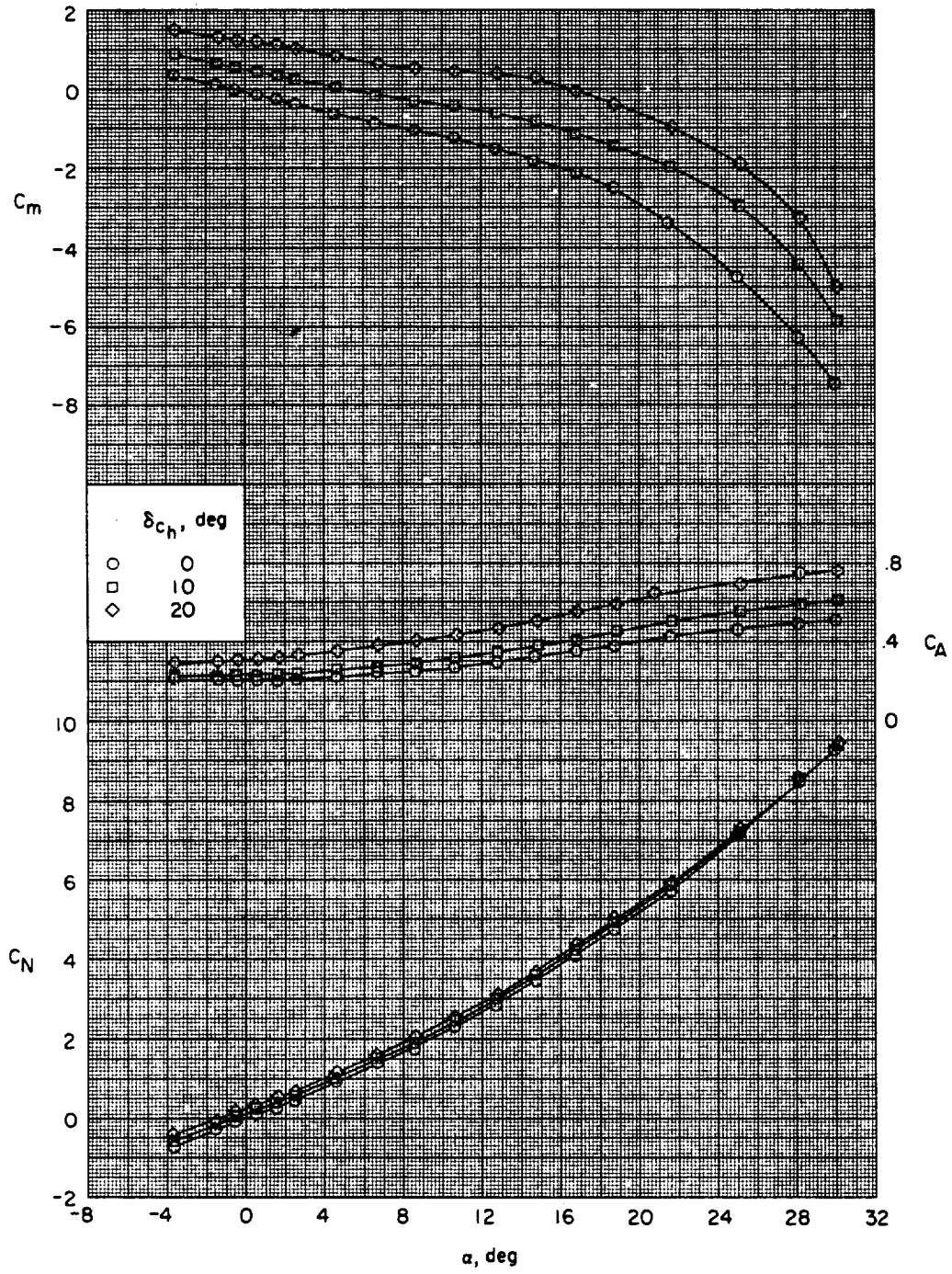

(l) M = 4.63.

Figure 4.- Continued.

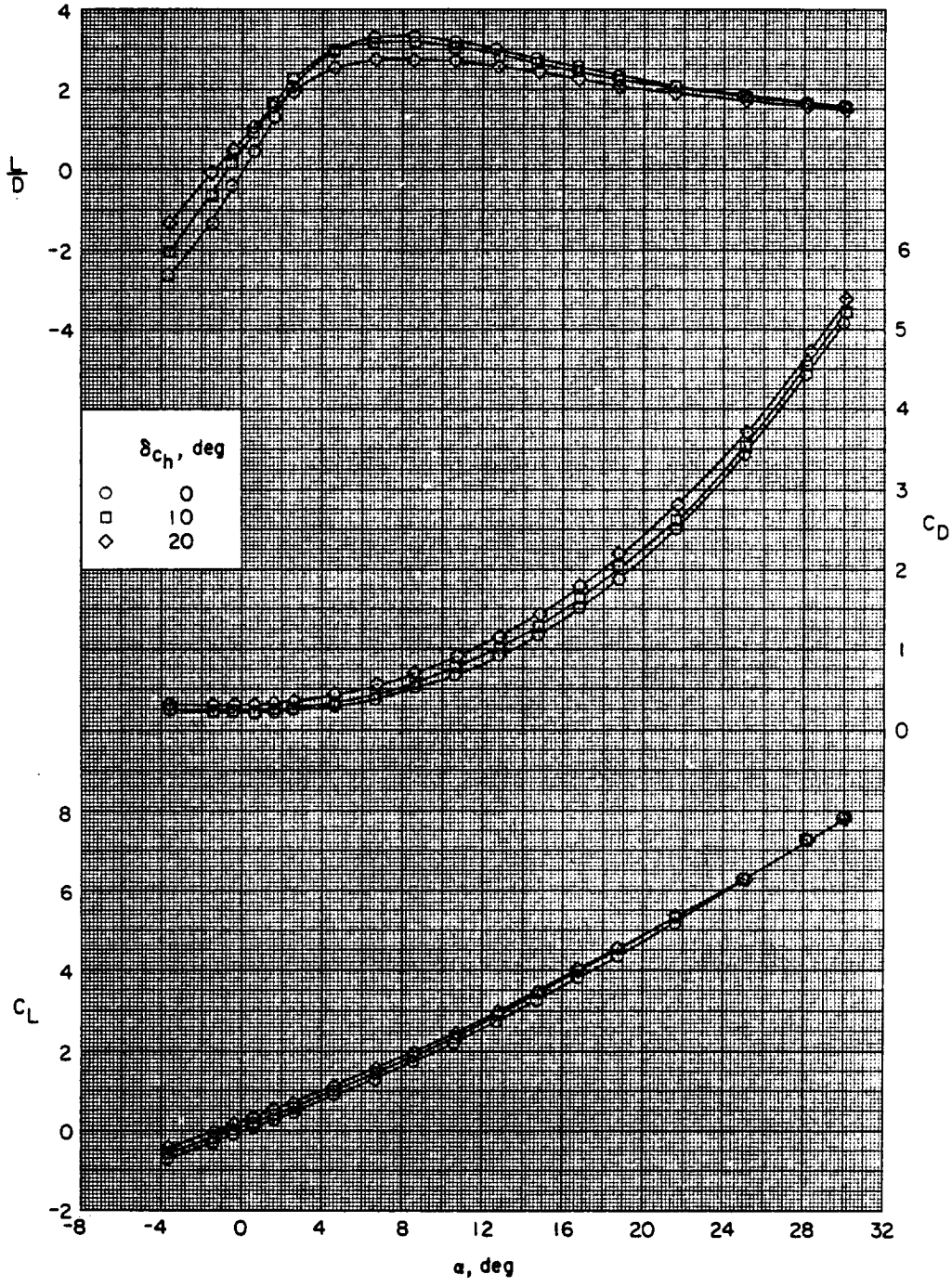

(l) Concluded.

Figure 4.- Concluded.

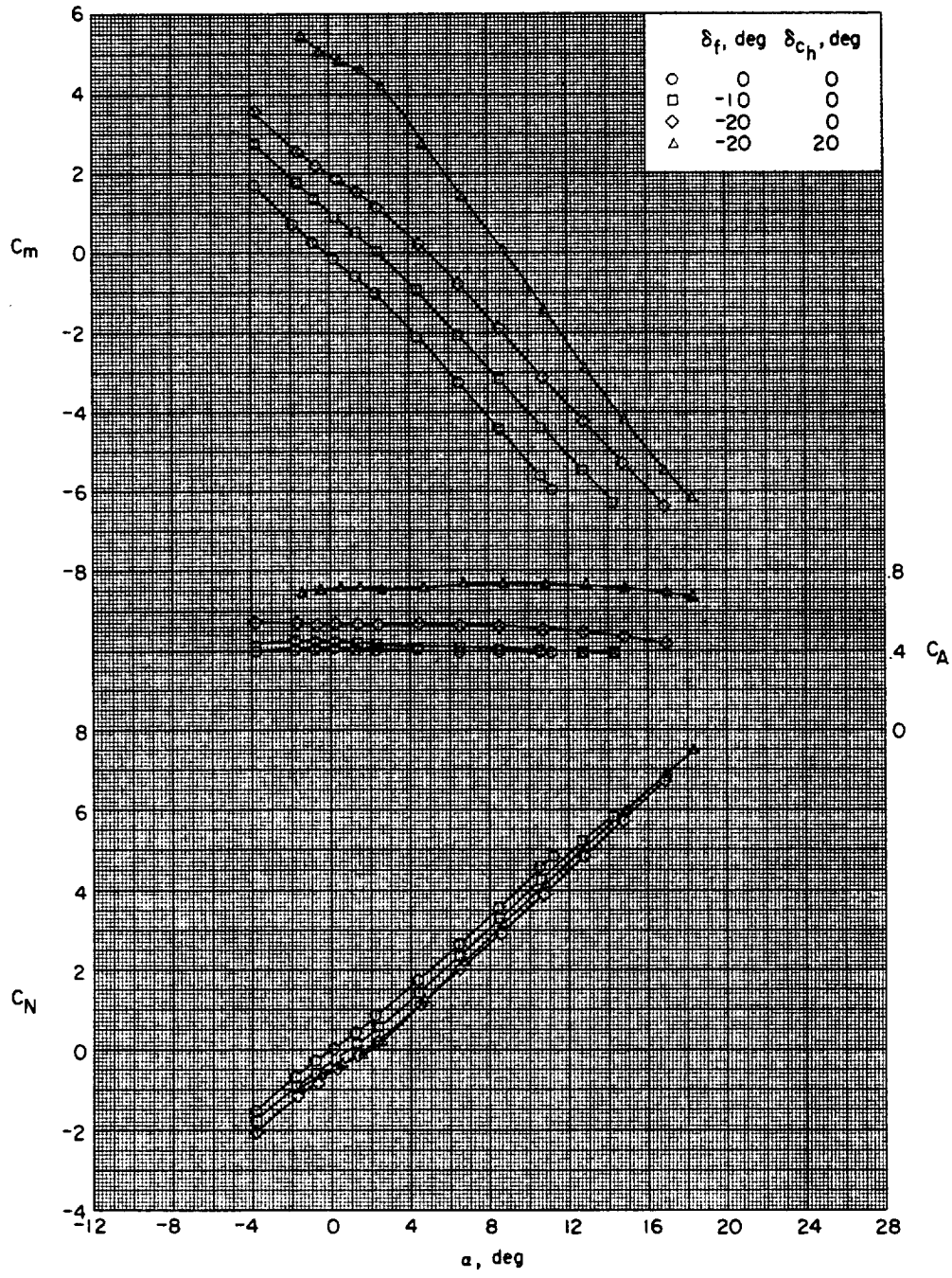

(a) M = 1.50.

Figure 5.- Effect of wing-flap deflection and horizontal-canard deflection on the longitudinal aerodynamic characteristics of configuration BWC. $\delta_{c_v} = 0^o$.

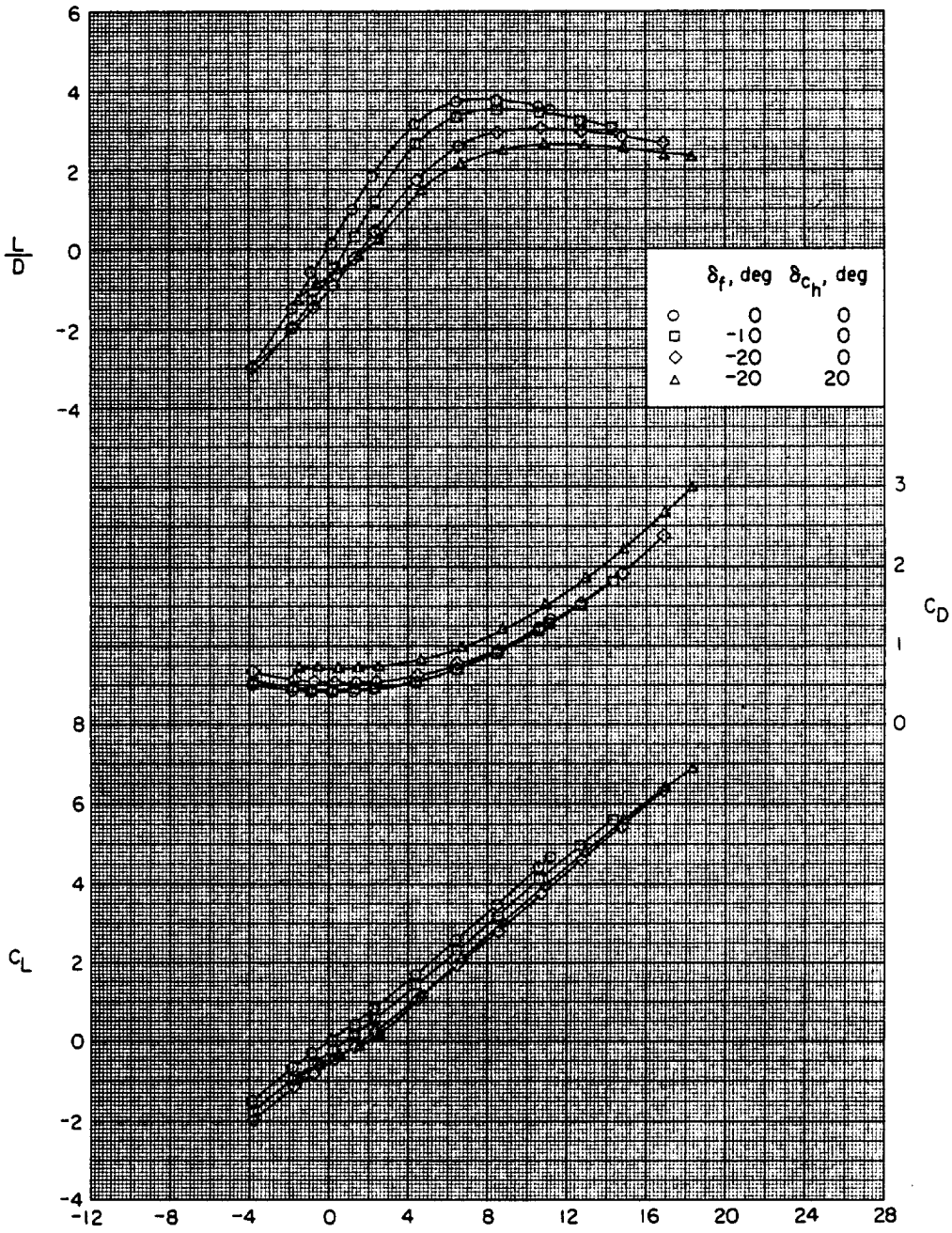

(a) Concluded.

Figure 5.- Continued.

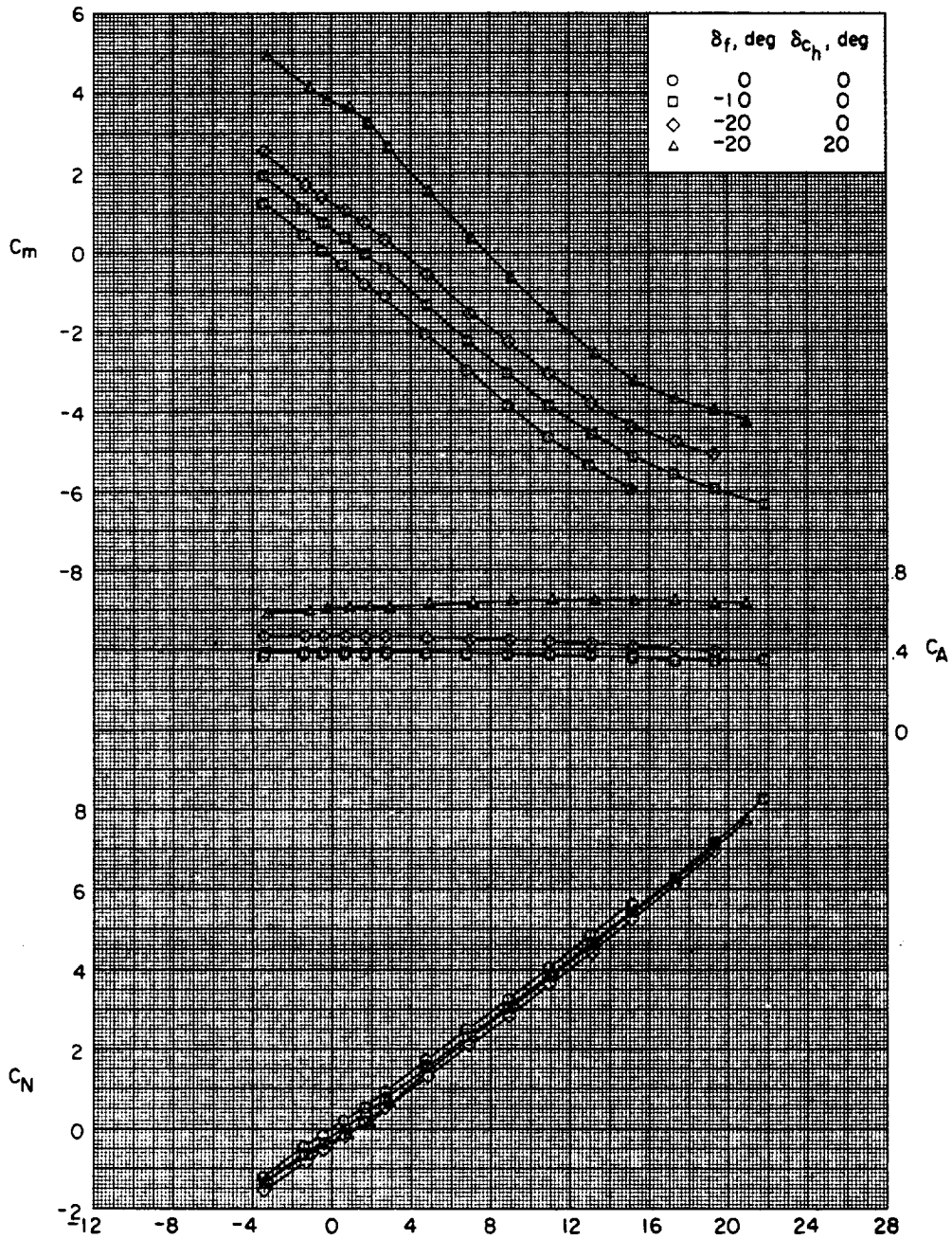

(b) M = 1.90.

Figure 5.- Continued.

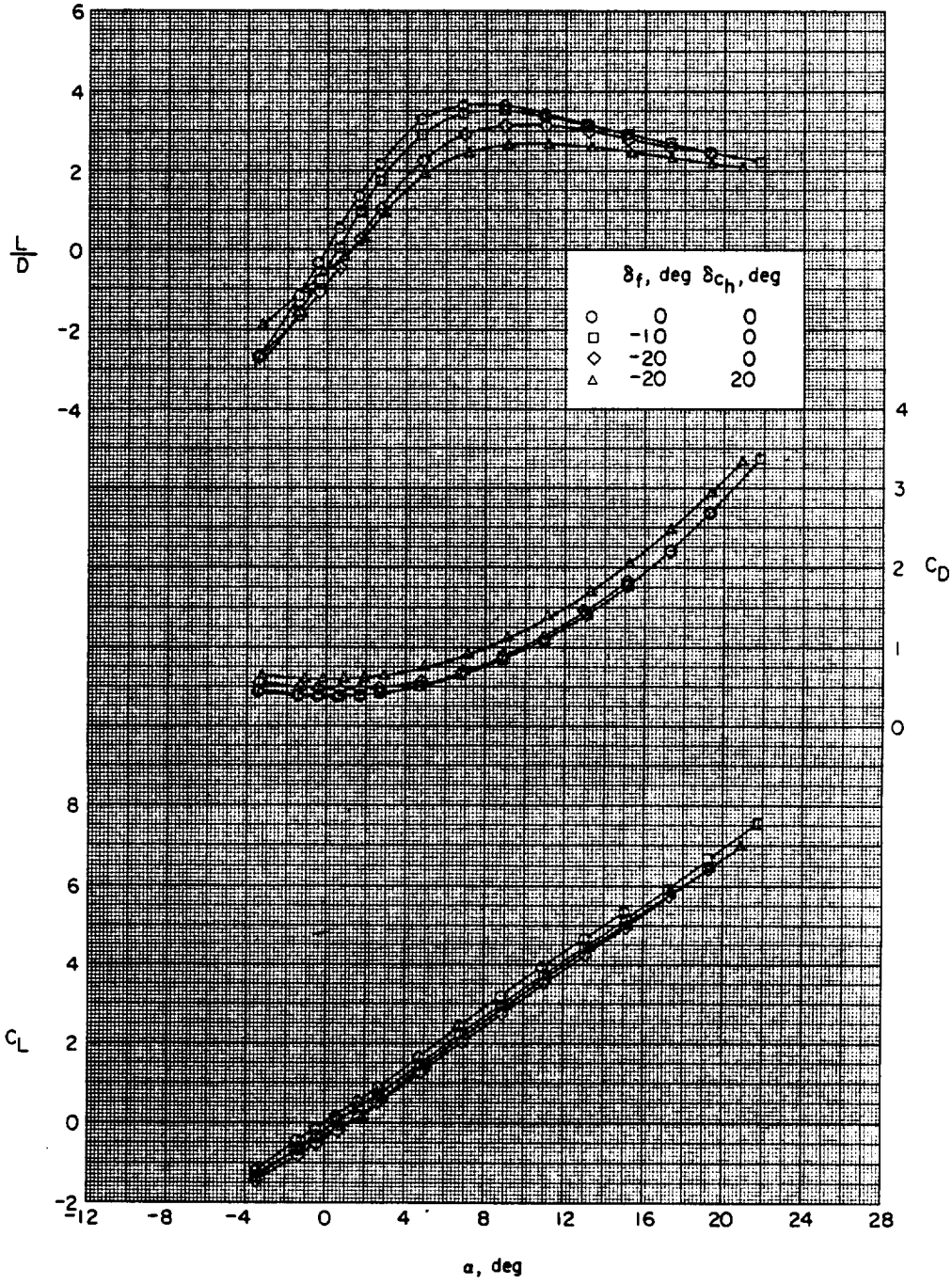

(b) Concluded.

Figure 5.- Continued.

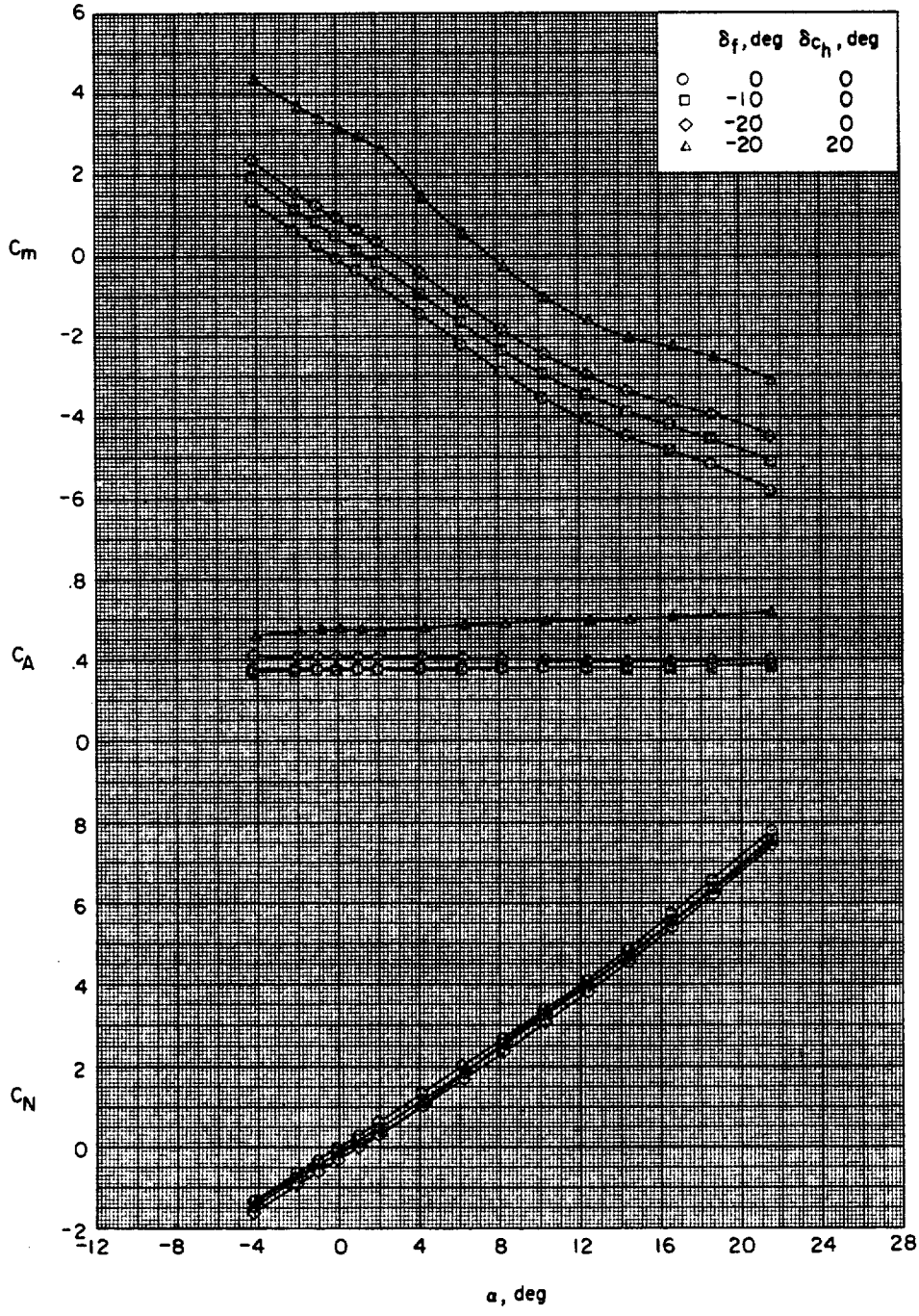

(c) M = 2.30.

Figure 5.- Continued.

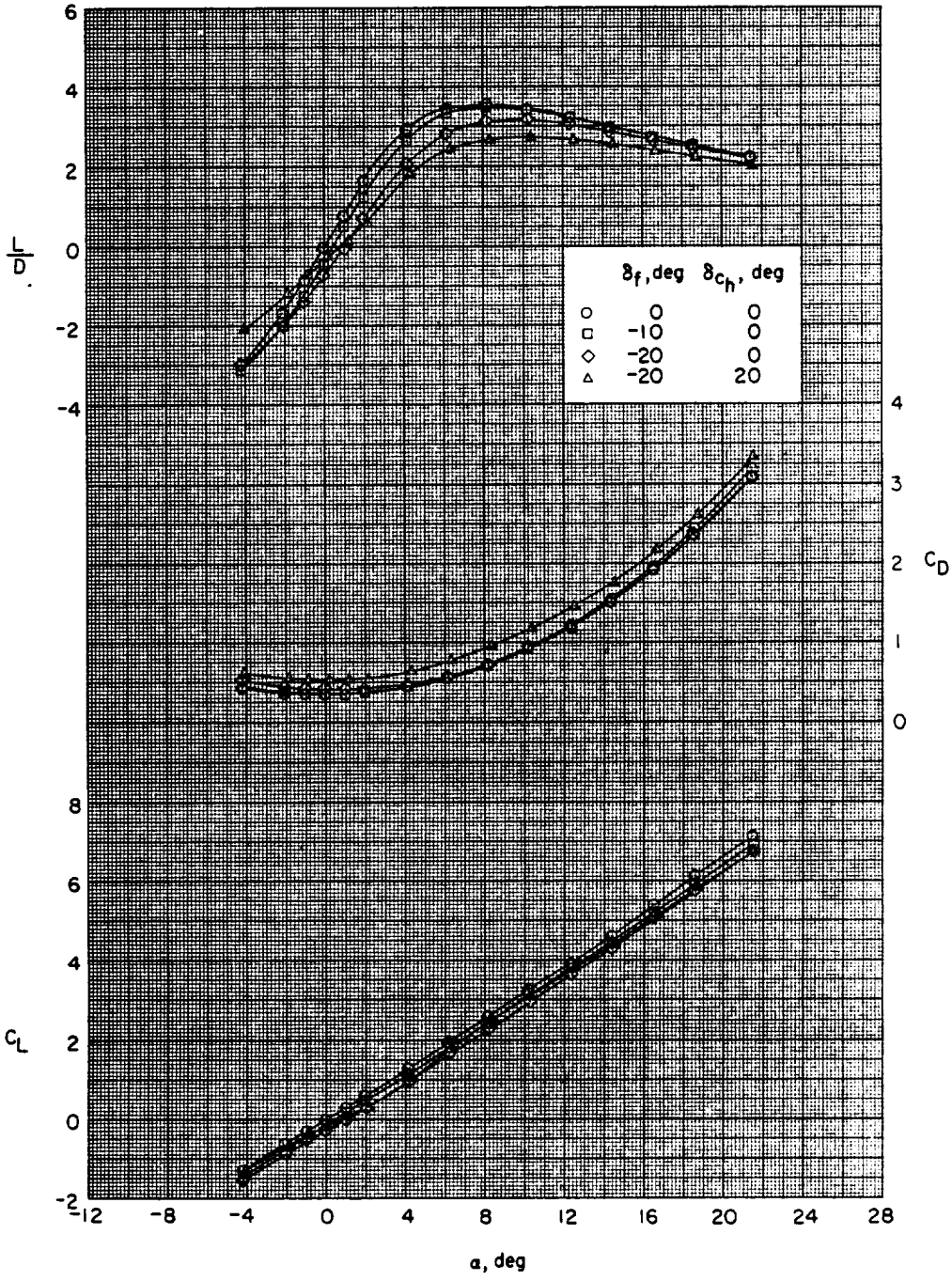

(c) Concluded.

Figure 5.- Continued.

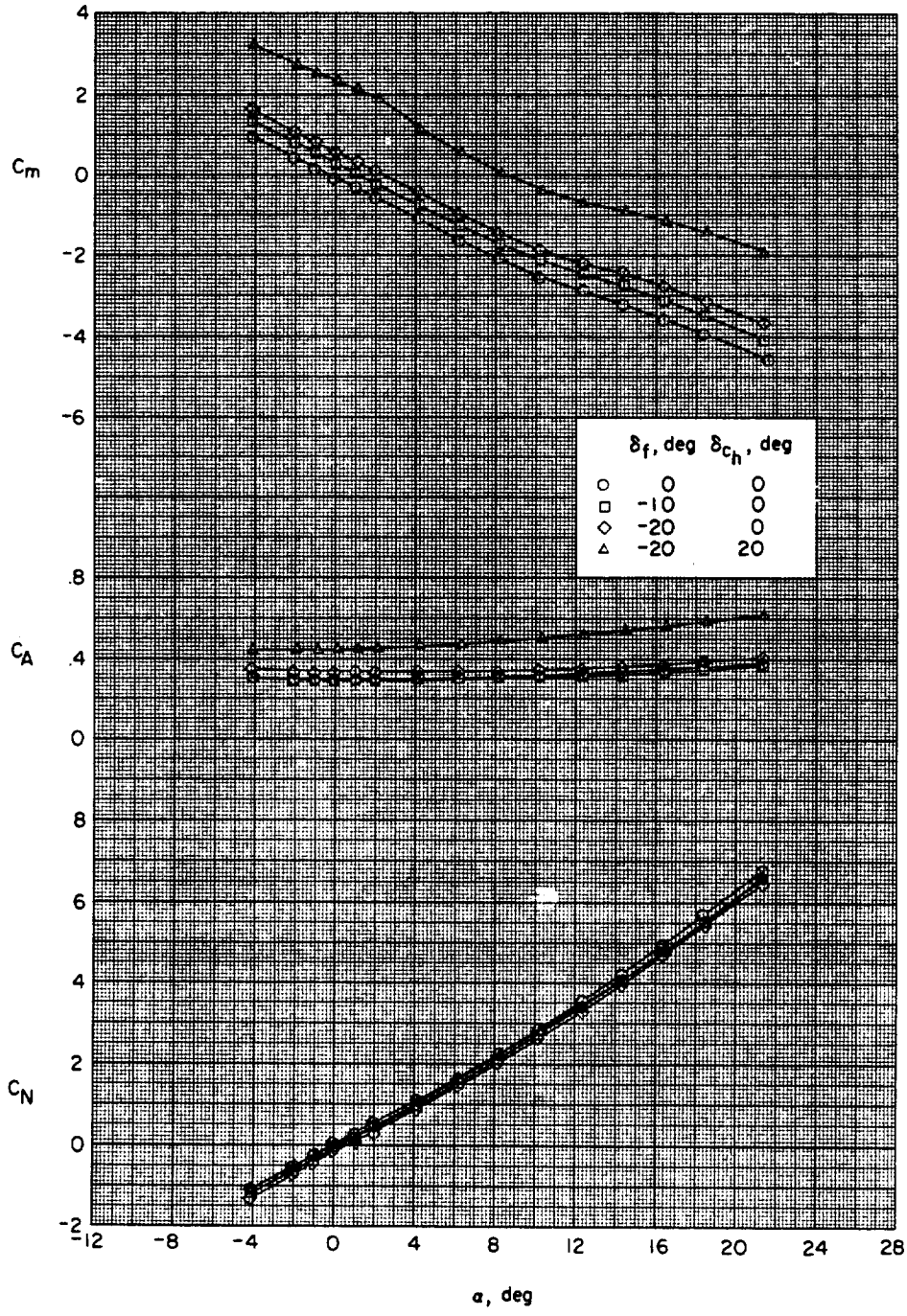

(d) M = 2.96.

Figure 5.- Continued.

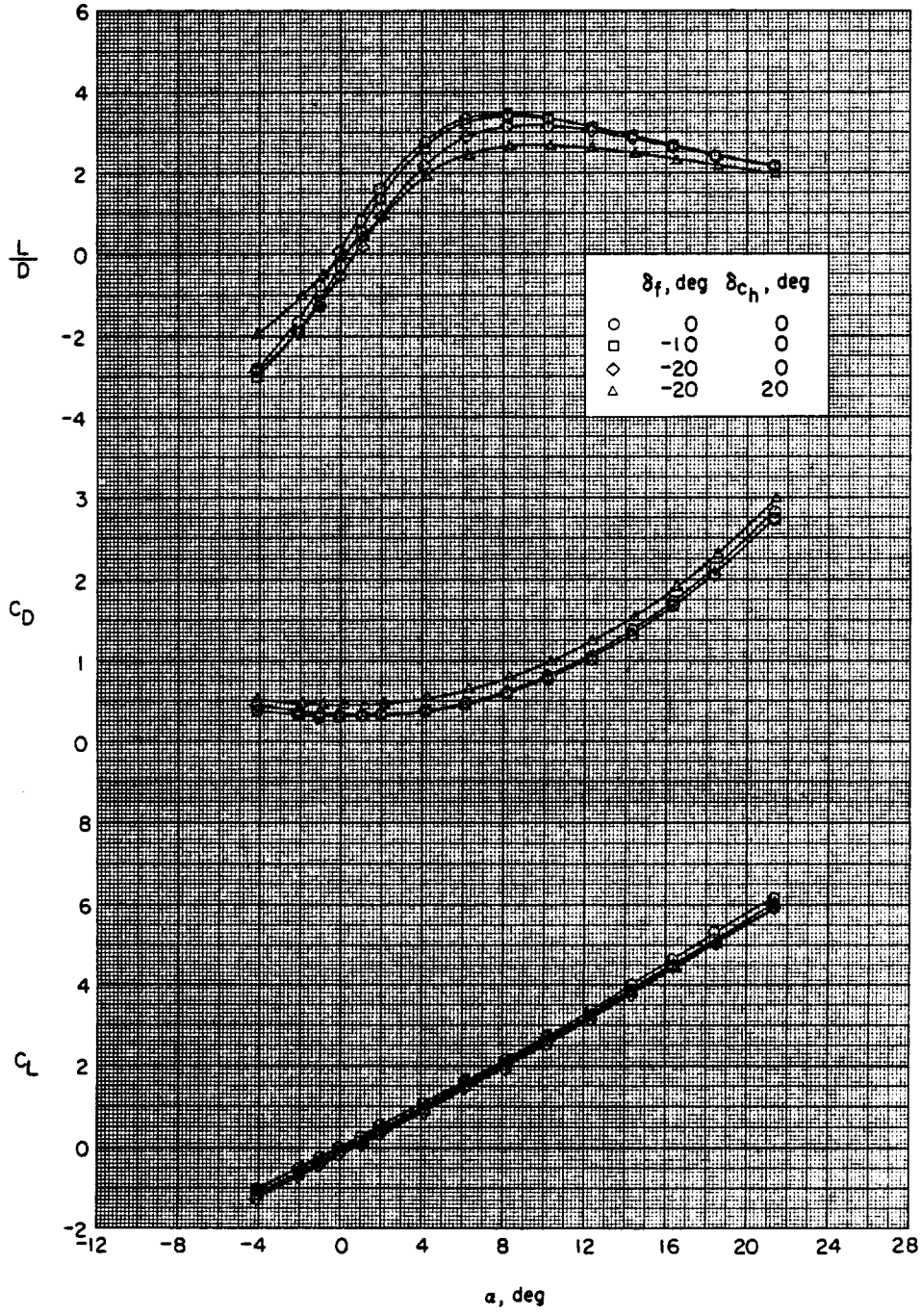

(d) Concluded.

Figure 5.- Continued.

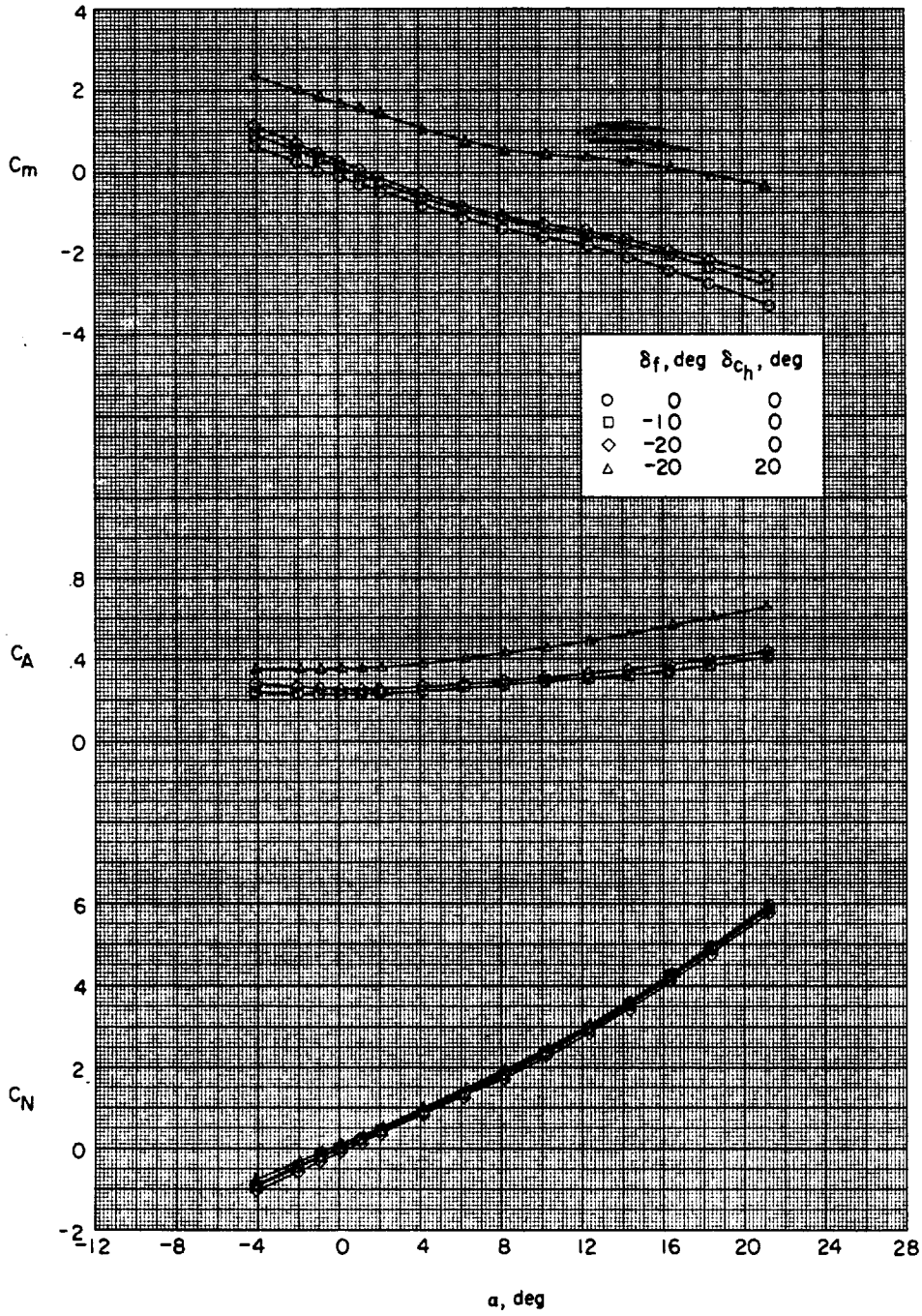

(e) M = 3.95.

Figure 5.- Continued.

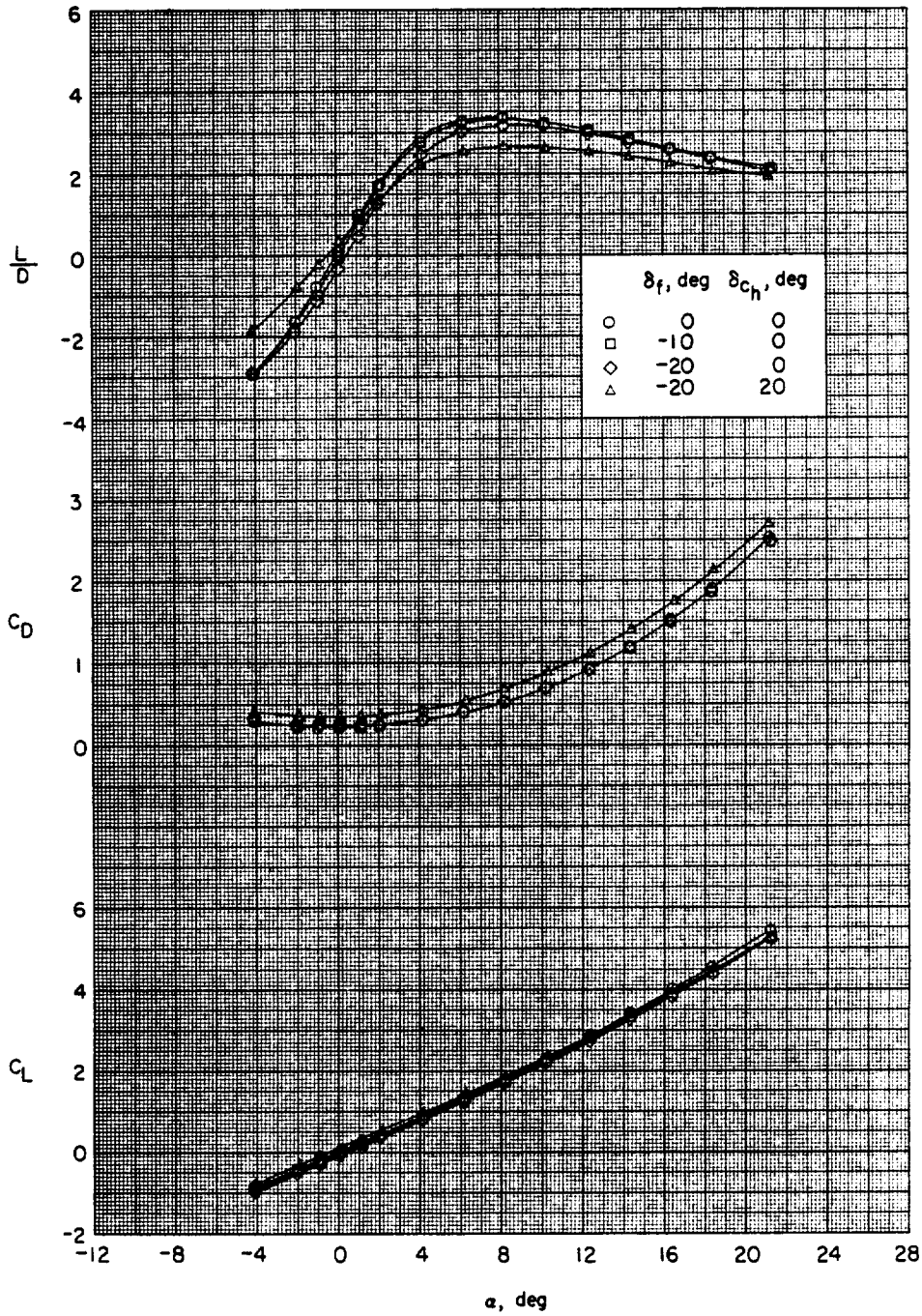

(e) Concluded.

Figure 5.- Continued.

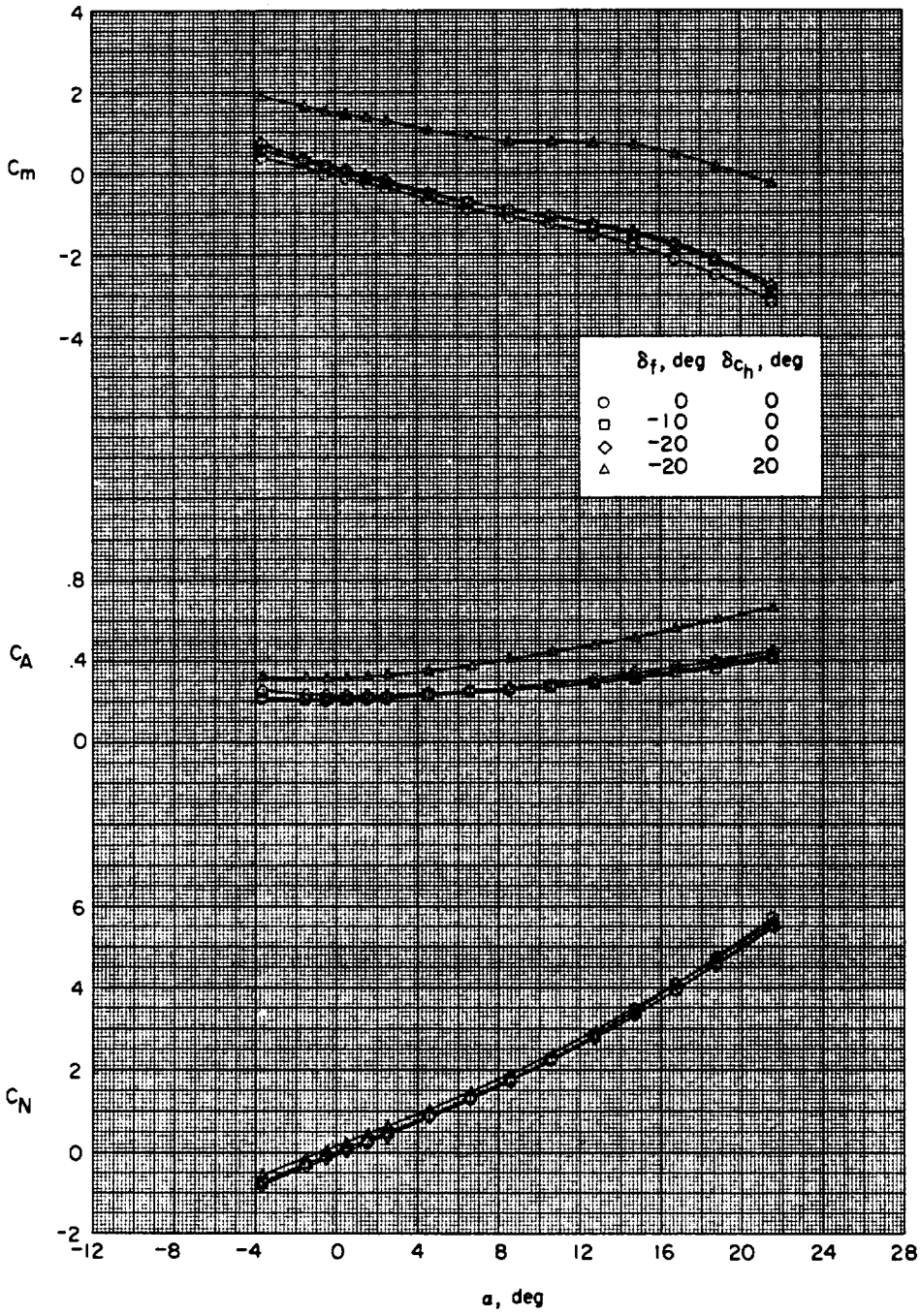

(f) M = 4.63.

Figure 5.- Continued.

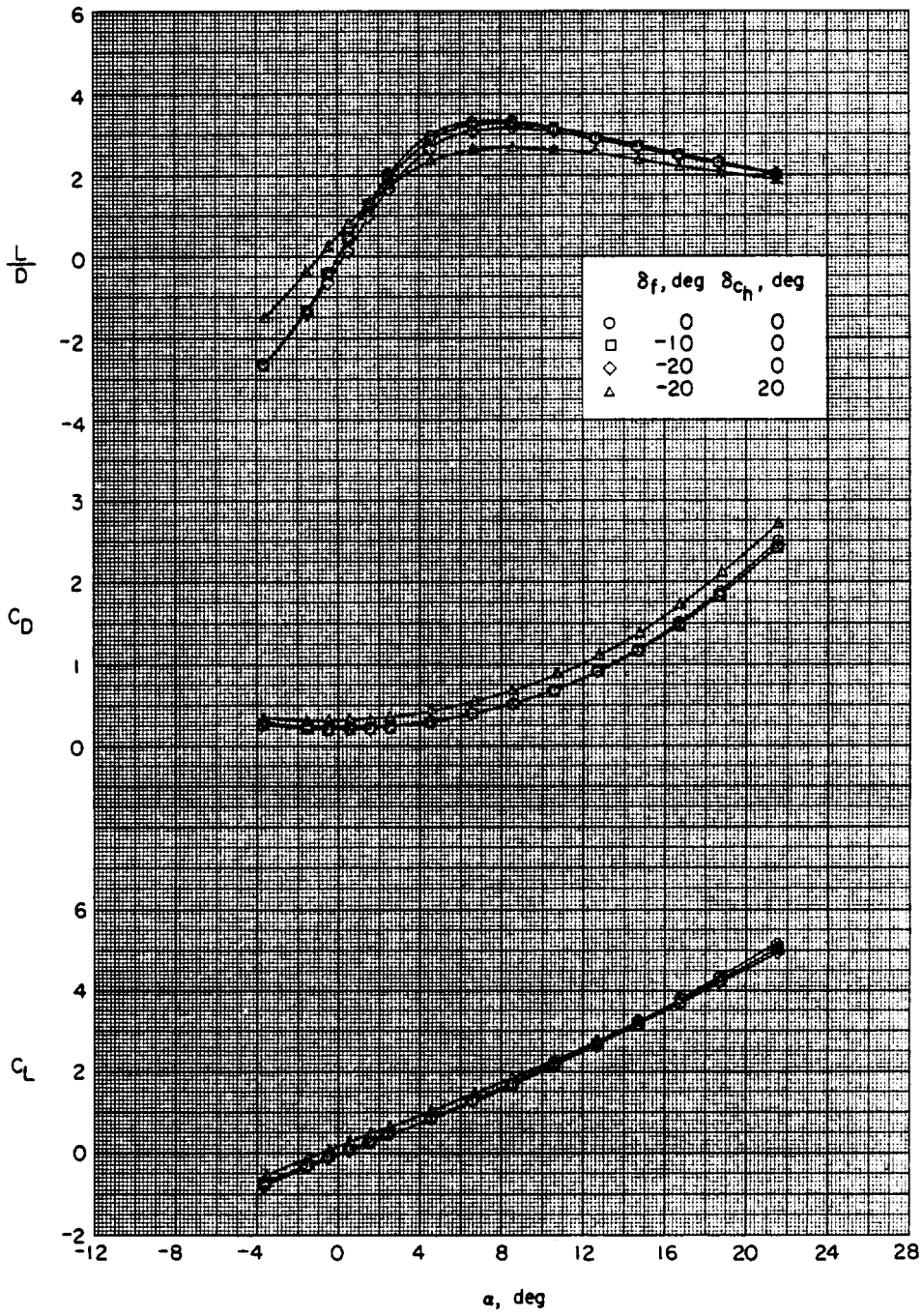

(f) Concluded.

Figure 5.- Concluded.

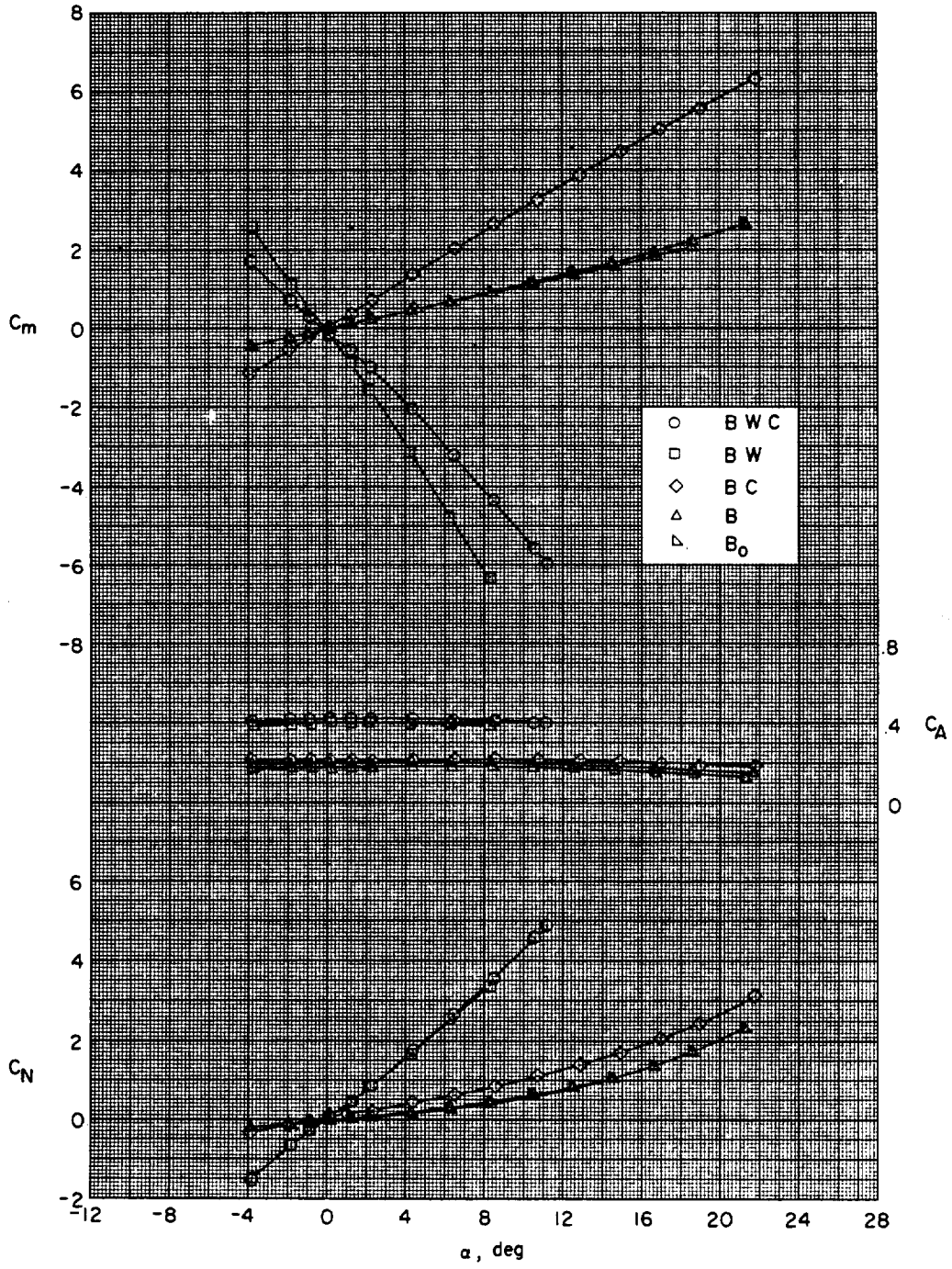

(a) M = 1.50.

Figure 6.- Effect of component parts on the longitudinal aerodynamic characteristics.

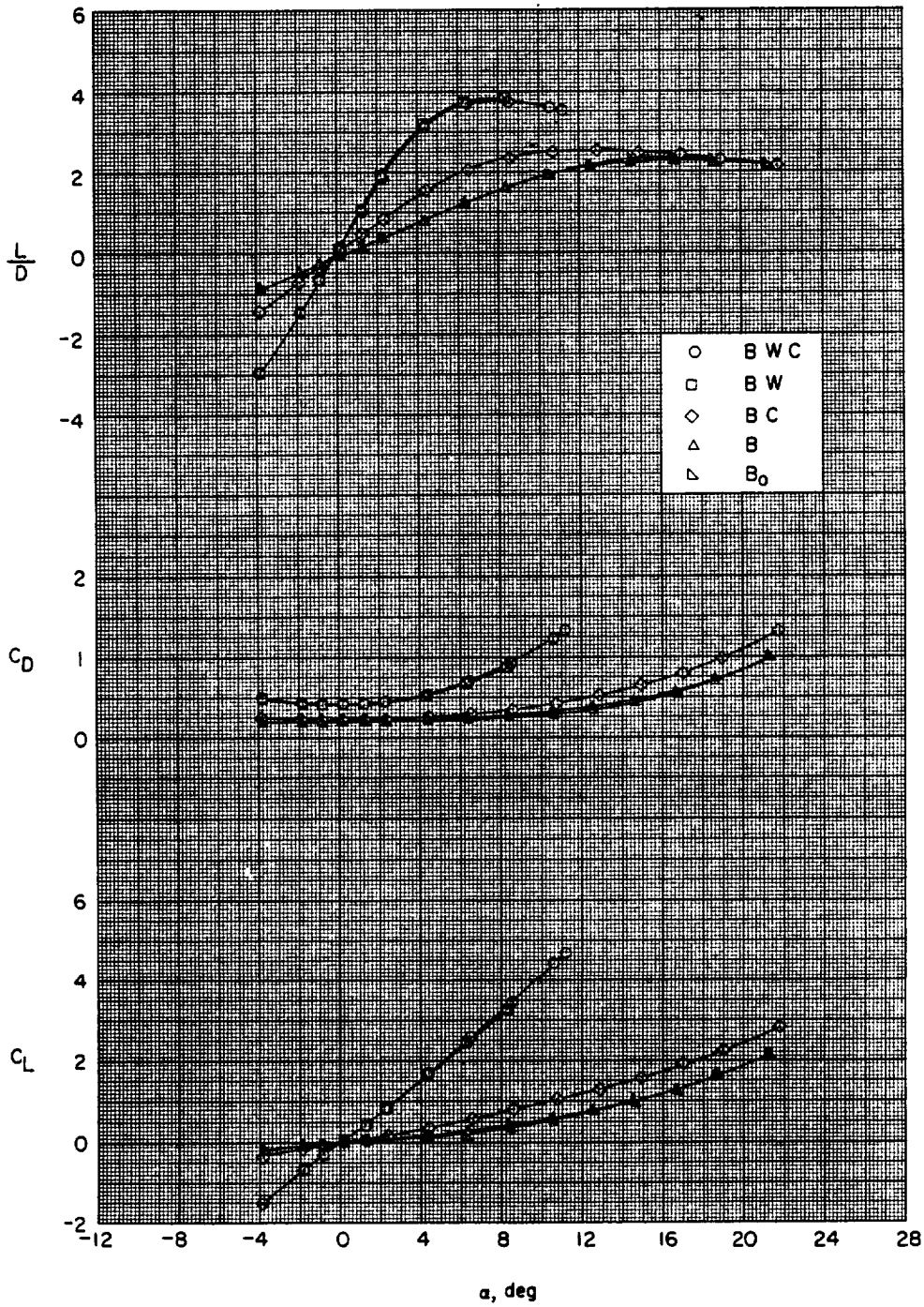

(a) Concluded.

Figure 6.- Continued.

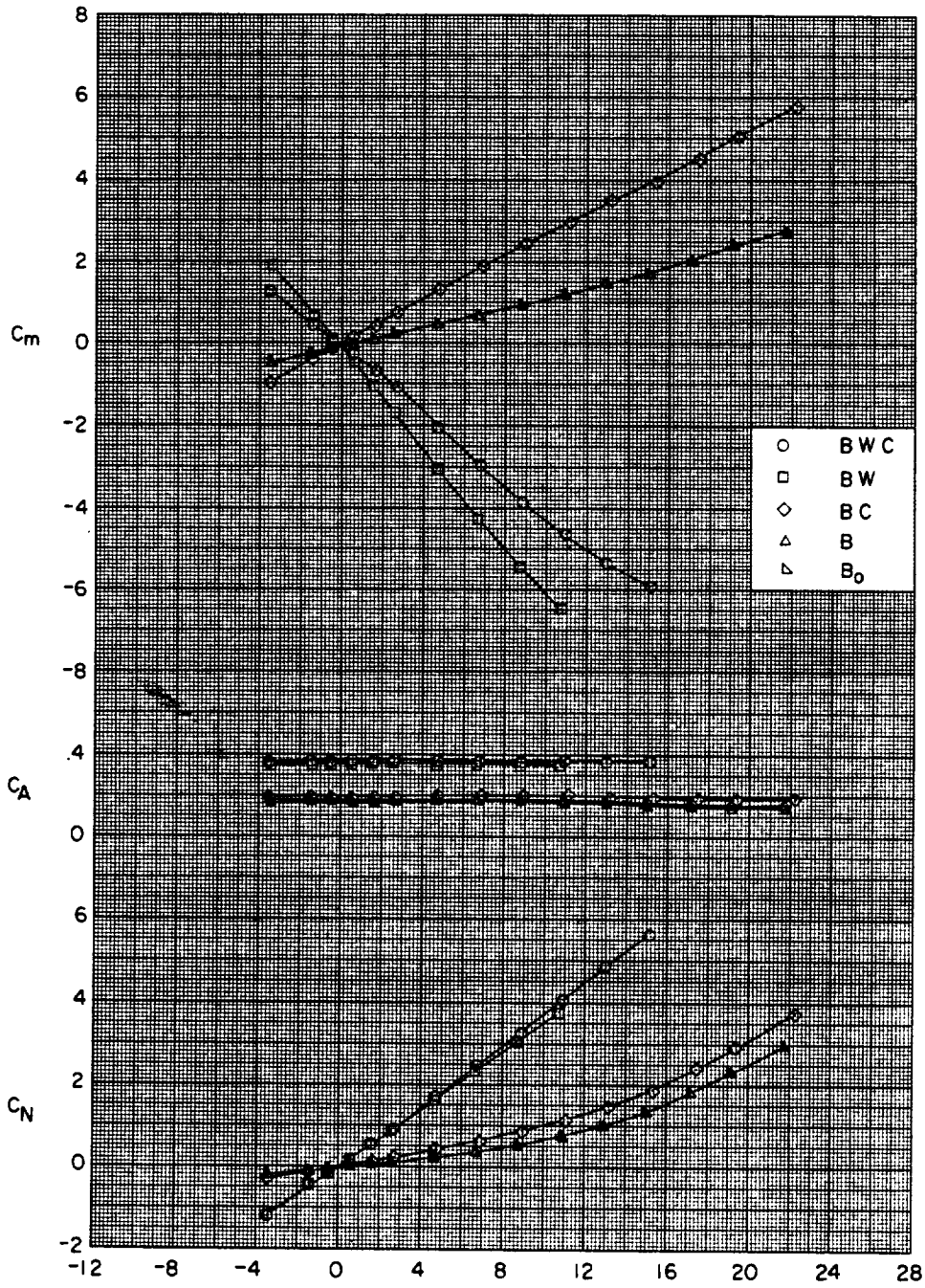

(b) M = 1.90.

Figure 6.- Continued.

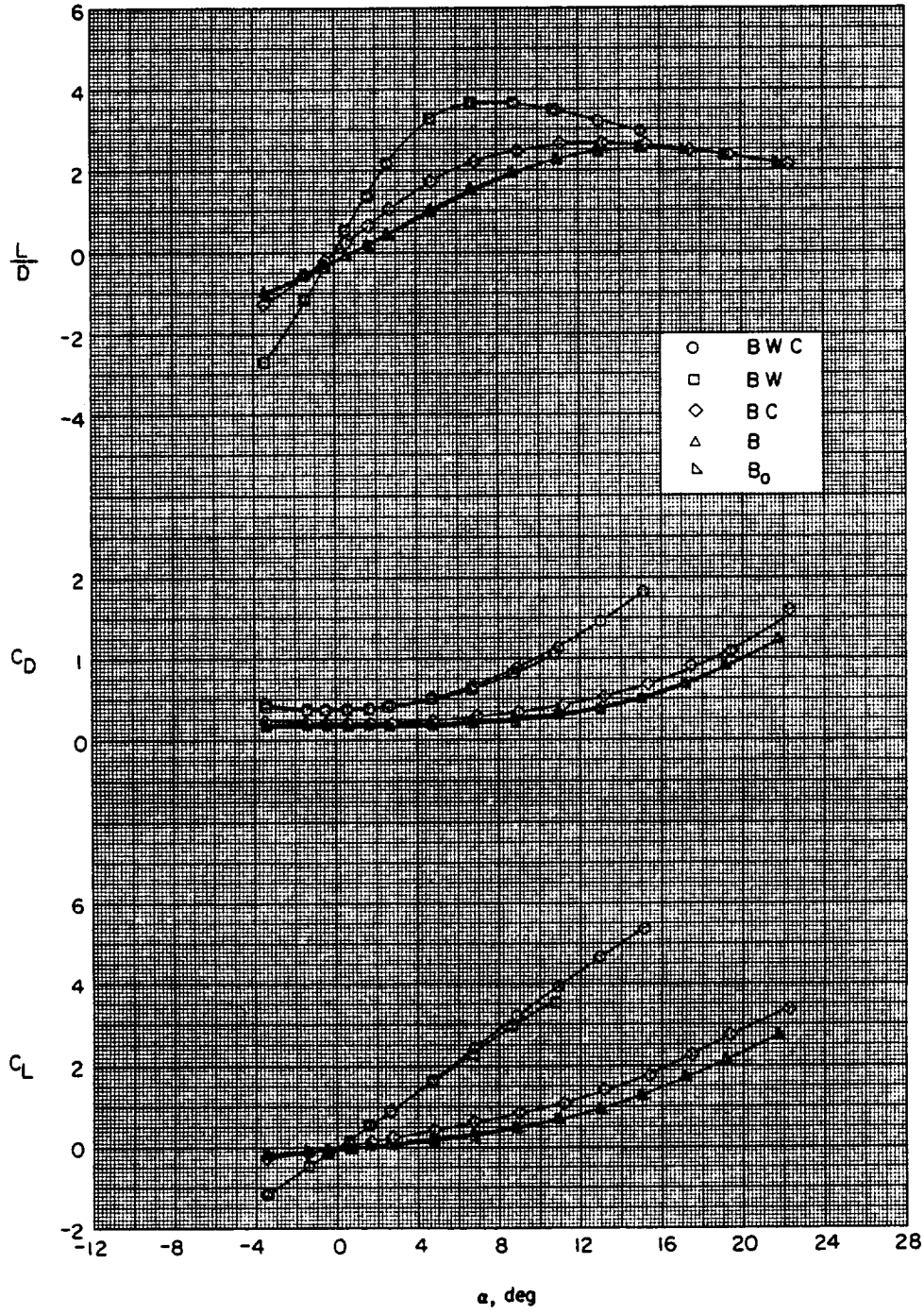

(b) Concluded.

Figure 6.- Continued.

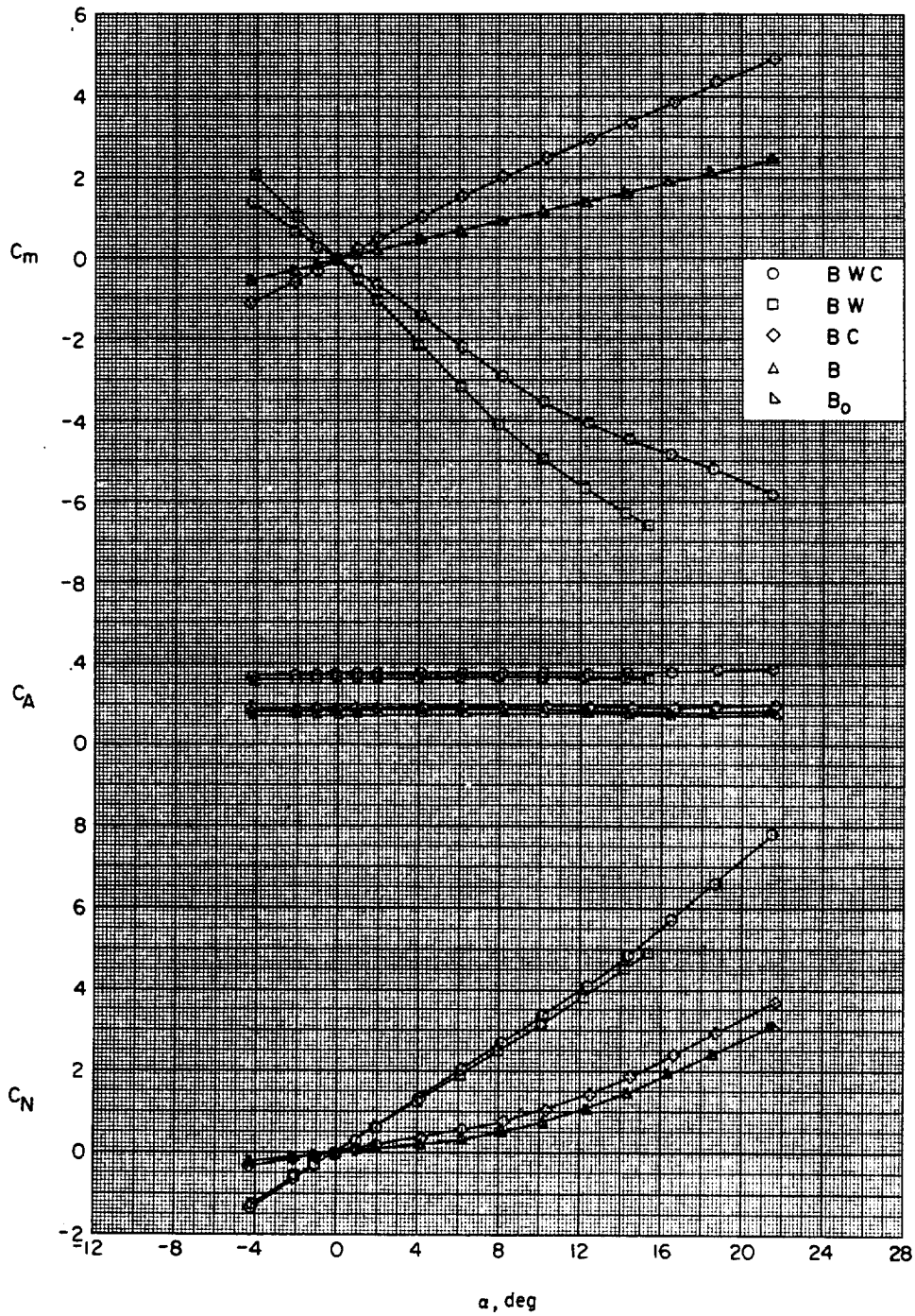

(c) M = 2.30.

Figure 6.- Continued.

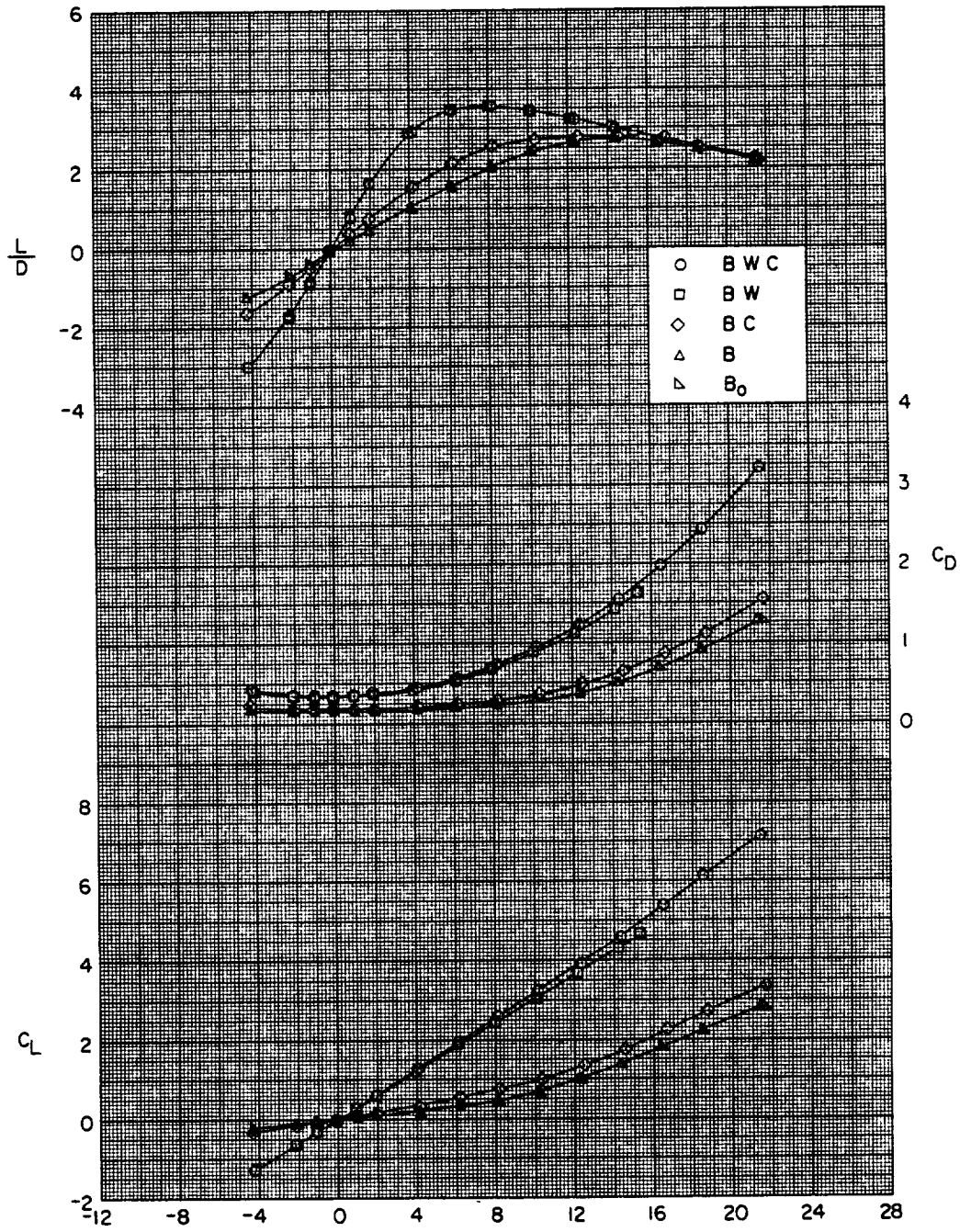

(c) Concluded.

Figure 6.- Continued.

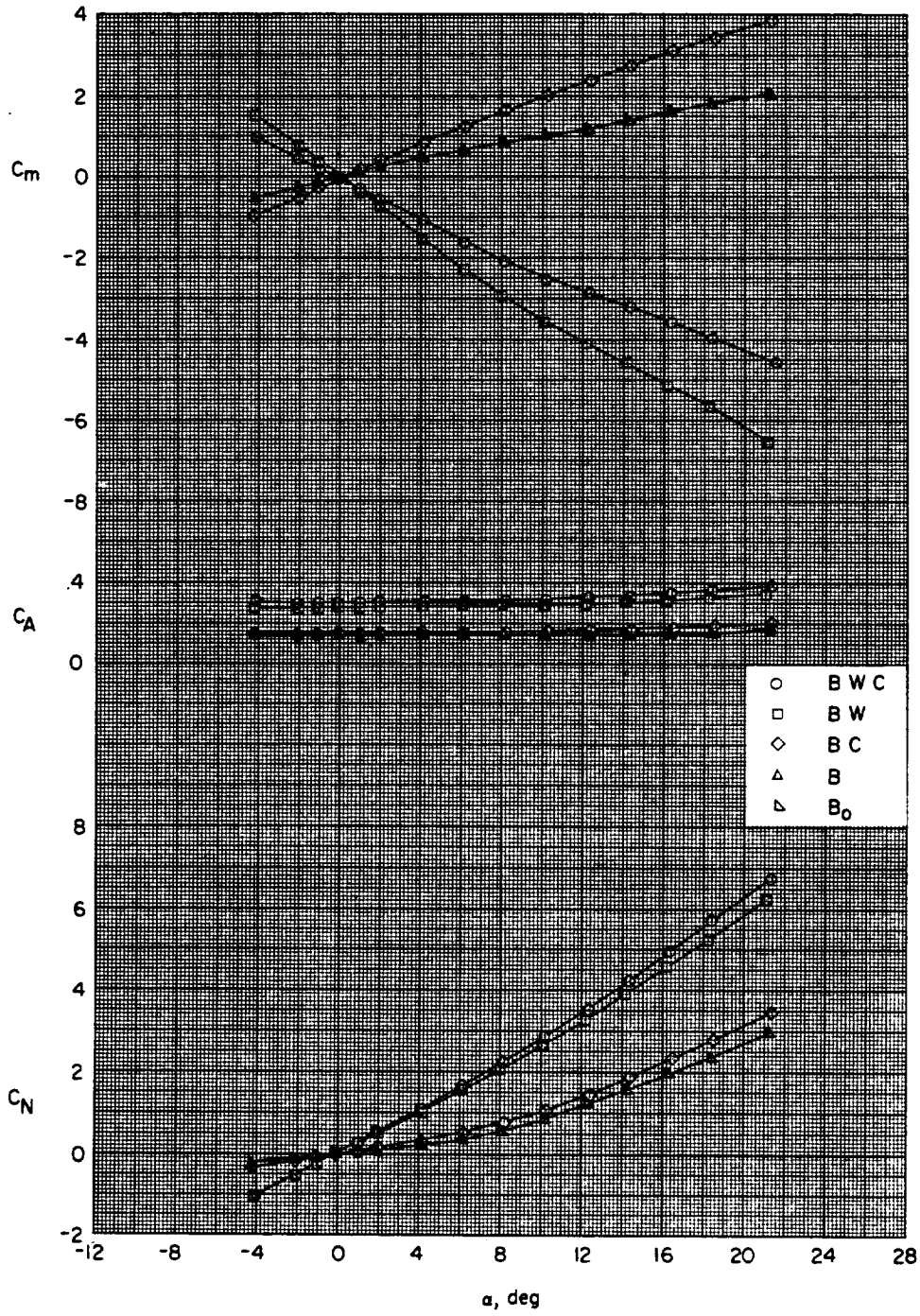

(d) M = 2.96.

Figure 6.- Continued.

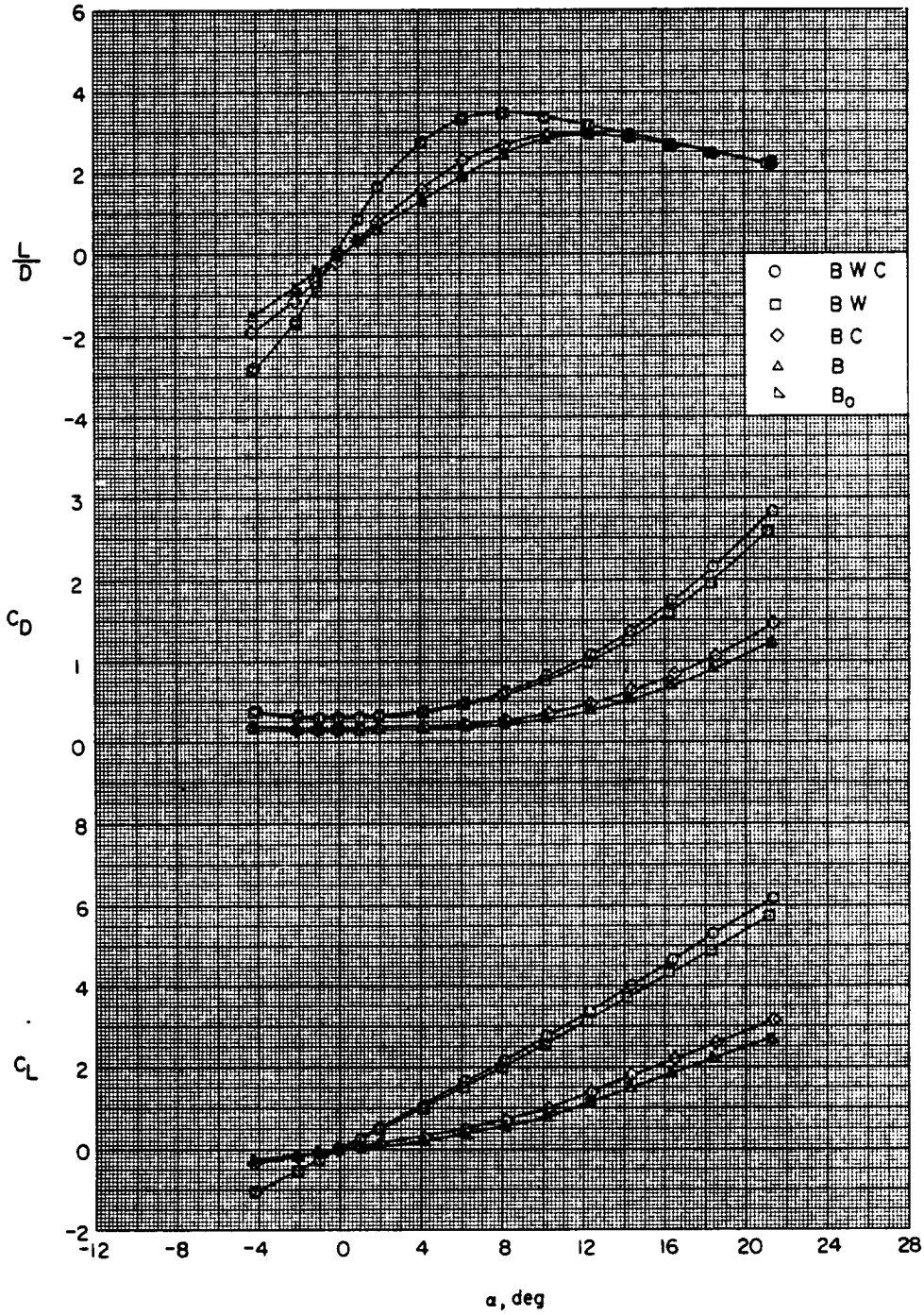

(d) Concluded.

Figure 6.- Continued.

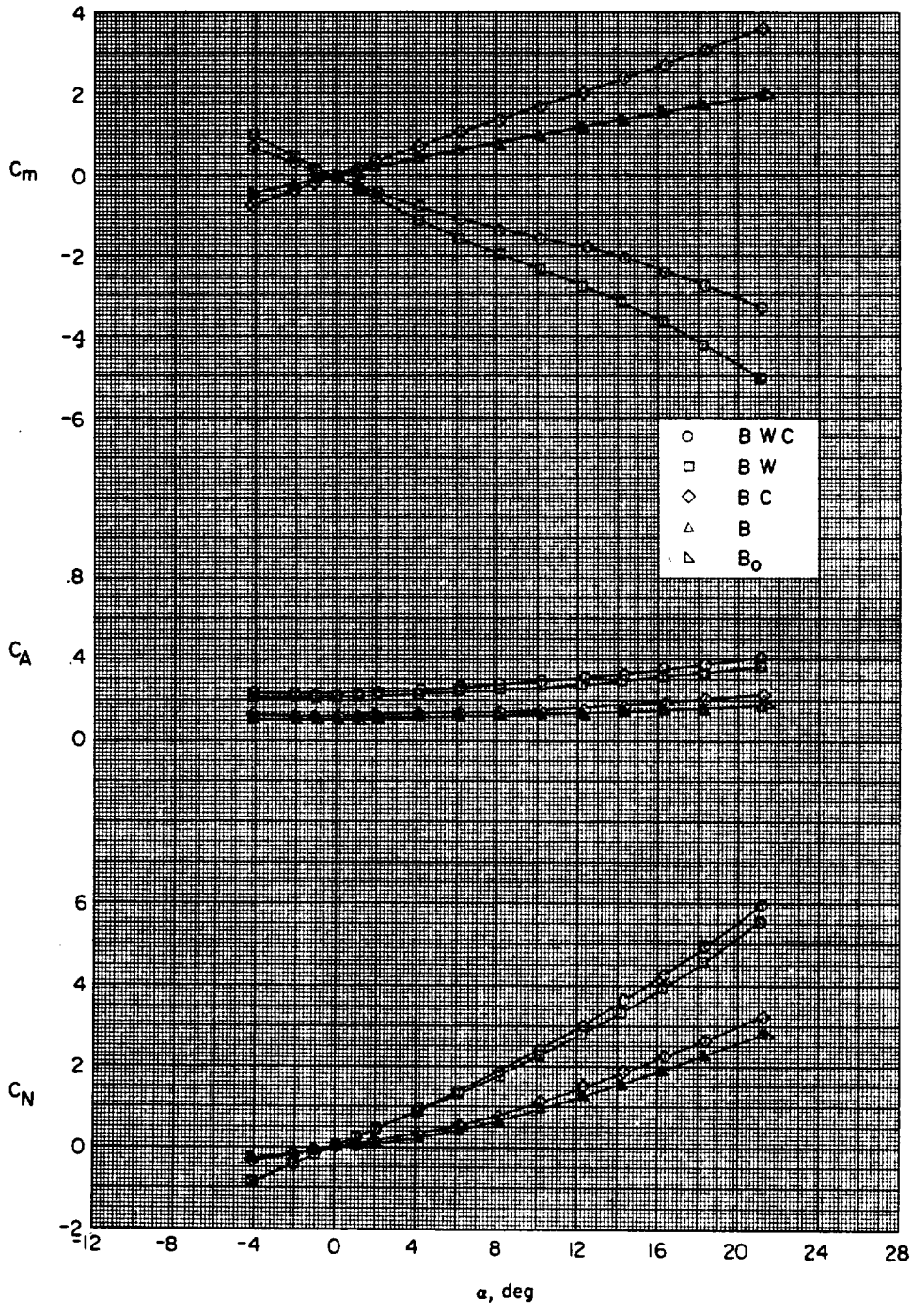

(e) M = 3.95.

Figure 6.- Continued.

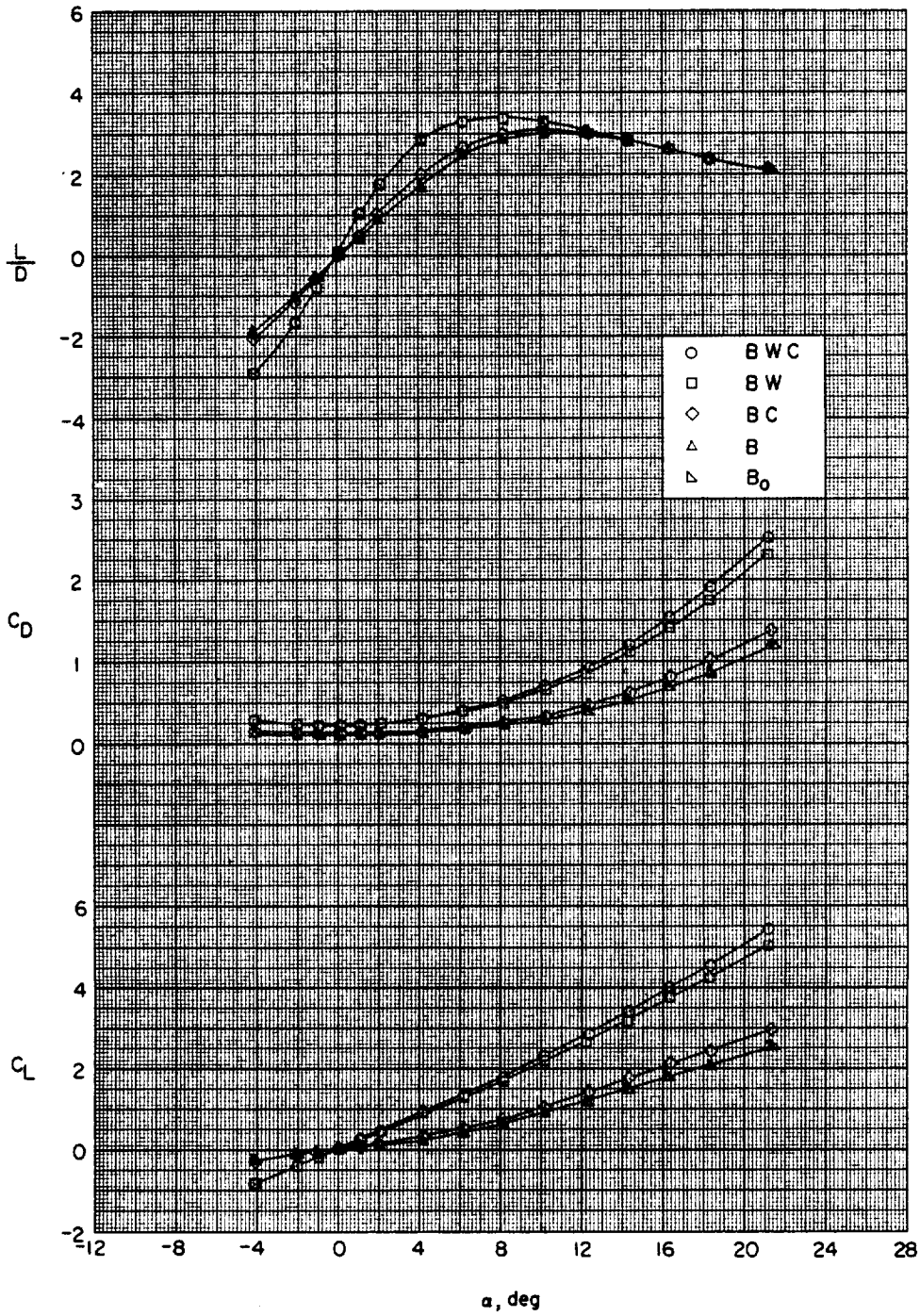

(e) Concluded.

Figure 6.- Continued.

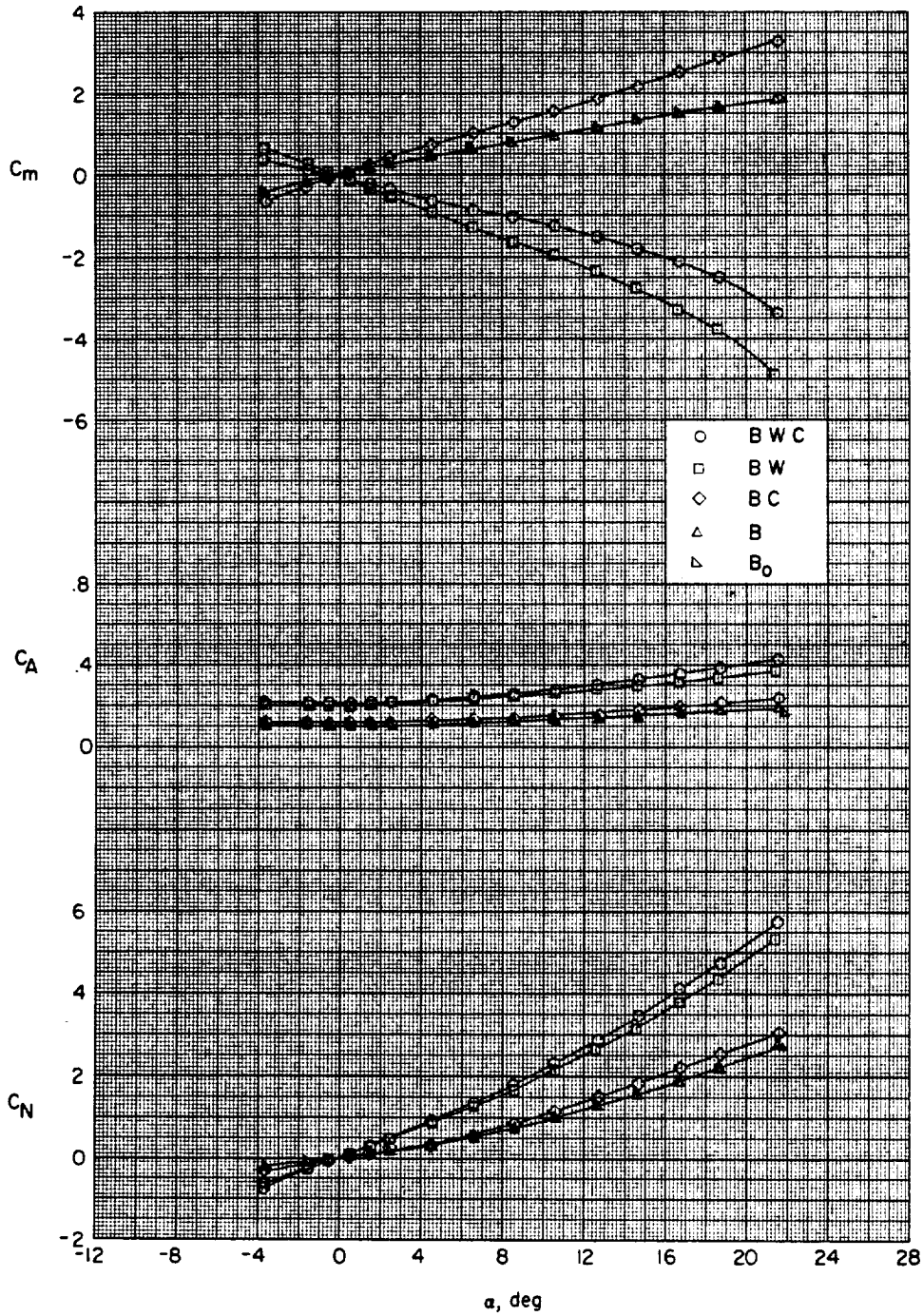

(f) M = 4.63.

Figure 6.- Continued.

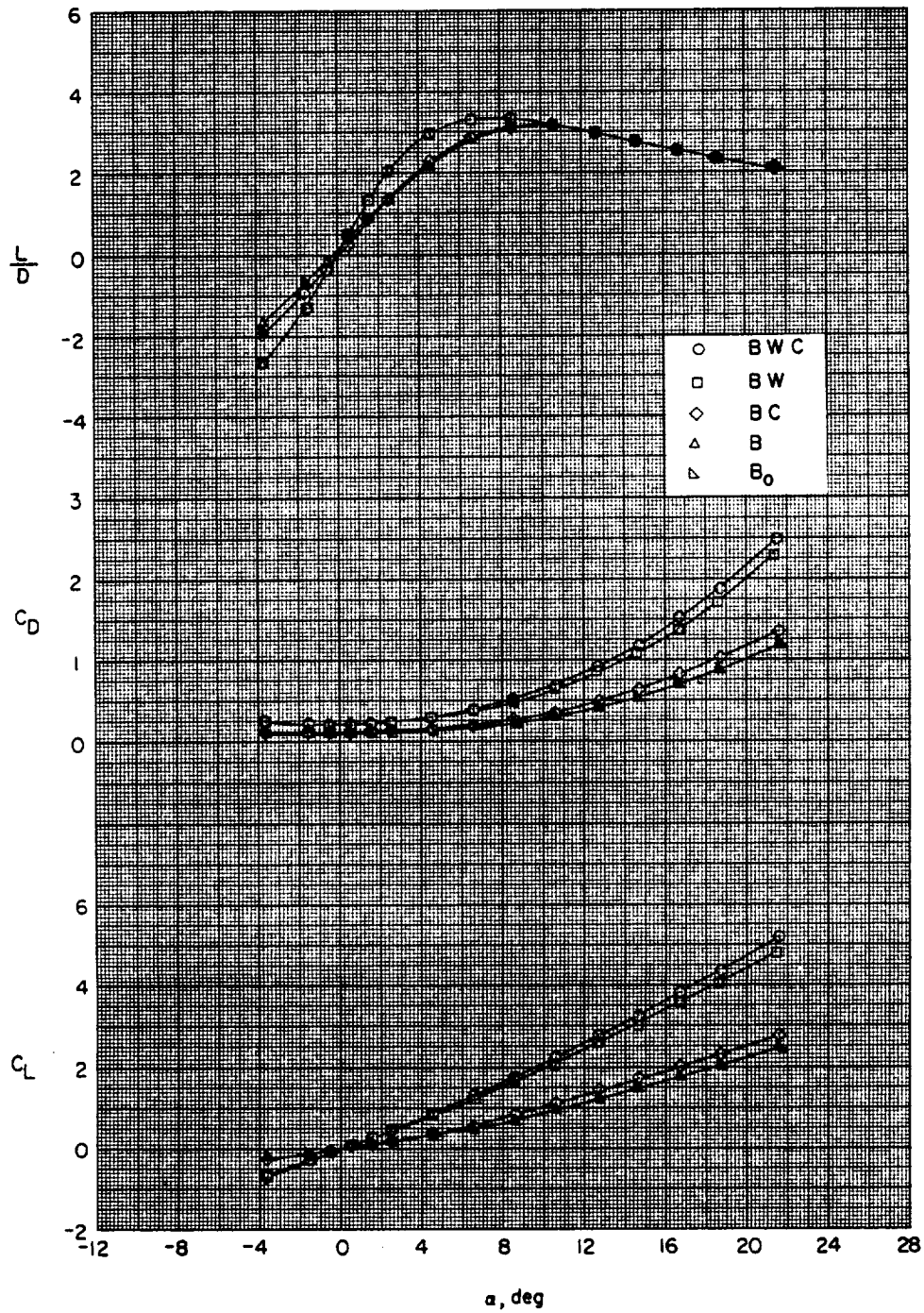

(f) Concluded.

Figure 6.- Concluded.

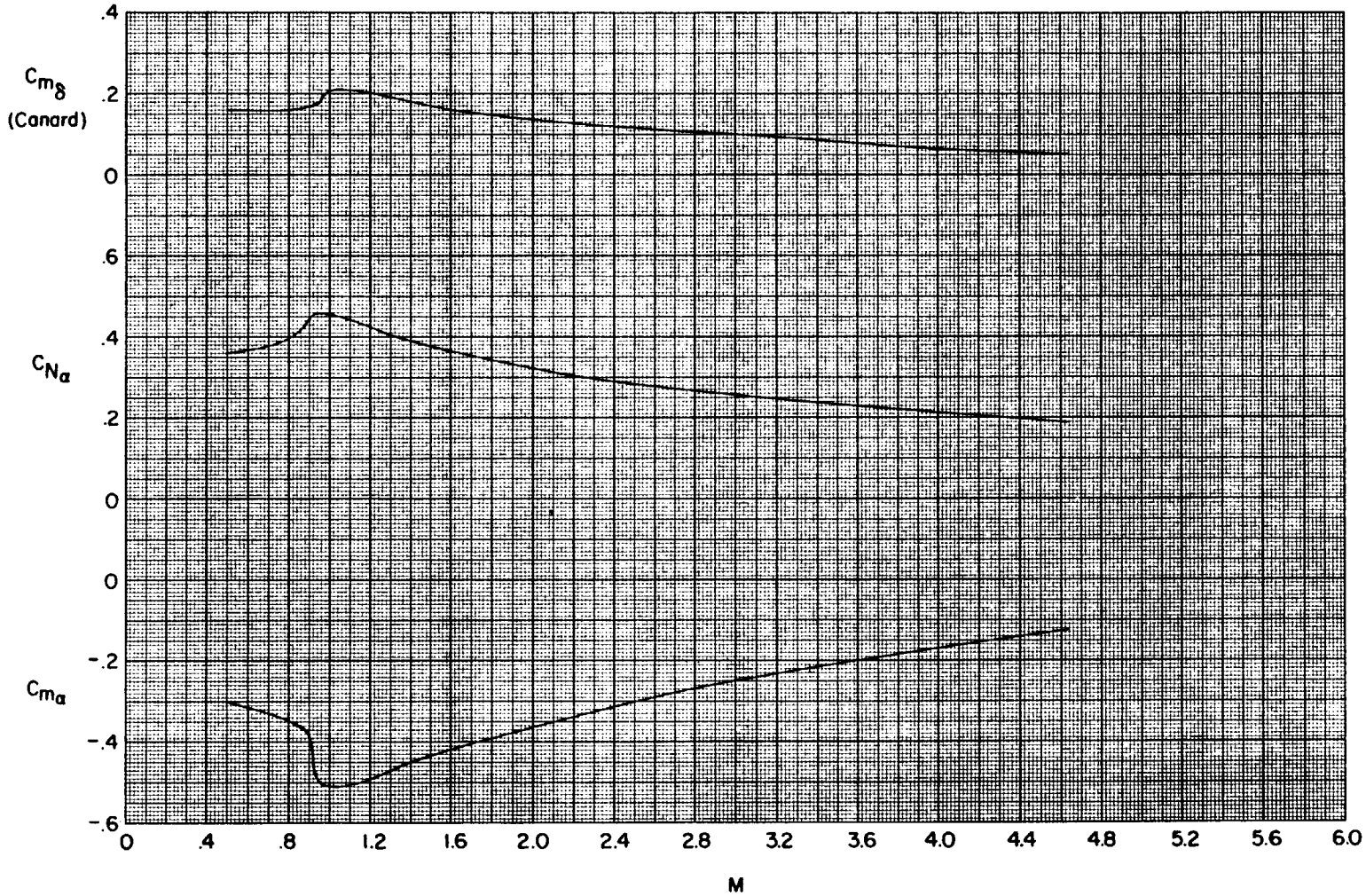

(a) Variation of C_{m_δ}, C_{N_α}, and C_{m_α} with M.

Figure 7.- Summary of the longitudinal aerodynamic characteristics of configuration BWC.

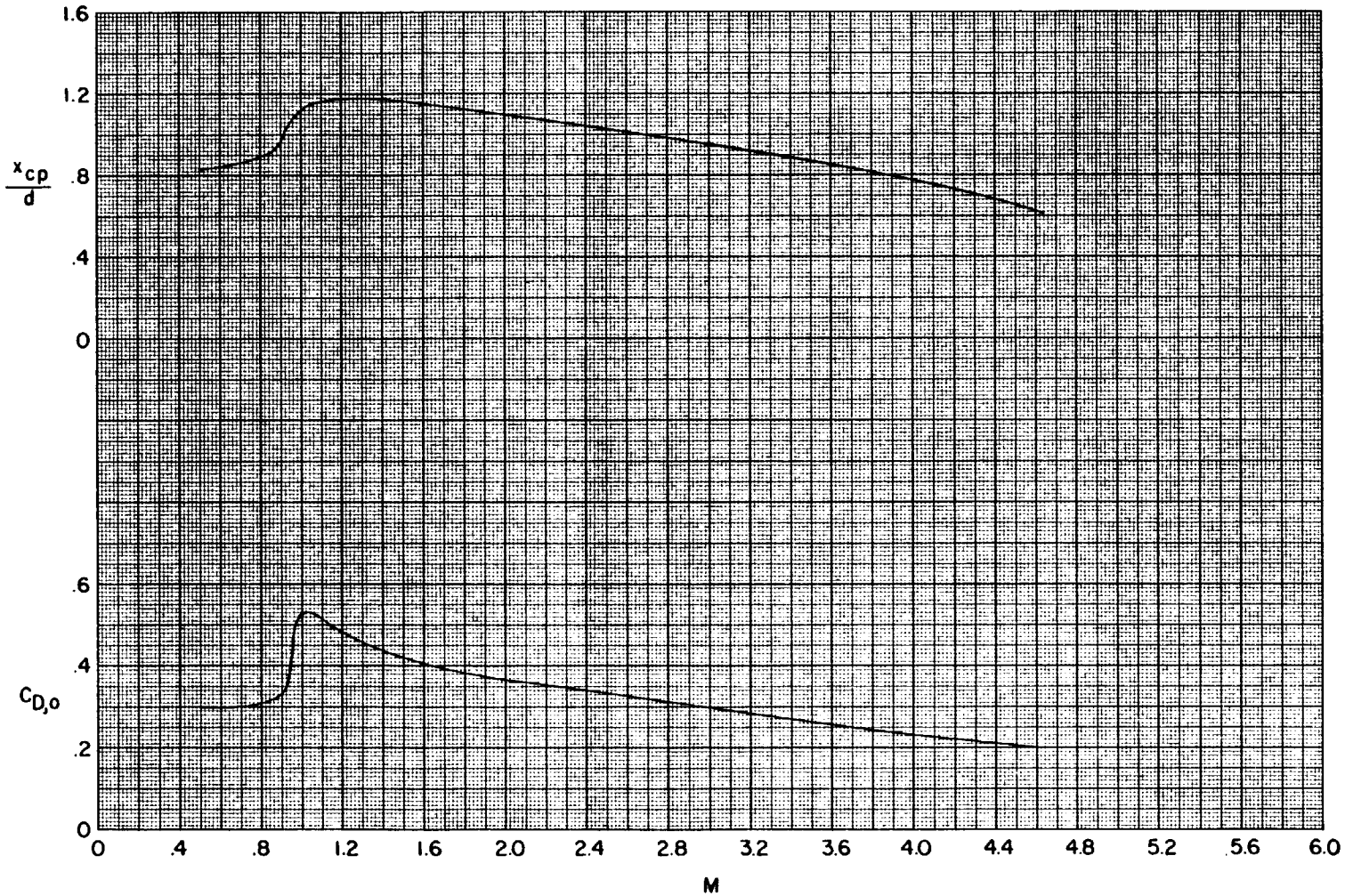

(b) Variation of x_{cp}/d and $C_{D,o}$ with M.

Figure 7.- Concluded.

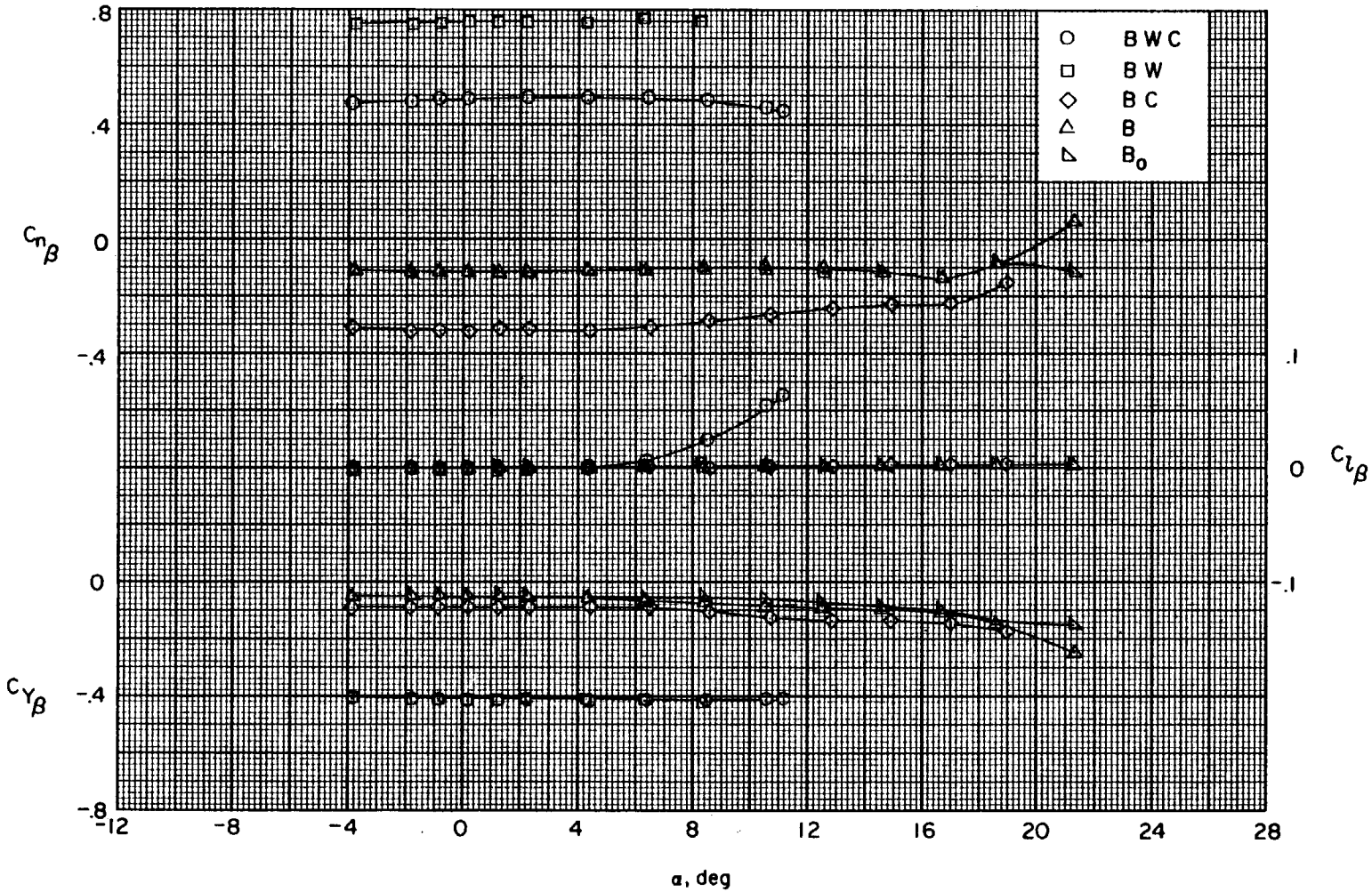

(a) M = 1.50.

Figure 8.- Effect of component parts on the sideslip derivatives.

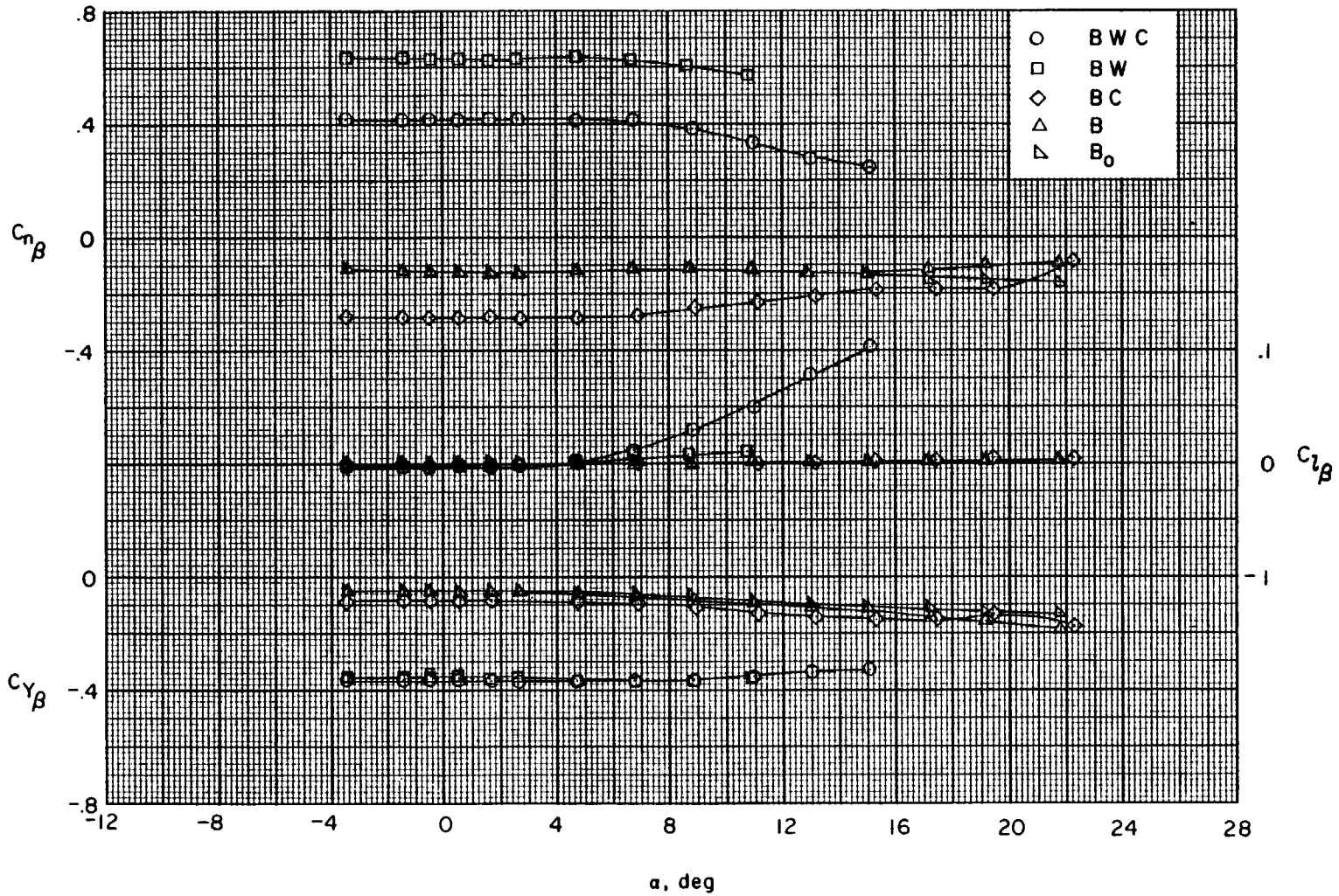

(b) M = 1.90.

Figure 8.- Continued.

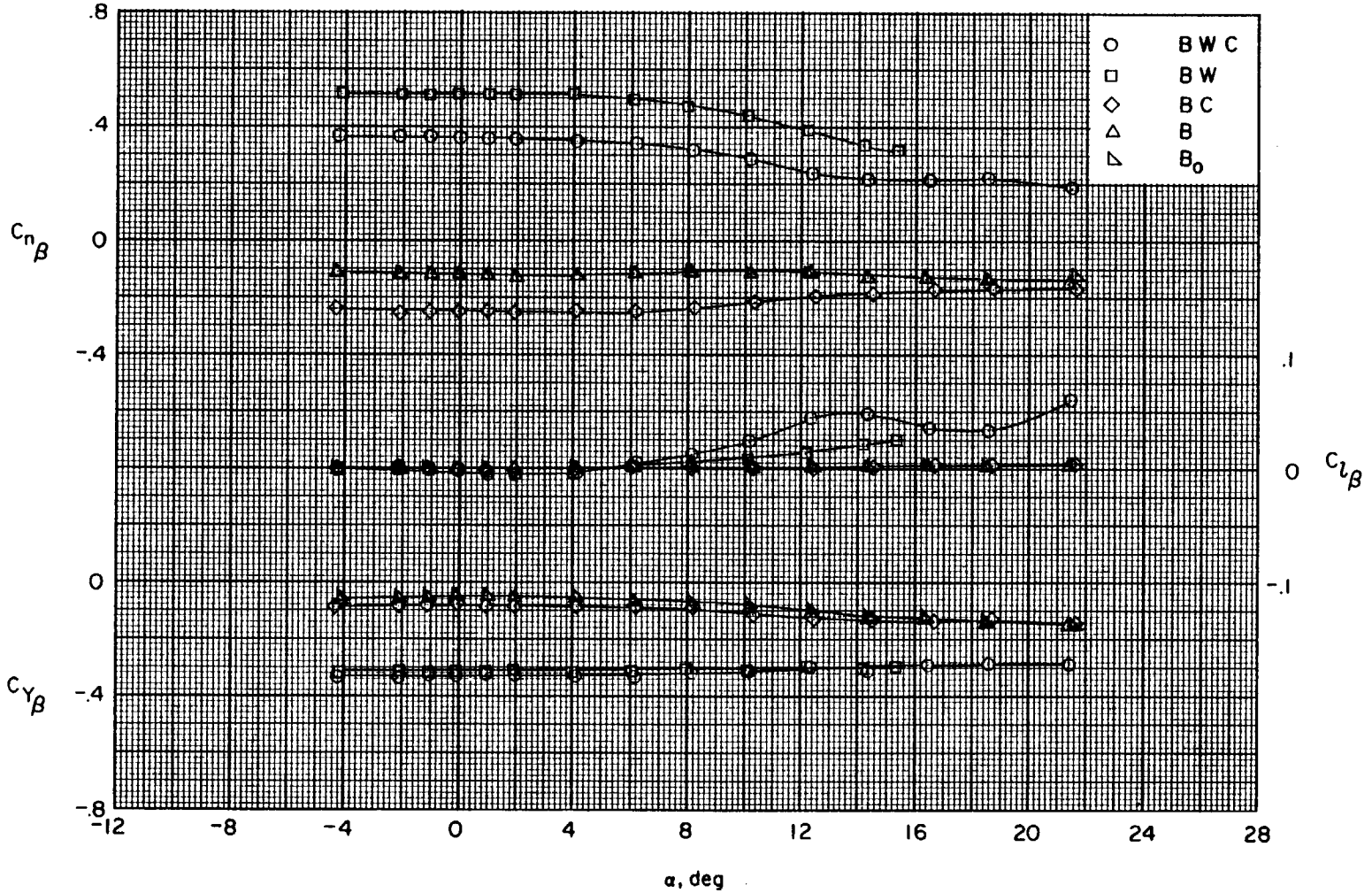

(c) M = 2.30.

Figure 8.- Continued.

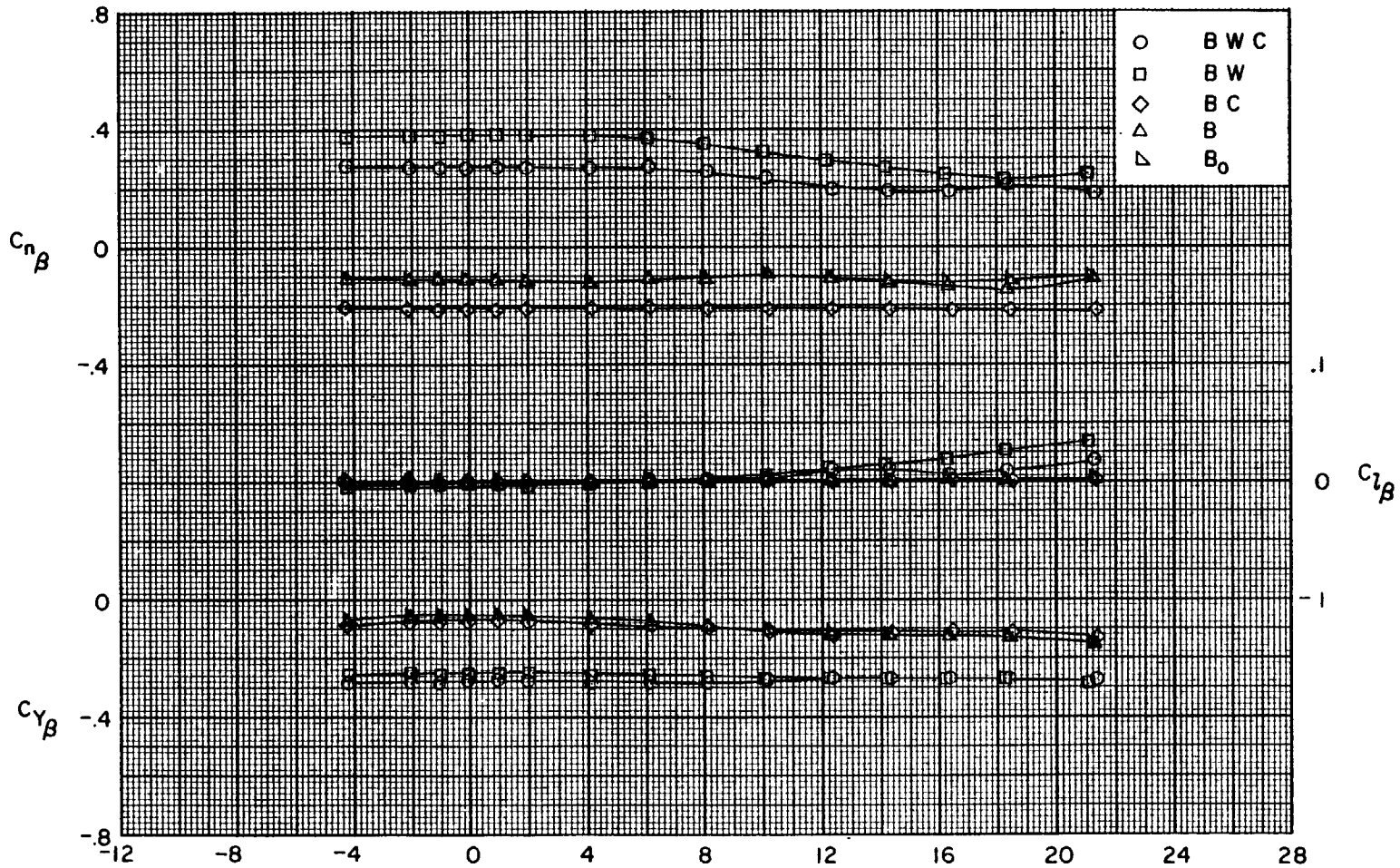

(d) M = 2.96.

Figure 8.- Continued.

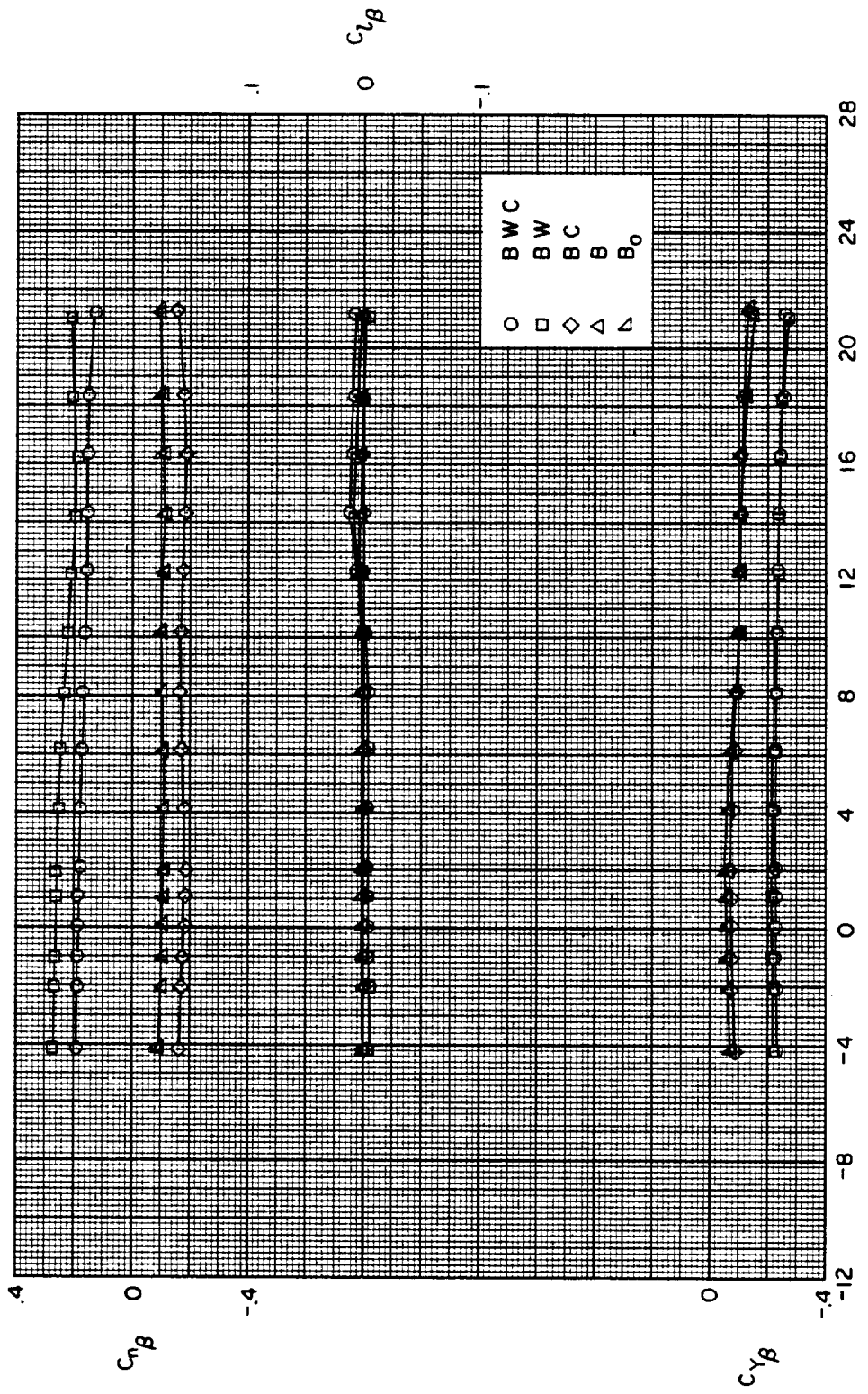

(e) M = 3.95.

Figure 8.- Continued.

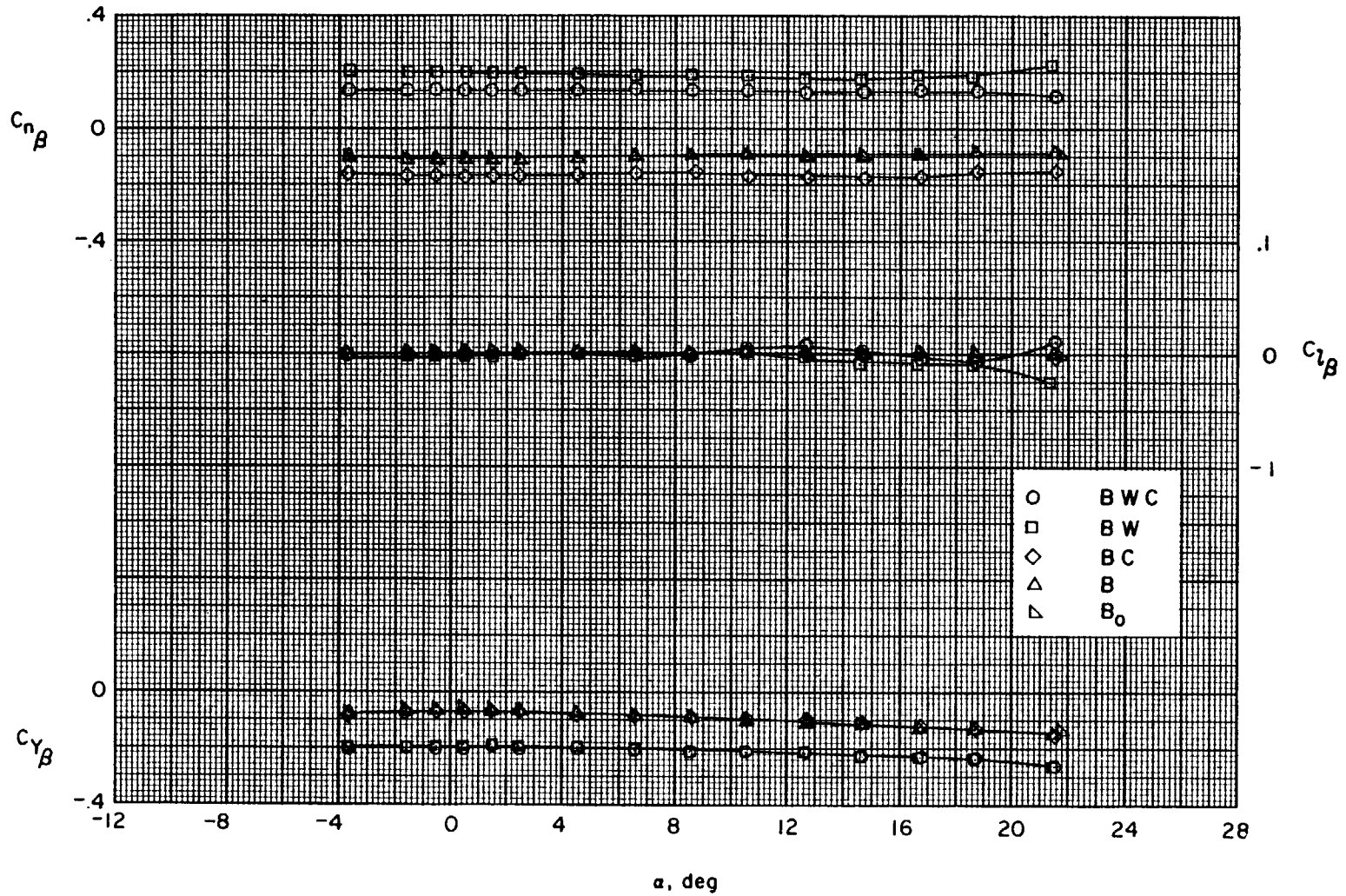

(f) M = 4.63.

Figure 8.- Concluded.

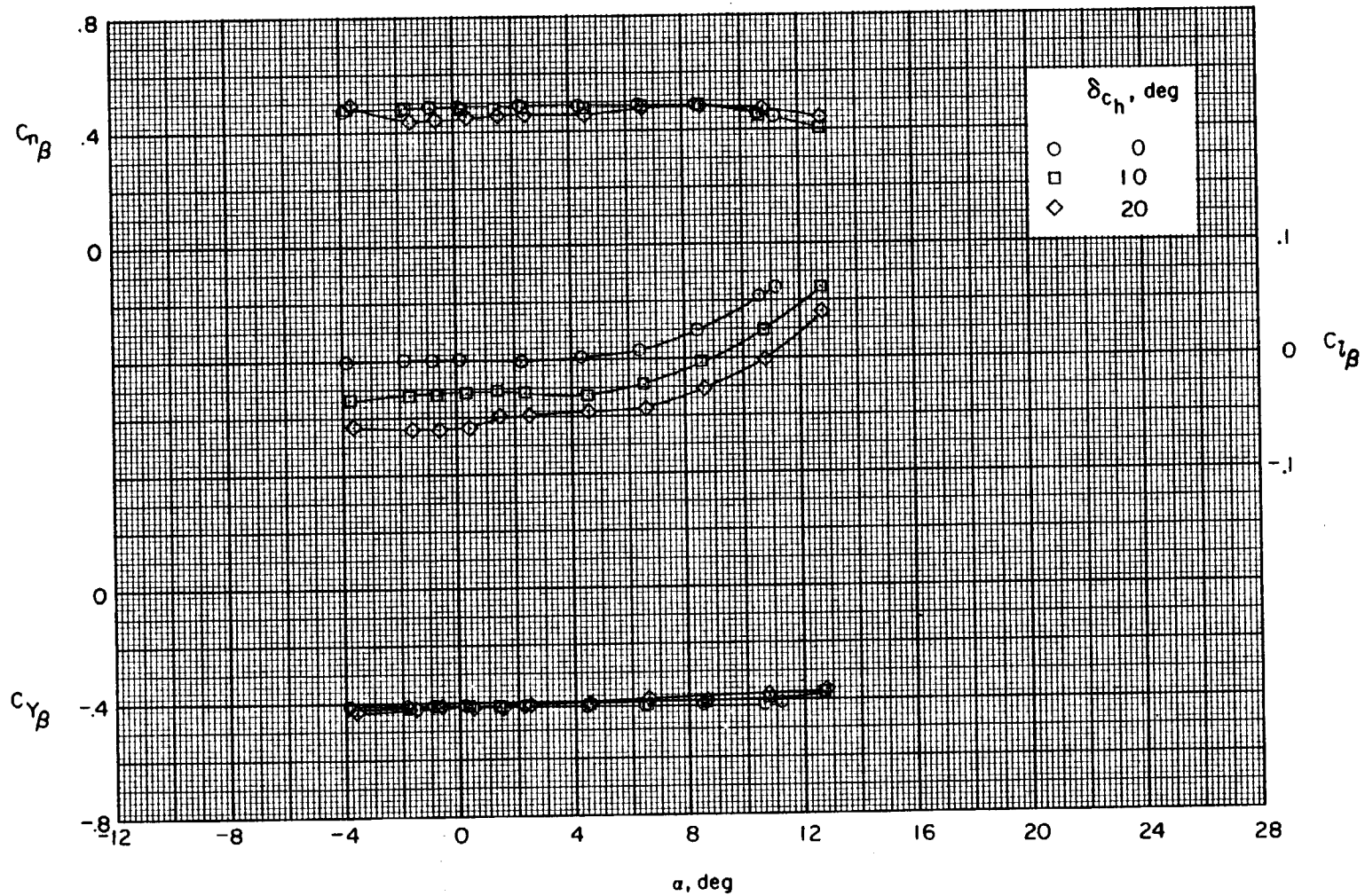

(a) M = 1.50.

Figure 9.- Effect of horizontal-canard deflection on the sideslip derivatives of configuration BWC. $\delta_f = 0^0$; $\delta_{c_v} = 0^0$.

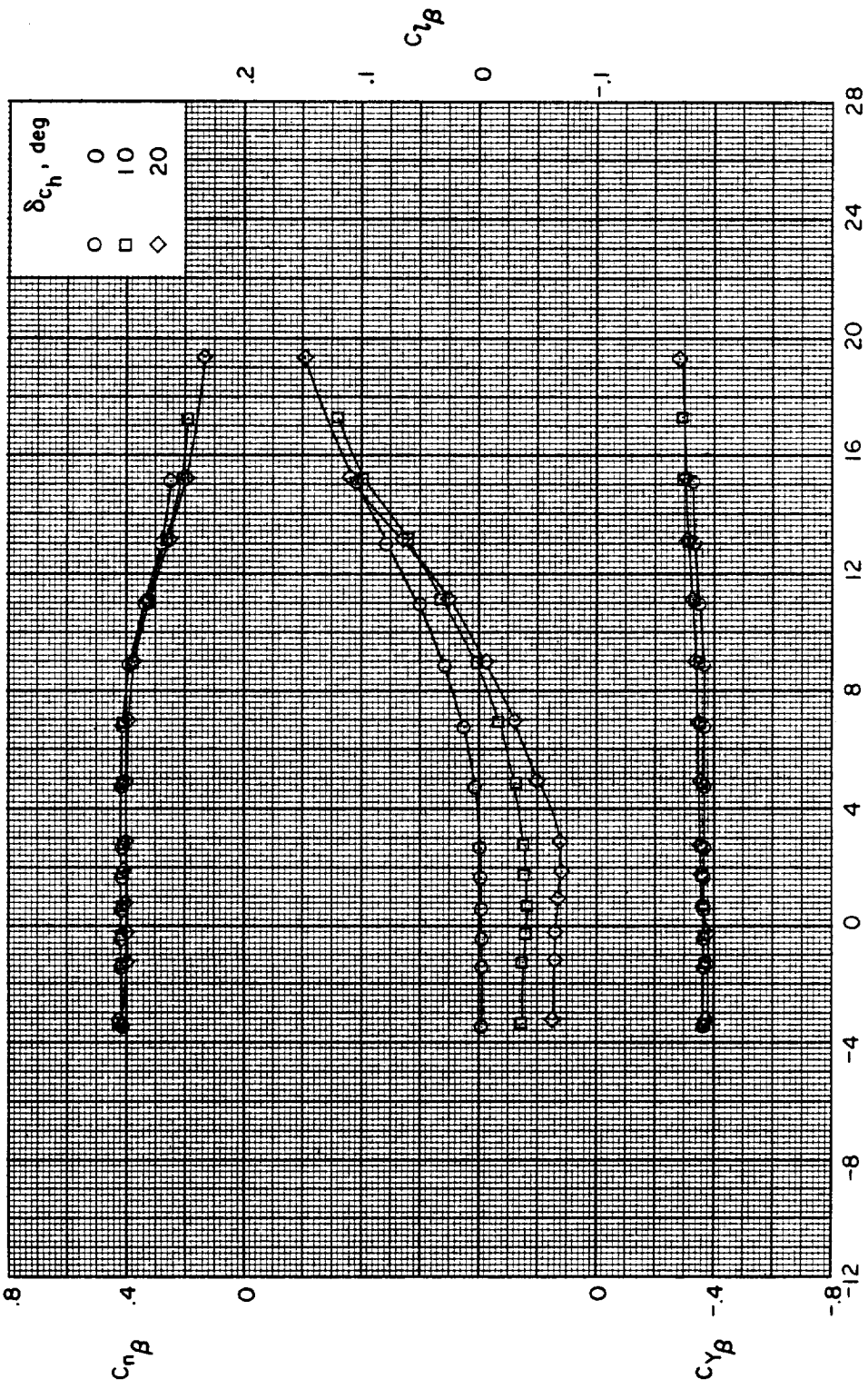

(b) M = 1.90.

Figure 9.- Continued.

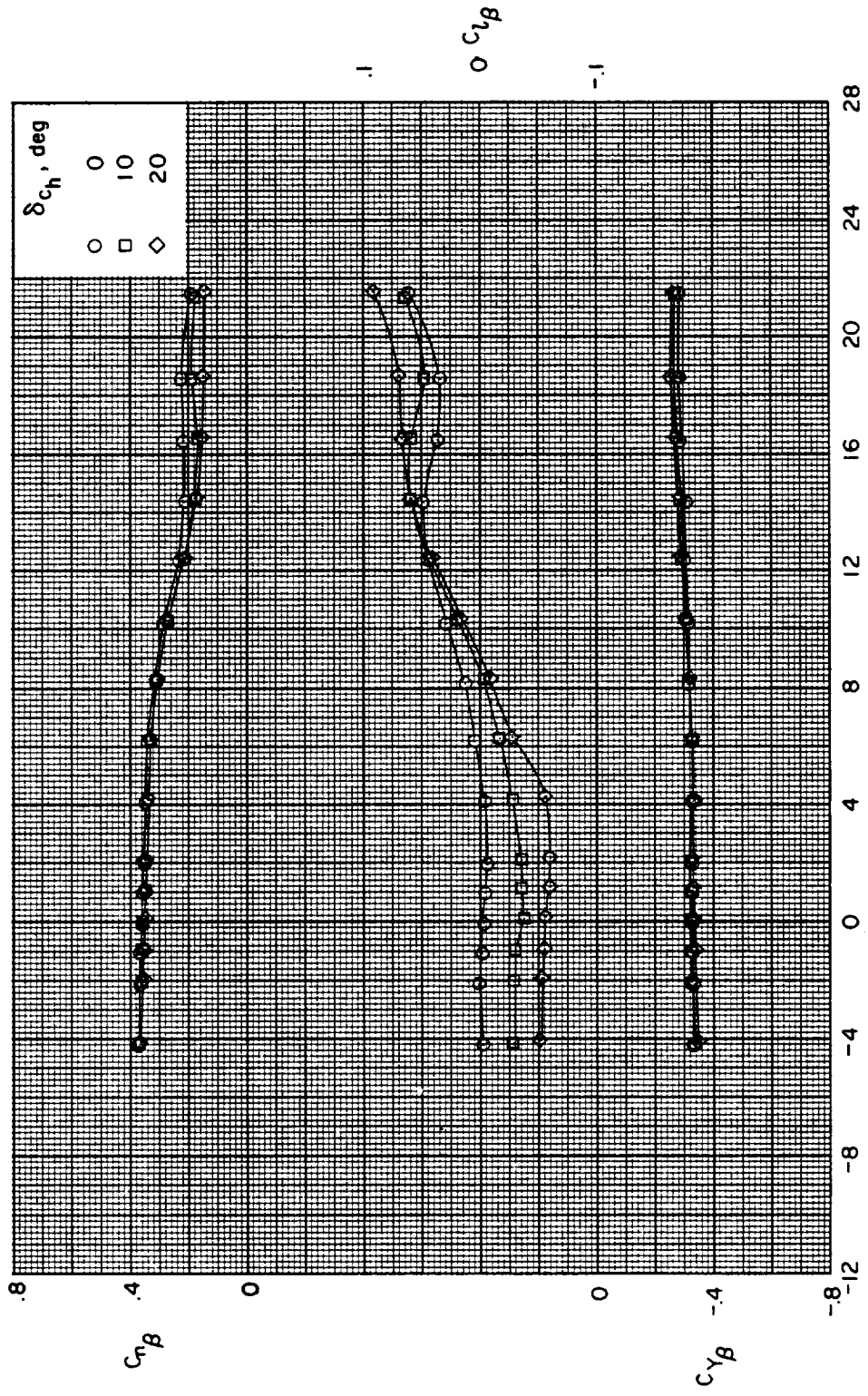

(c) M = 2.30.

Figure 9.- Continued.

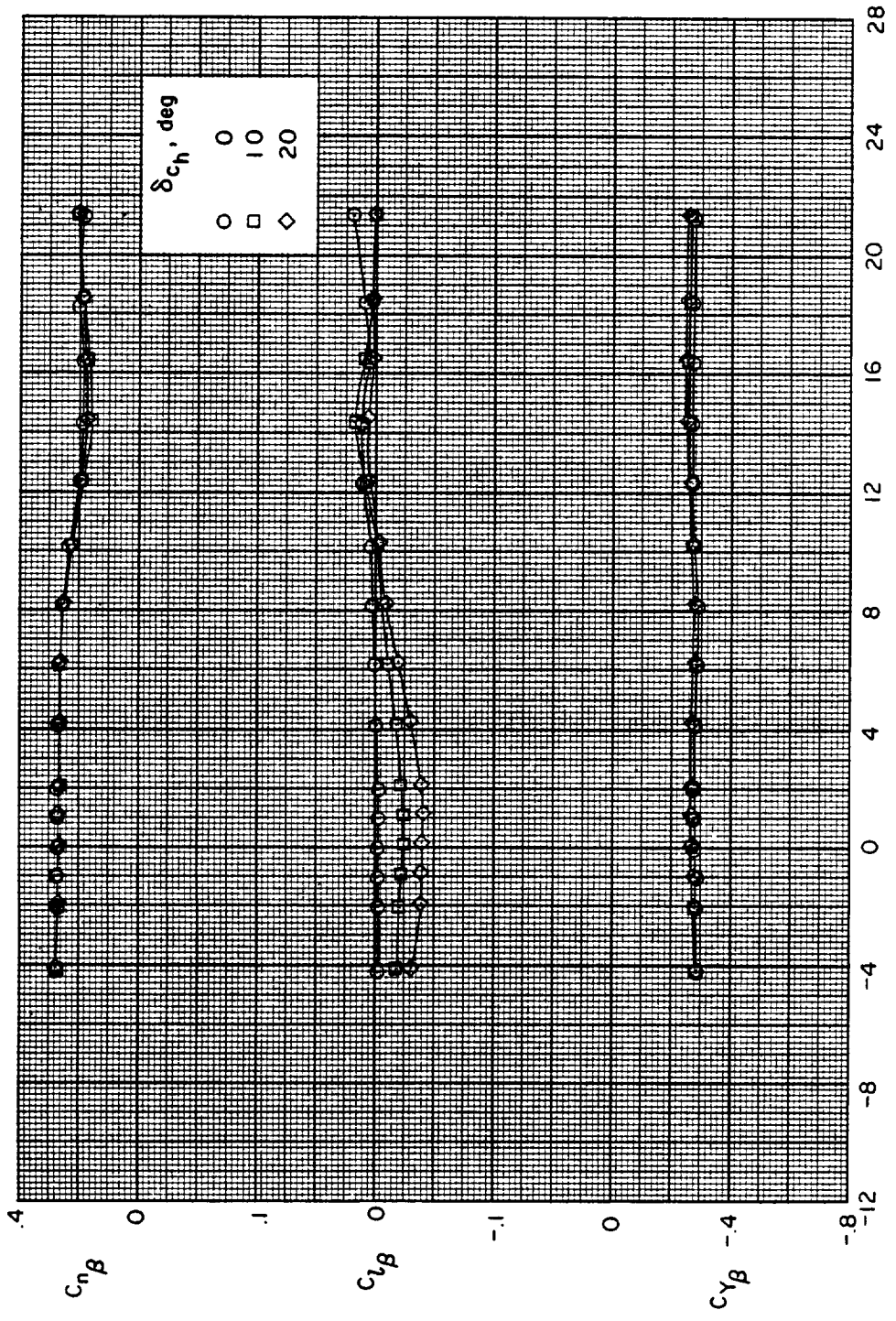

(d) M = 2.96.

Figure 9.- Continued.

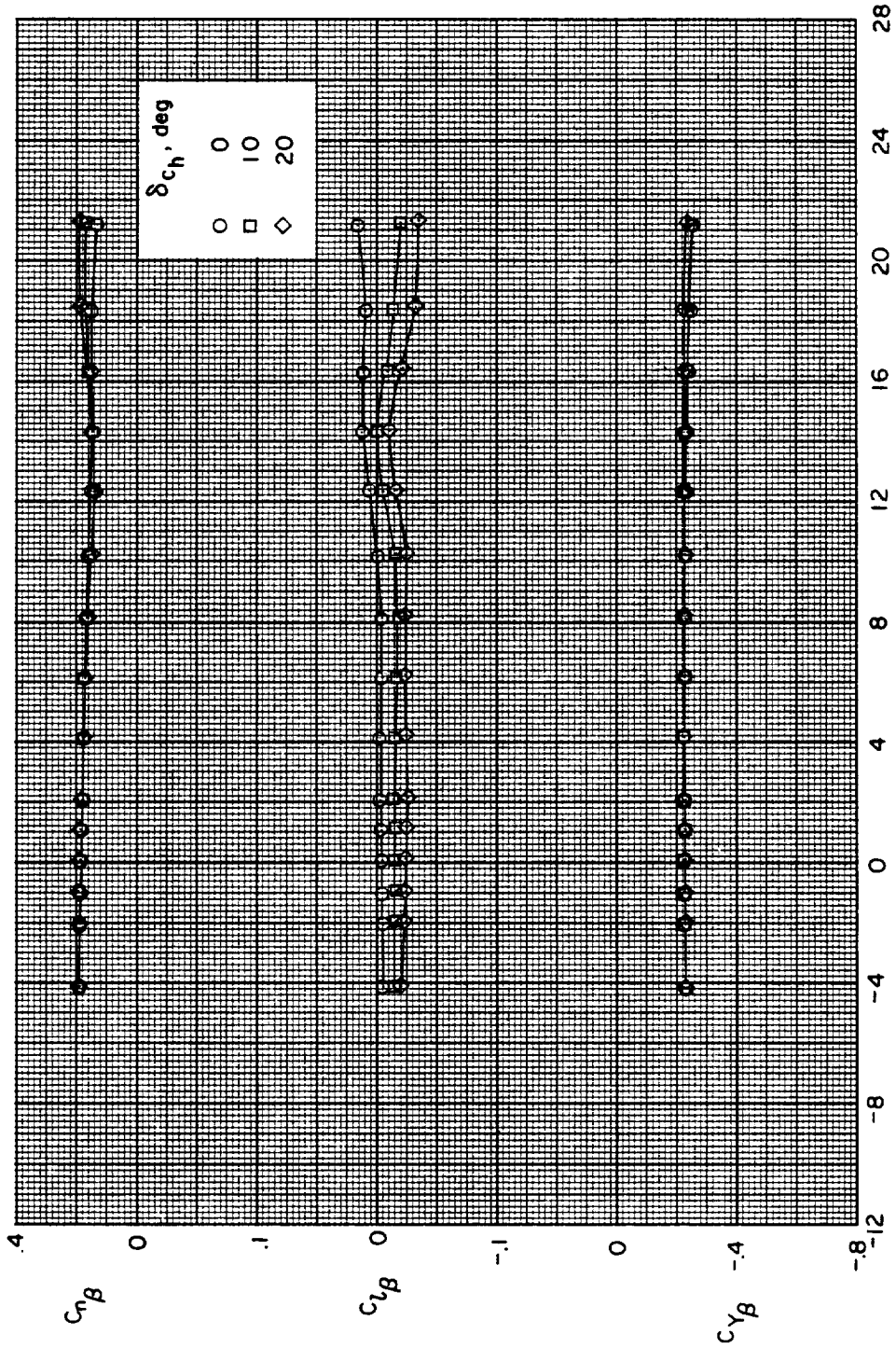

(e) M = 3.95.

Figure 9.- Continued.

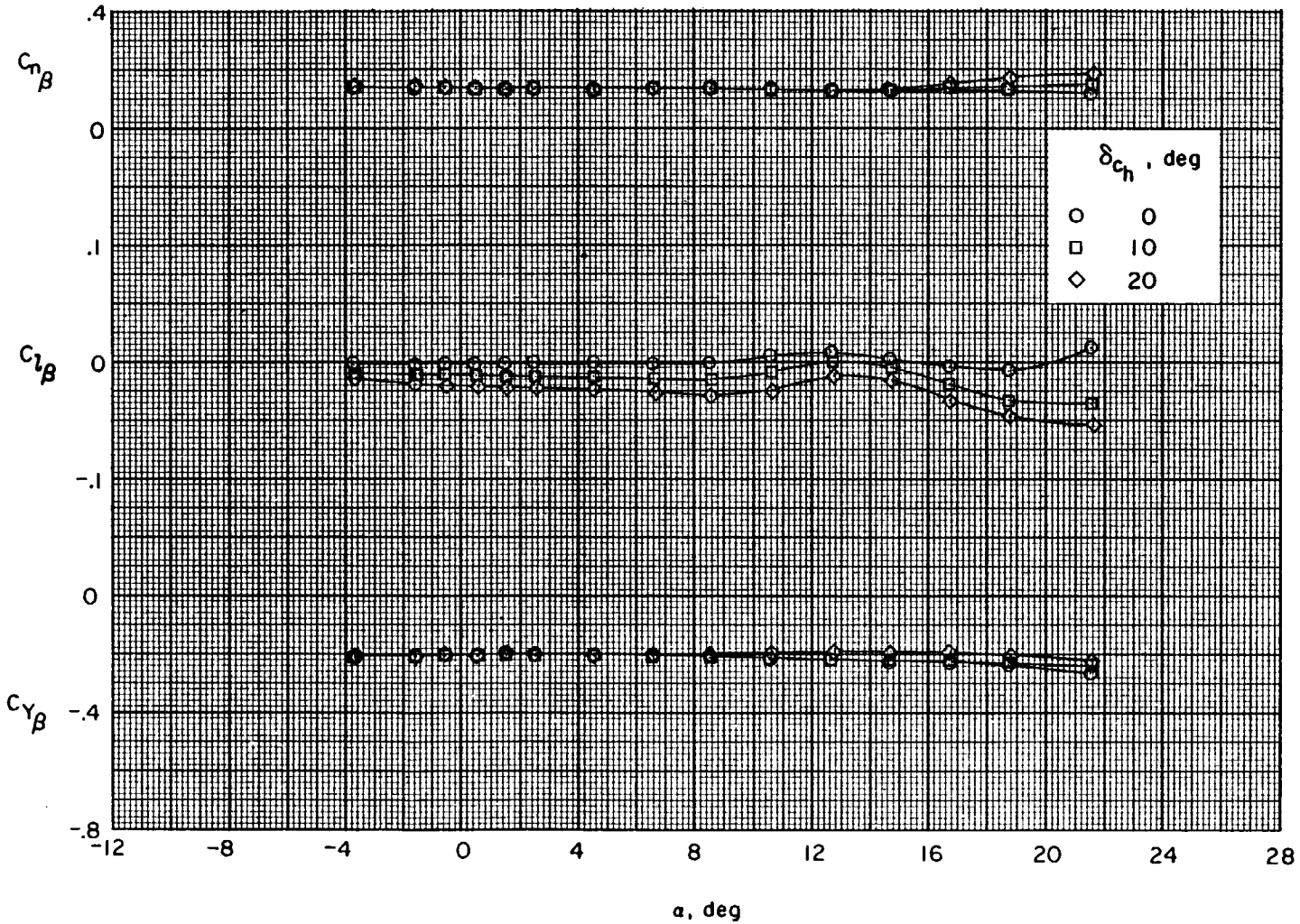

(f) M = 4.63.

Figure 9.- Concluded.

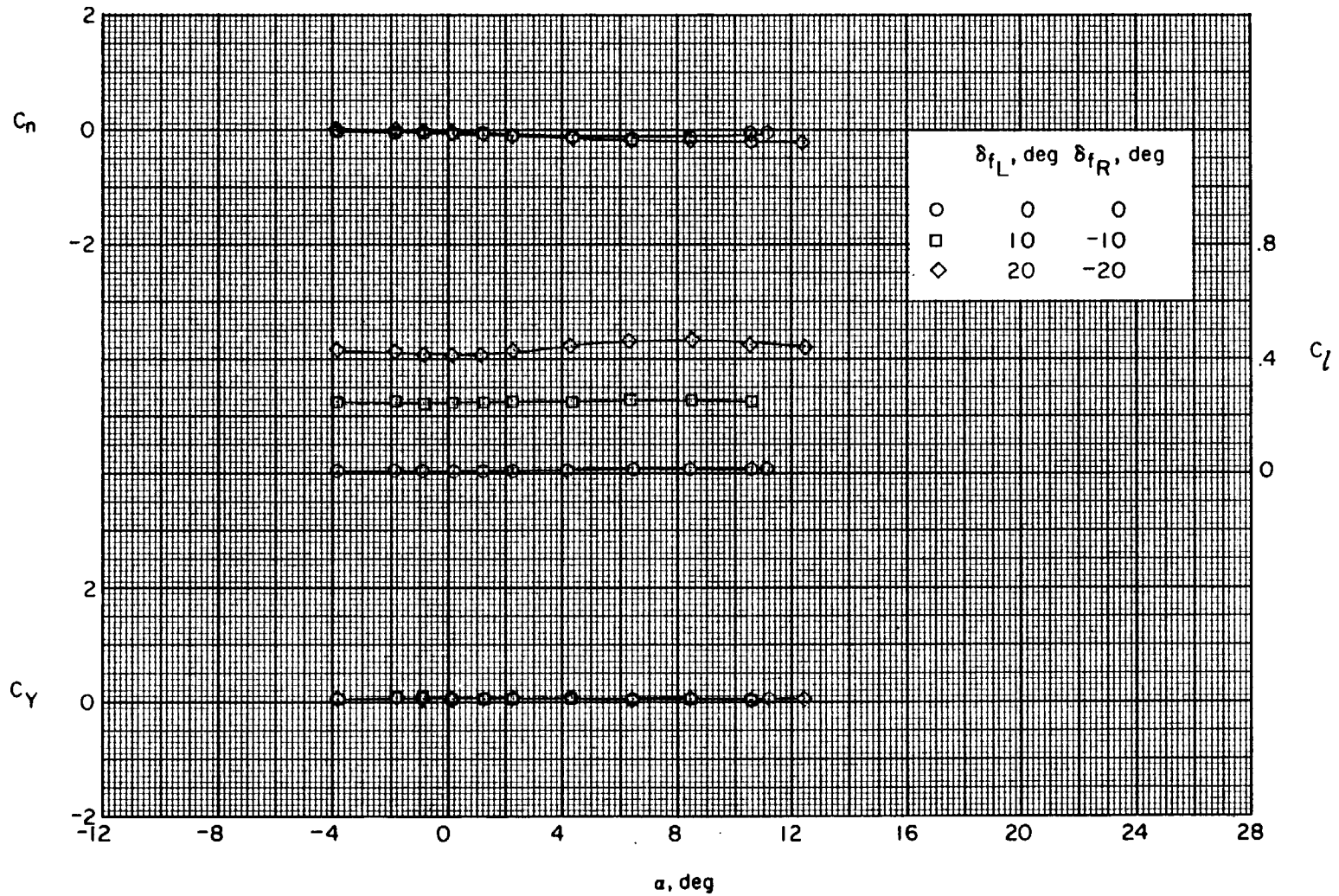

(a) M = 1.50.

Figure 10.- Effect of wing-flap deflection on the lateral control characteristics of configuration BWC with $\delta_{c_h} = 0^0$. $\delta_{c_v} = 0^0$.

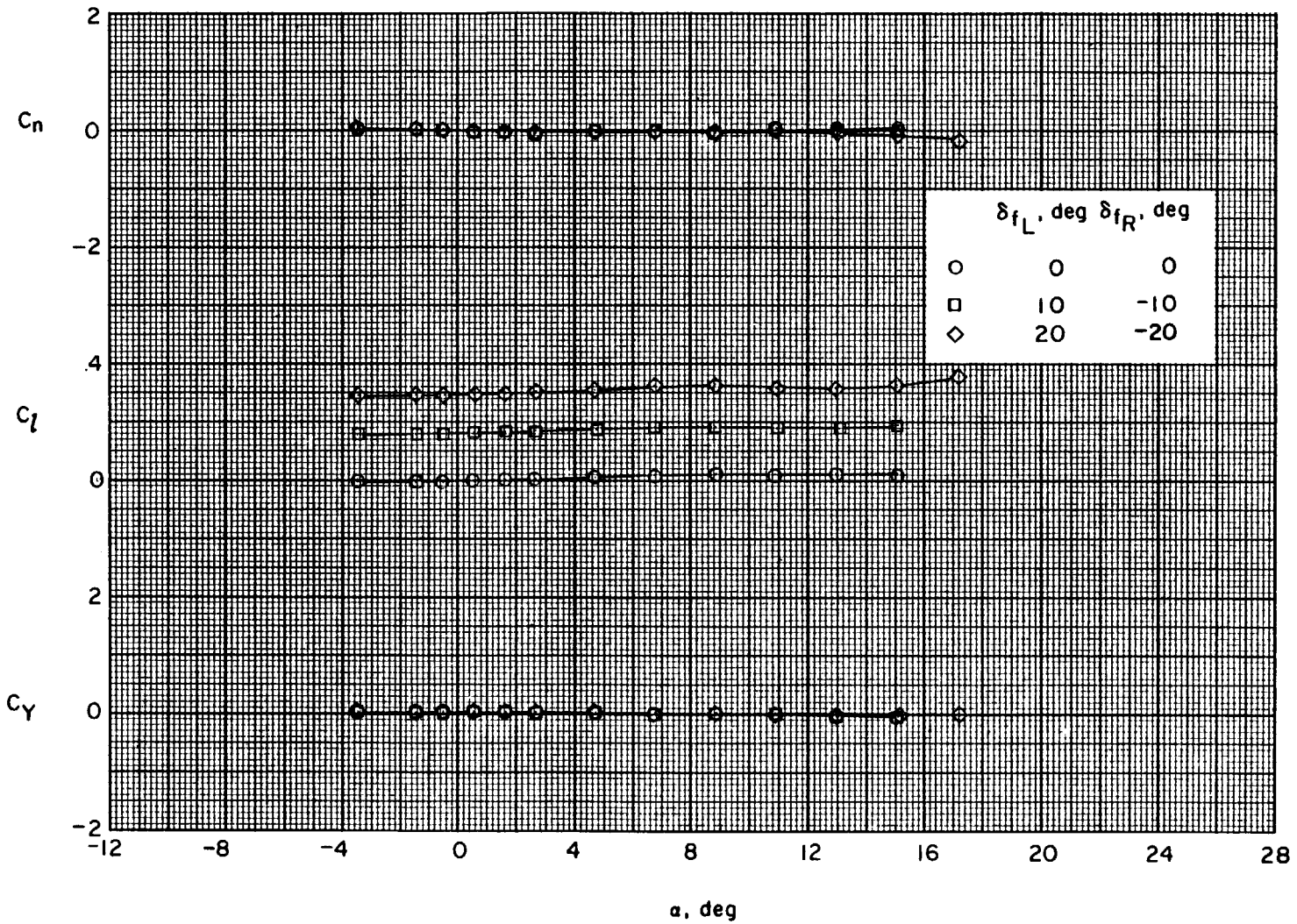

(b) M = 1.90.

Figure 10.- Continued.

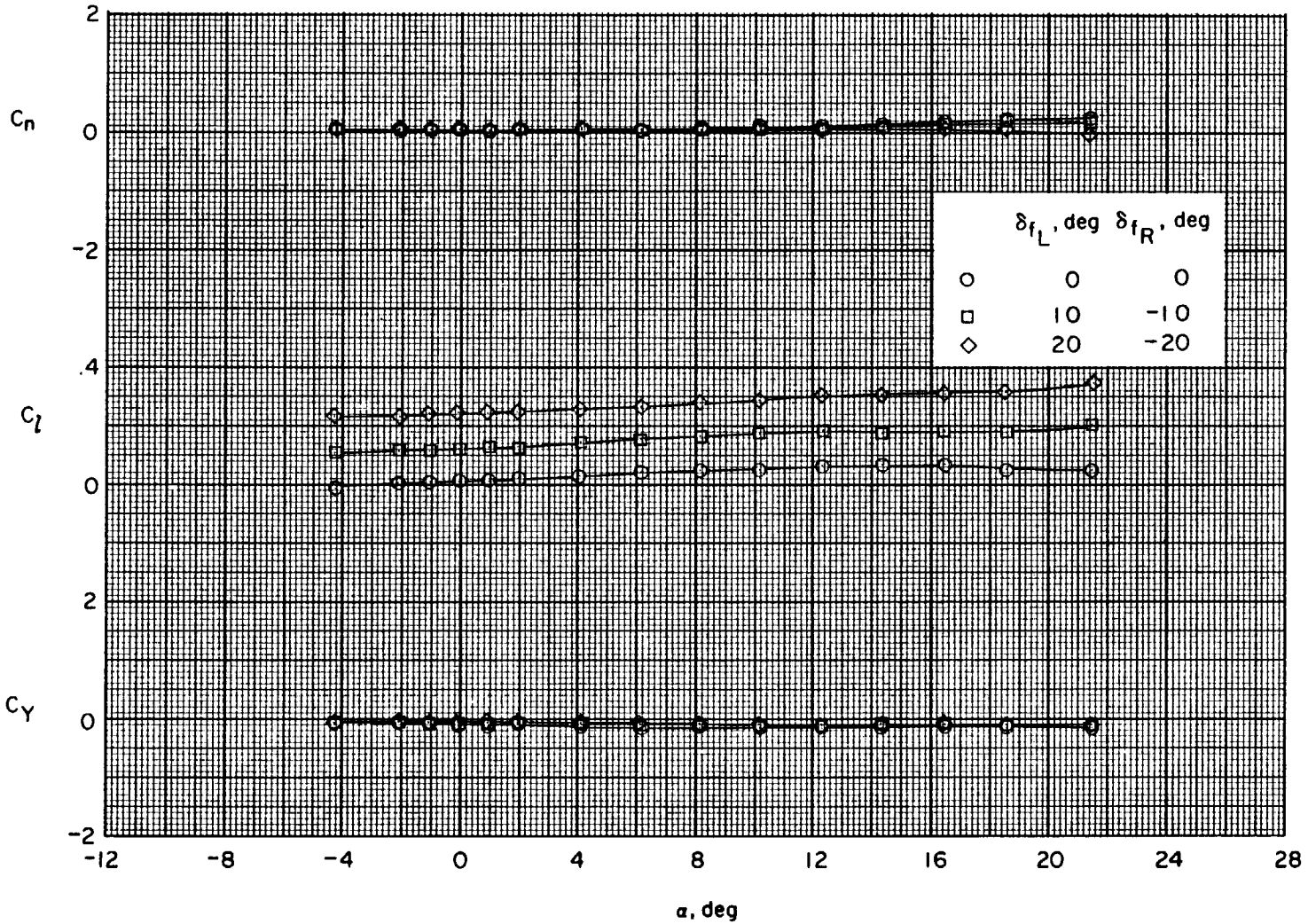

(c) M = 2.30.

Figure 10.- Continued.

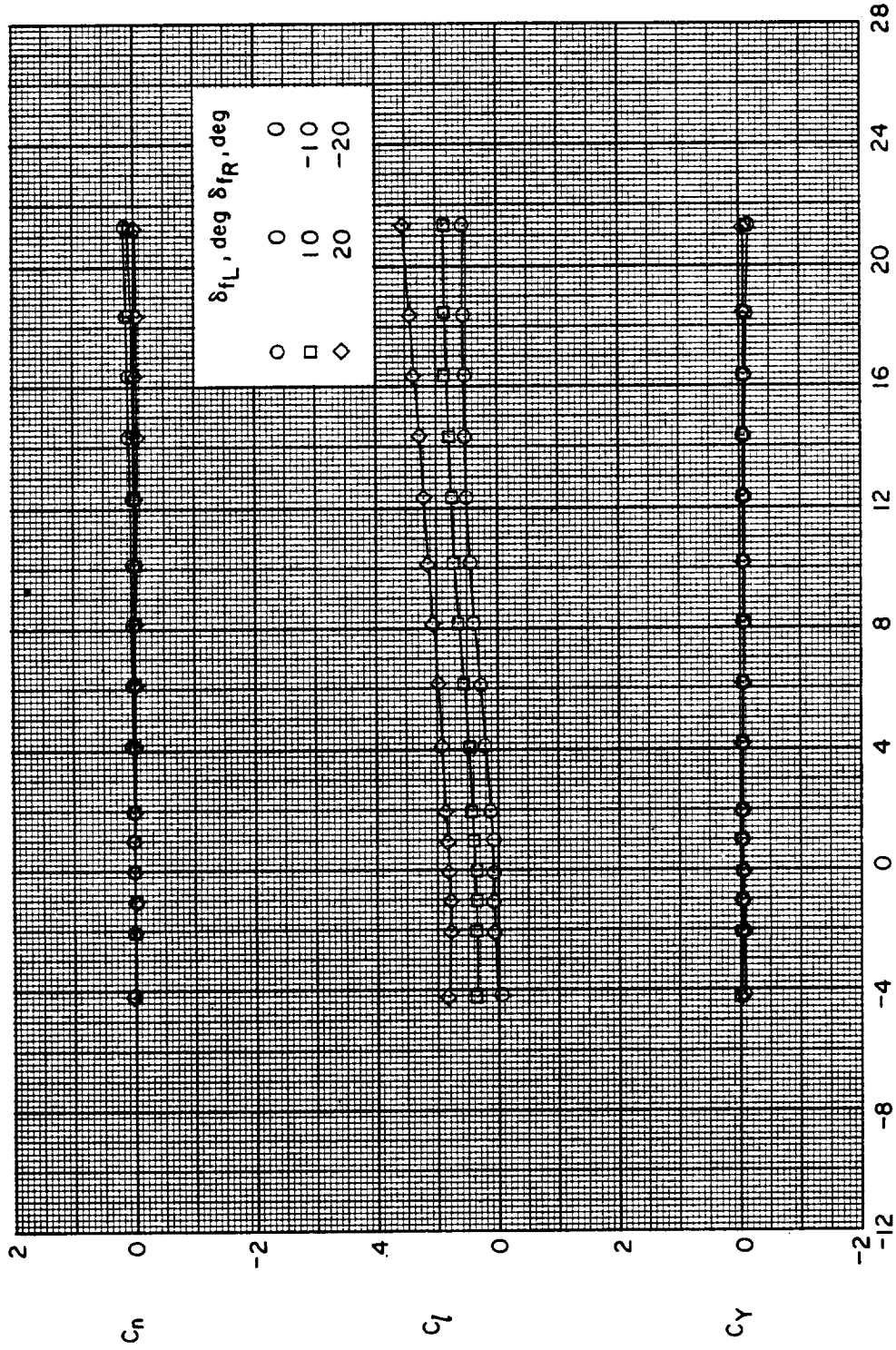

(d) M = 2.96.

Figure 10.- Continued.

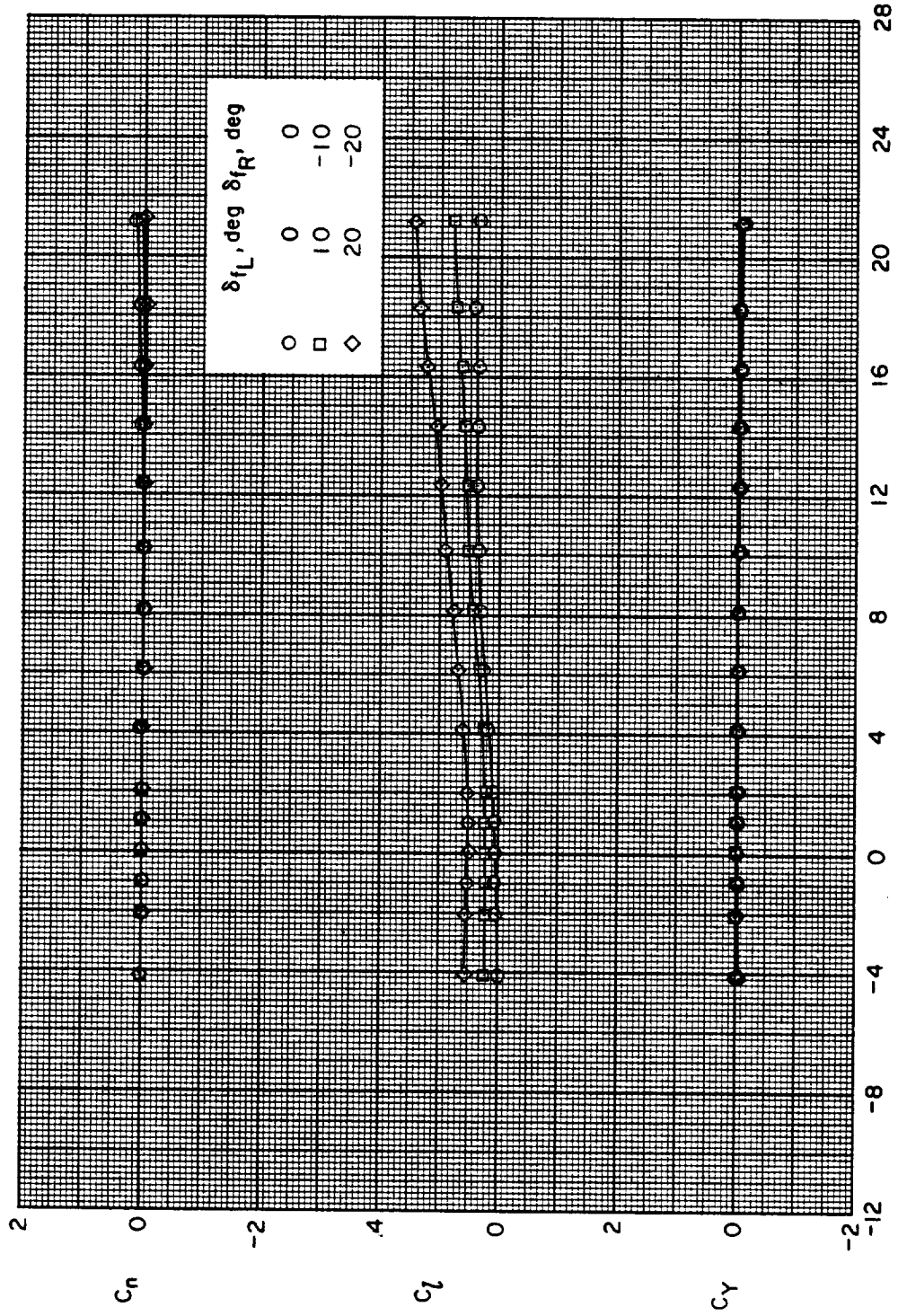

(e) M = 3.95.

Figure 10.- Continued.

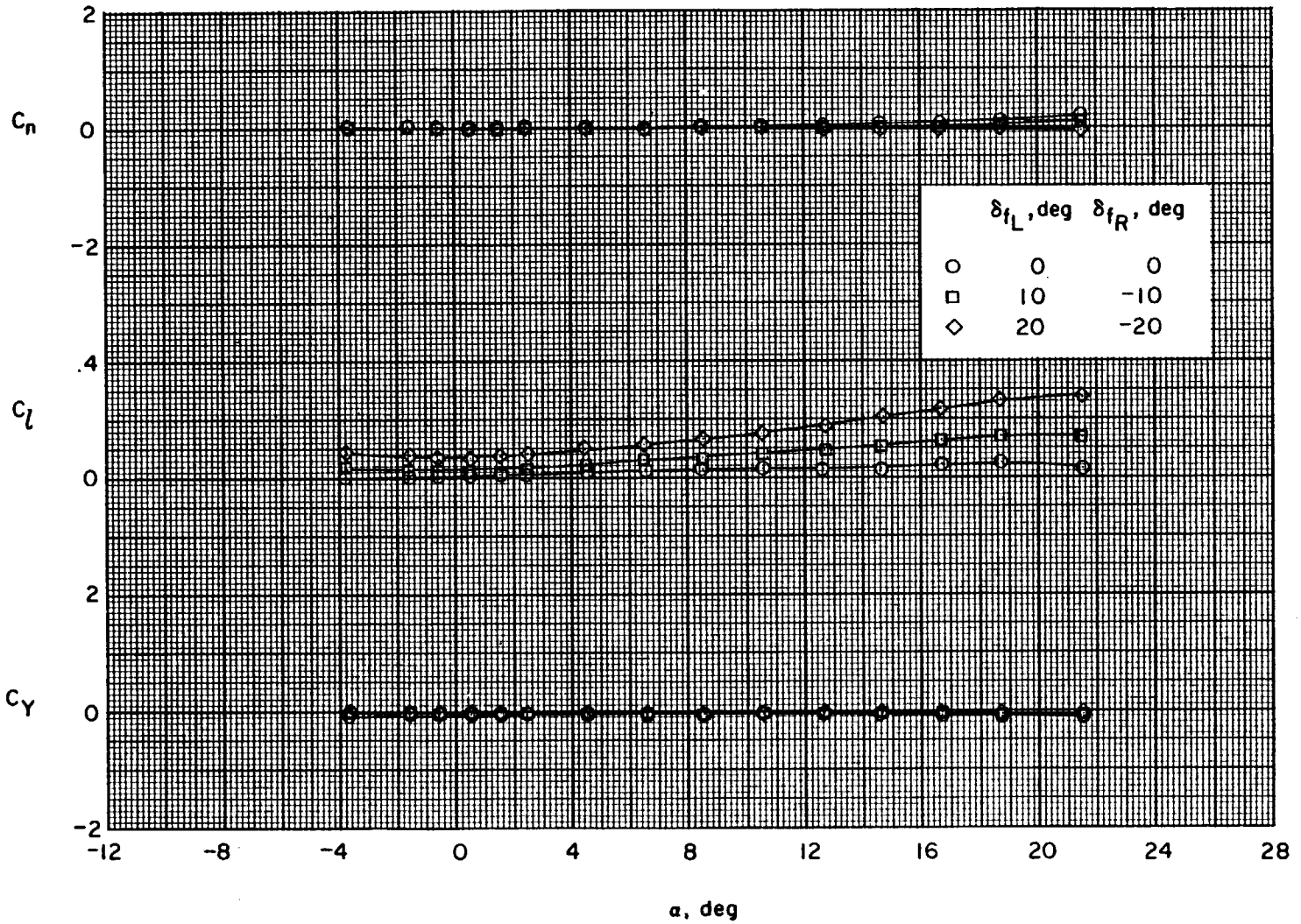

(f) M = 4.63.

Figure 10.- Concluded.

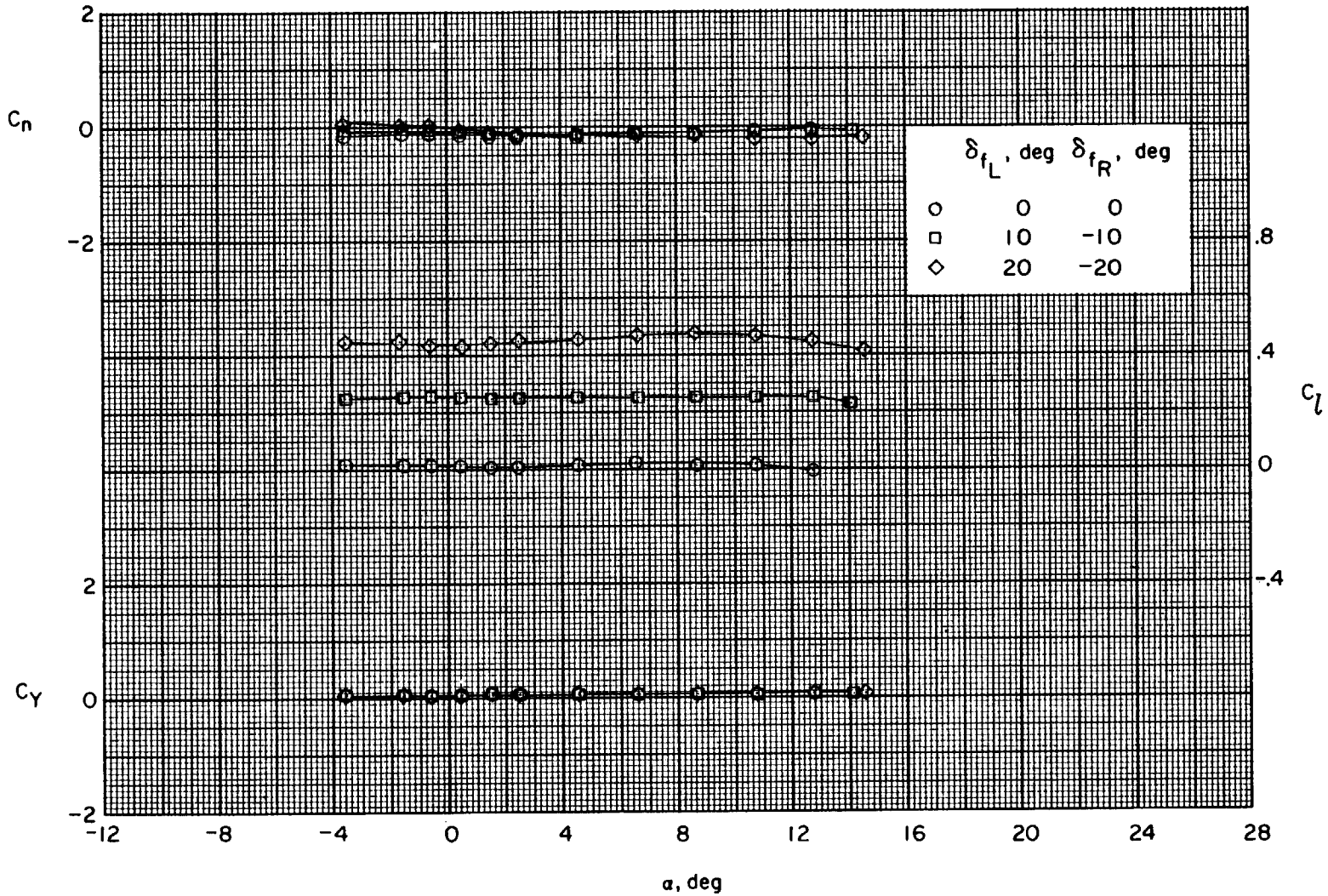

(a) M = 1.50.

Figure 11.- Effect of wing-flap deflection on the lateral control characteristics of configuration BWC with $\delta_{c_h} = 20^0$. $\delta_{c_v} = 0^0$.

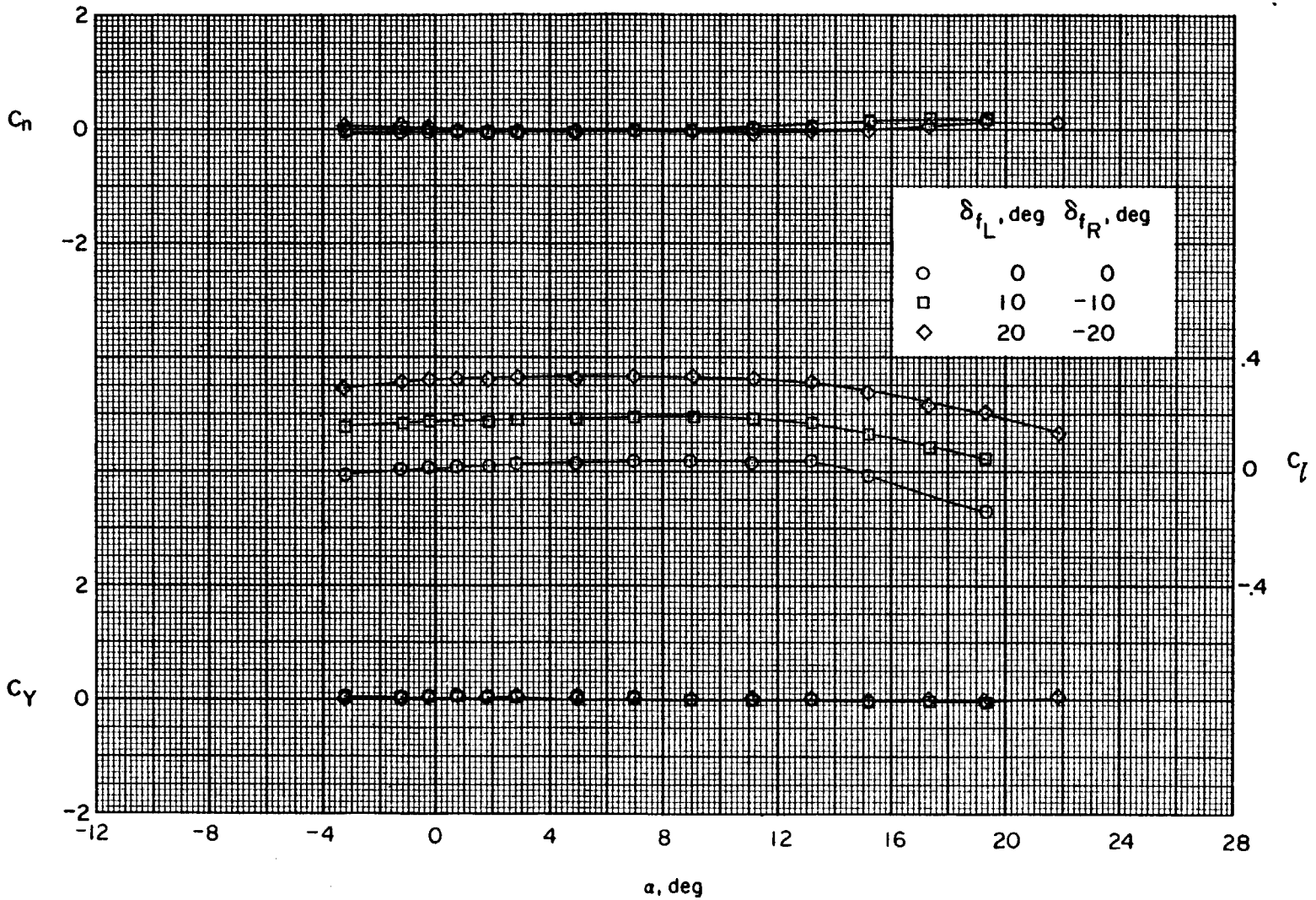

(b) M = 1.90.

Figure 11.- Continued.

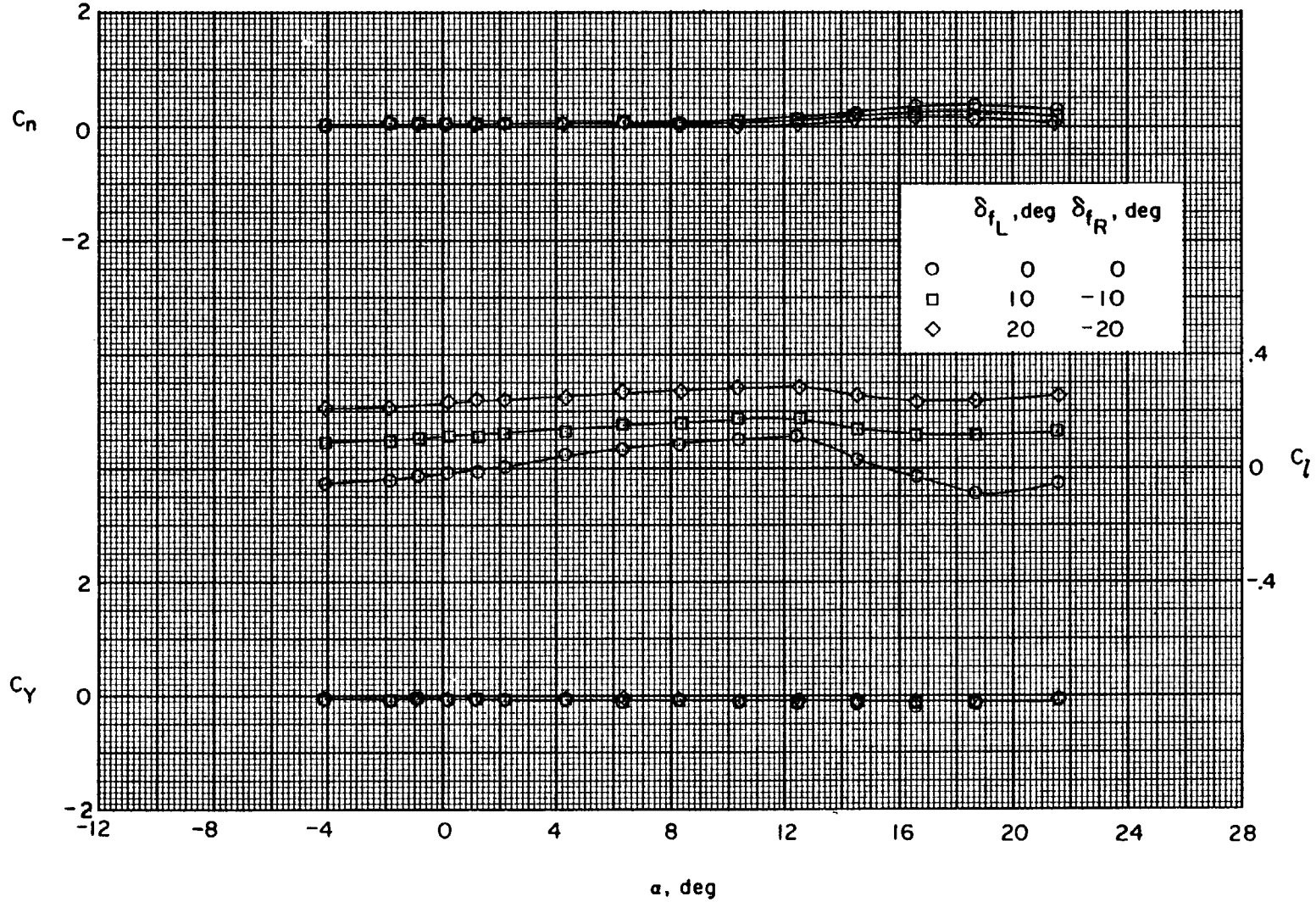

(c) M = 2.30.

Figure 11.- Continued.

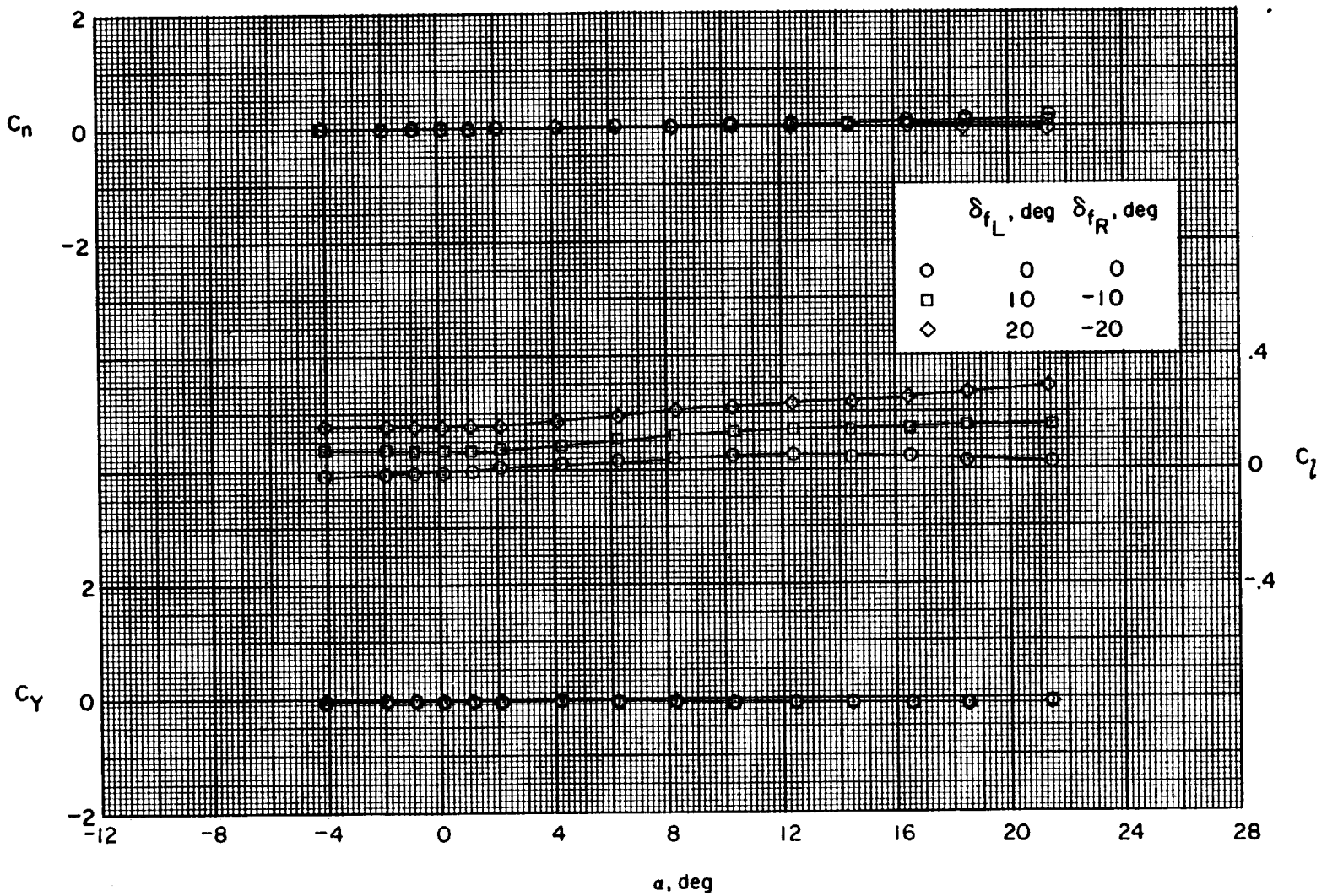

(d) M = 2.96.

Figure 11.- Continued.

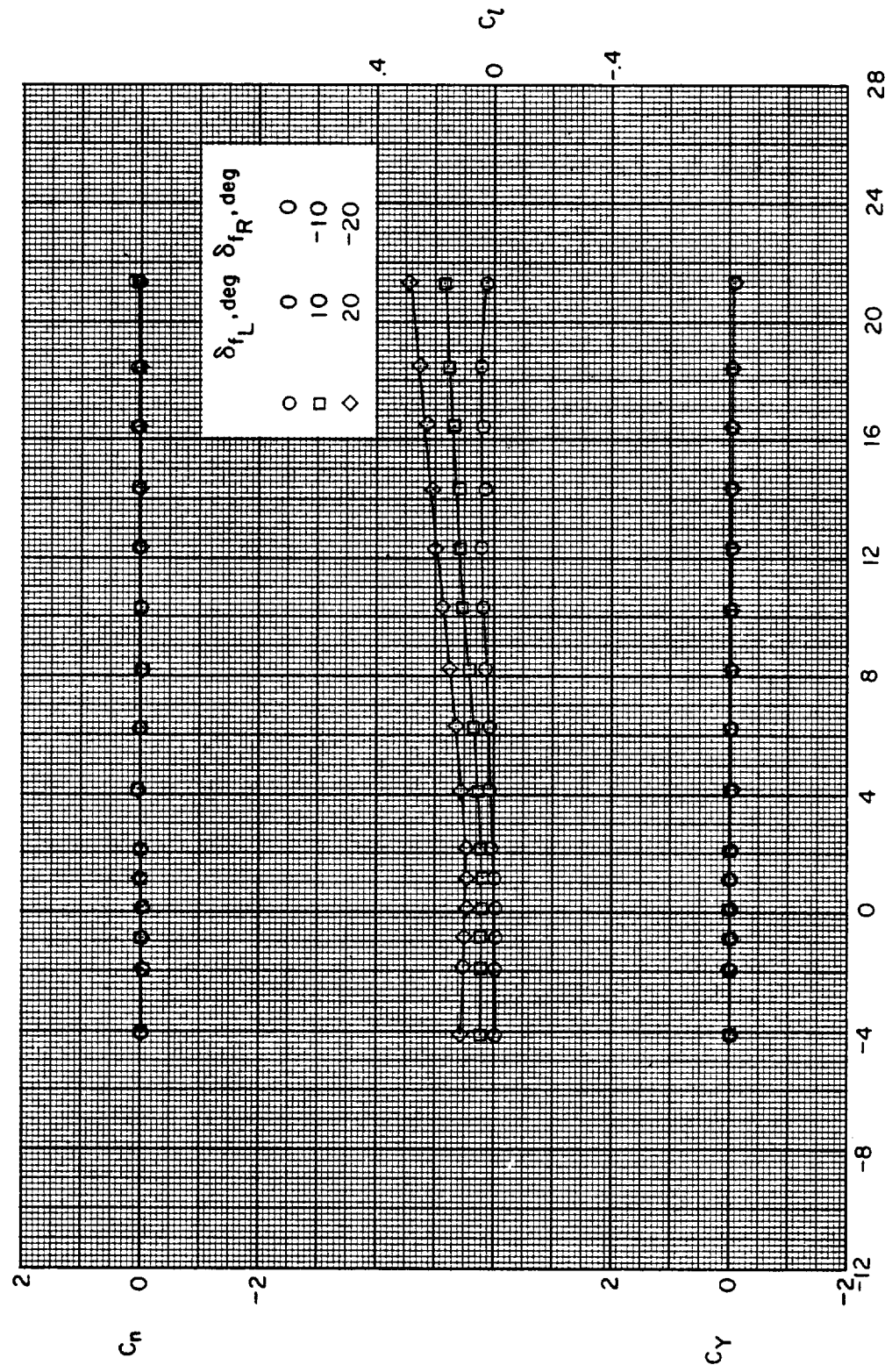

(e) M = 3.95.

Figure 11.- Continued.

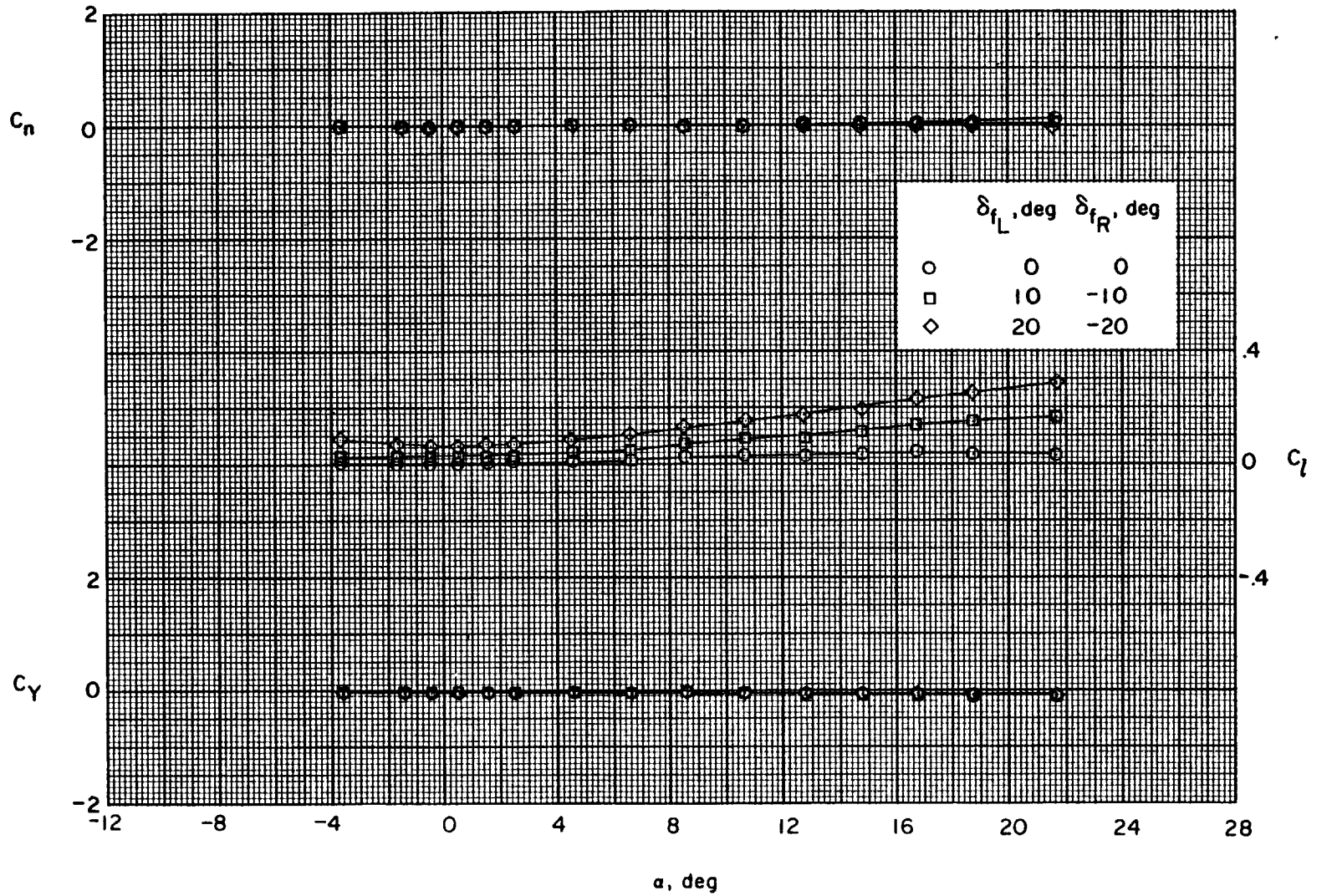

(f) M = 4.63.

Figure 11.- Concluded.

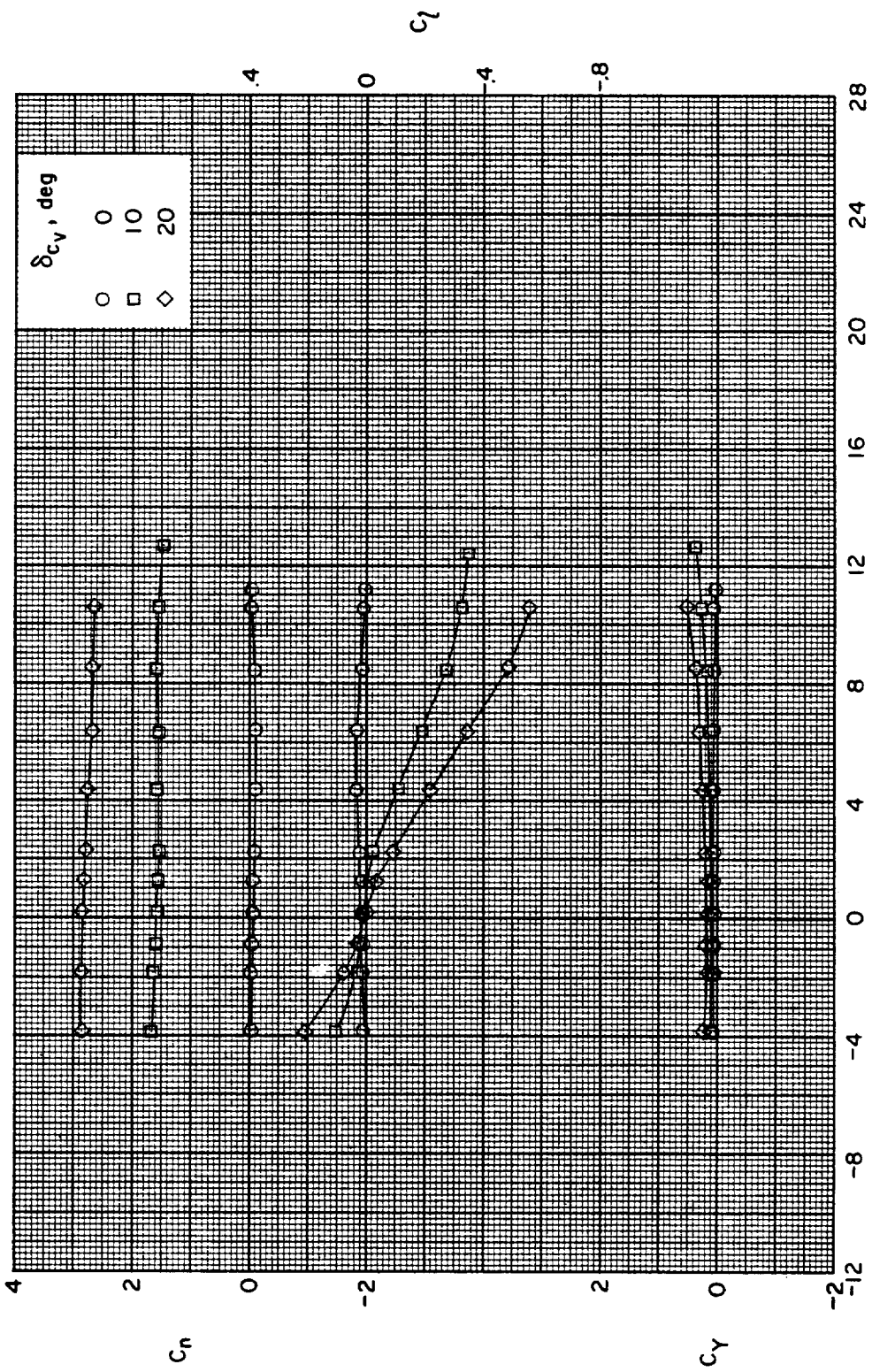

(a) M = 1.50.

Figure 12.- Effect of vertical-canard deflection on the lateral control characteristics of configuration BWC. $\delta_f = 0°$; $\delta_{c_h} = 0°$.

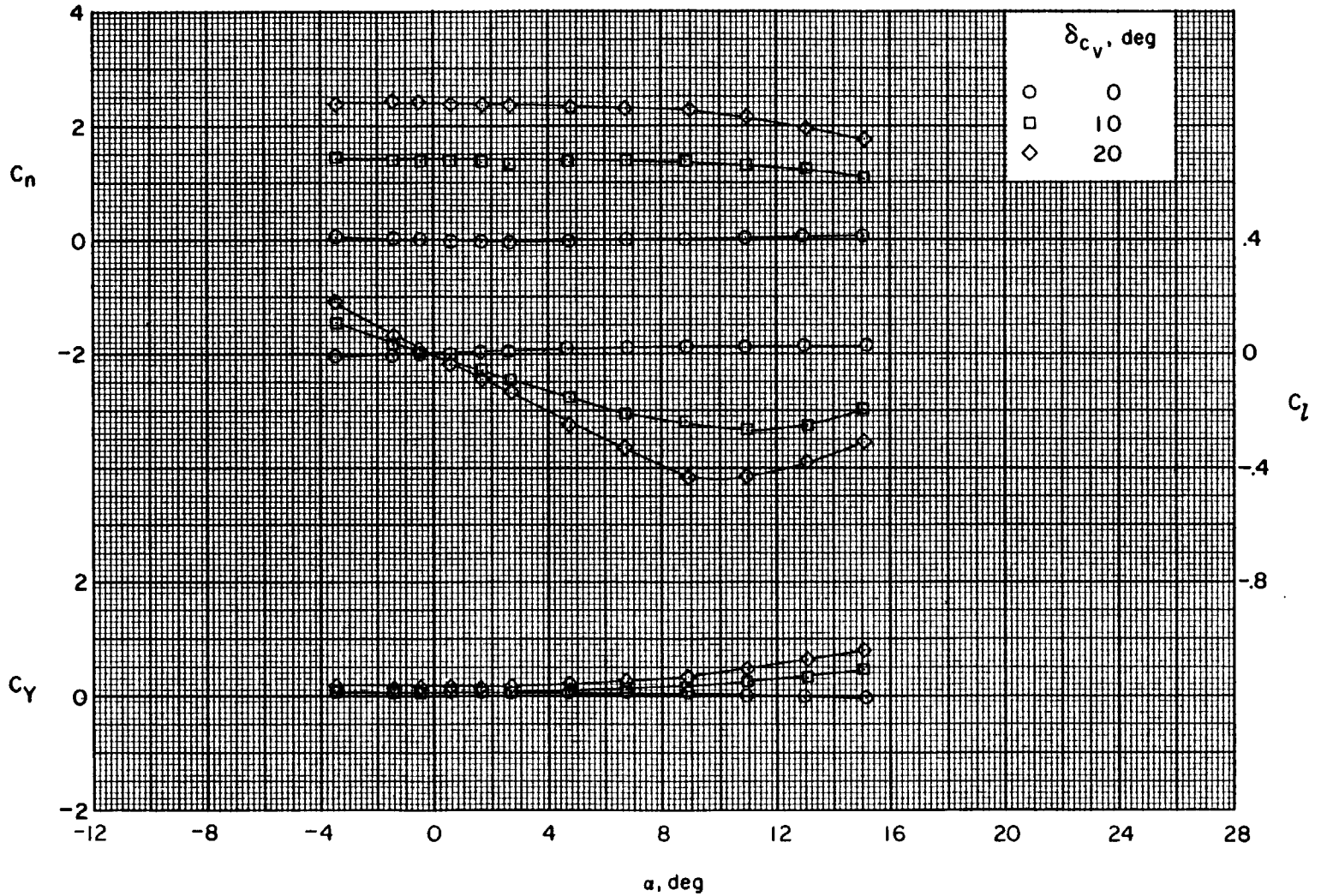

(b) M = 1.90.

Figure 12.- Continued.

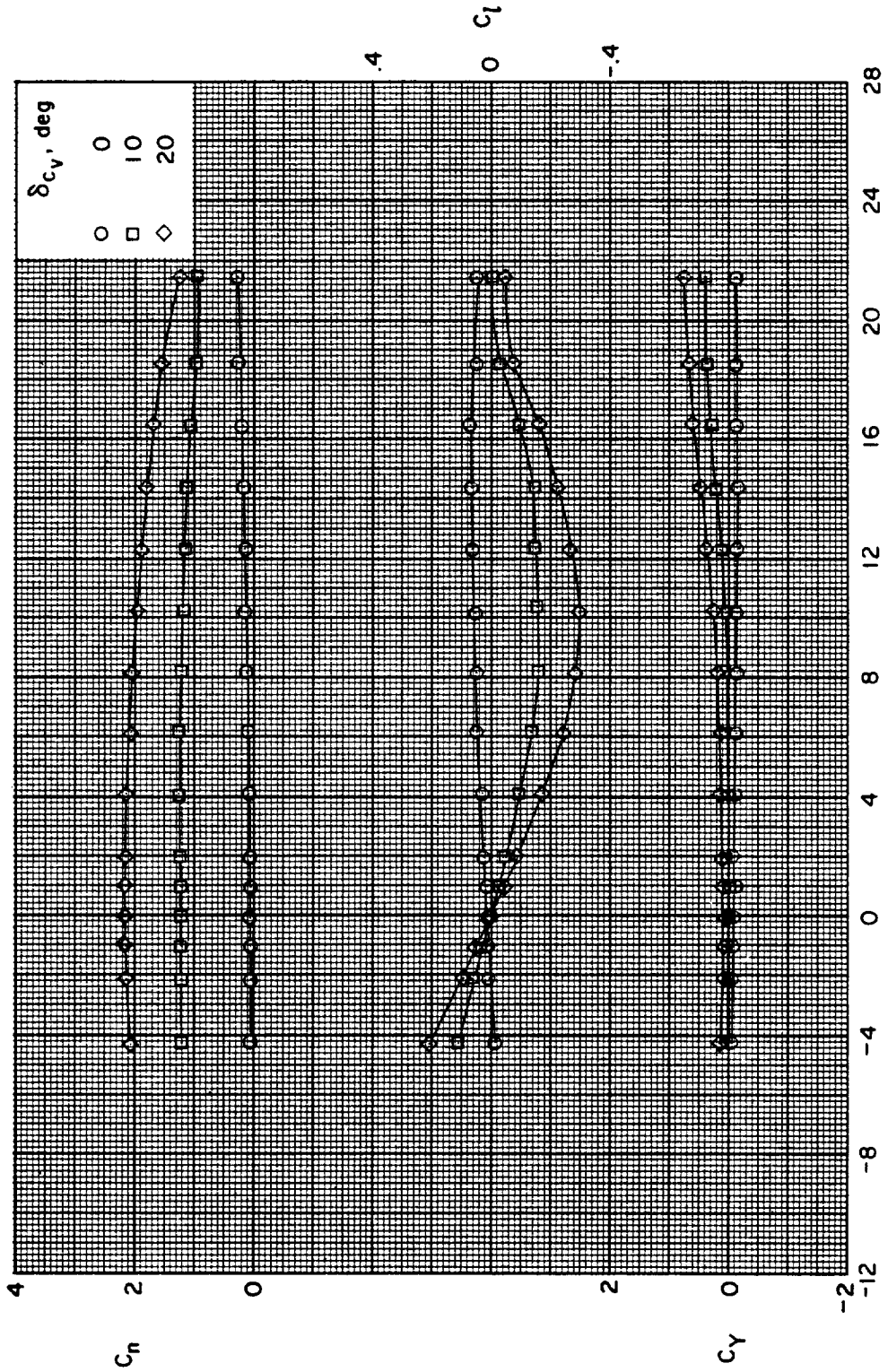

(c) M = 2.30.

Figure 12.- Continued.

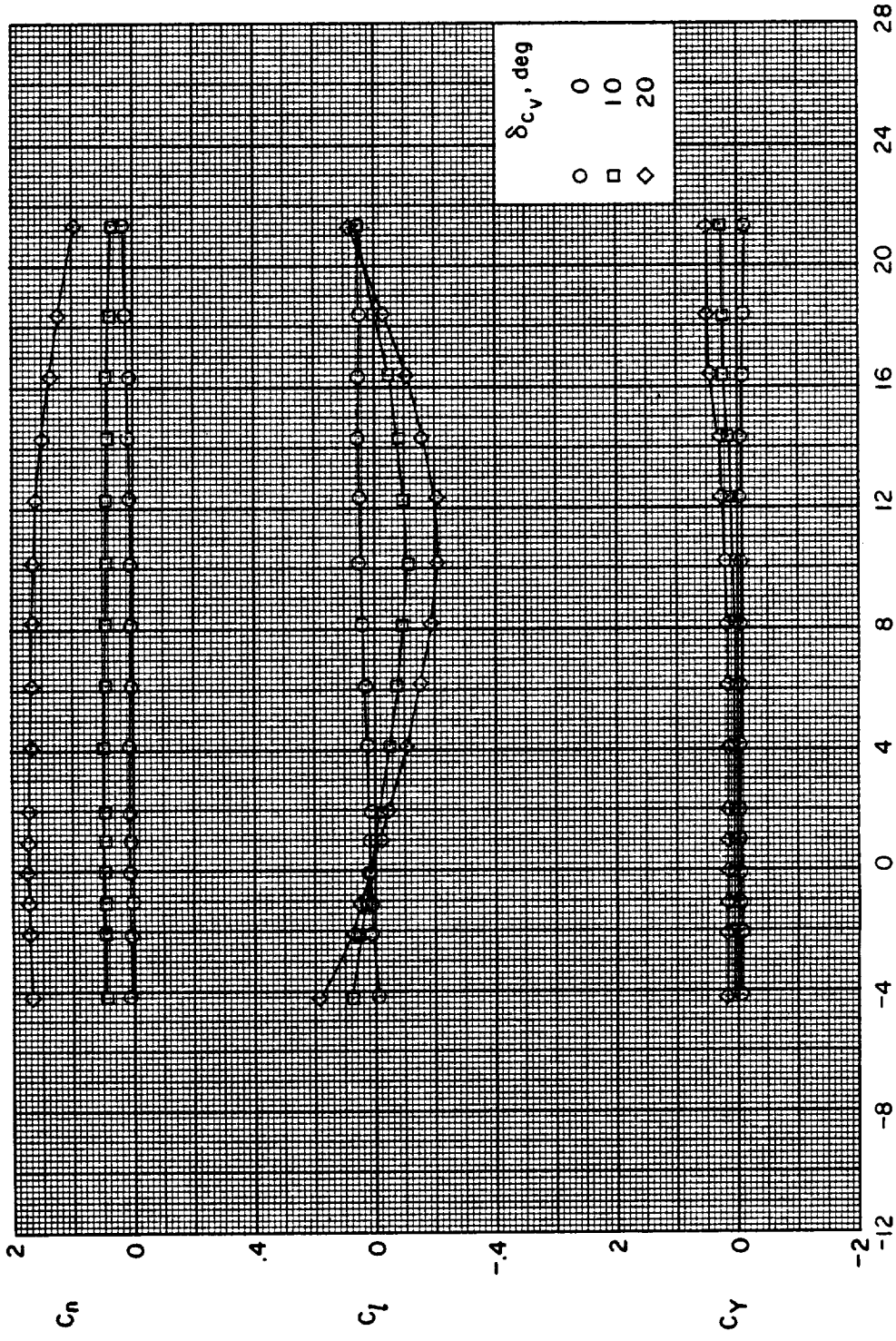

(d) M = 2.96.

Figure 12.- Continued.

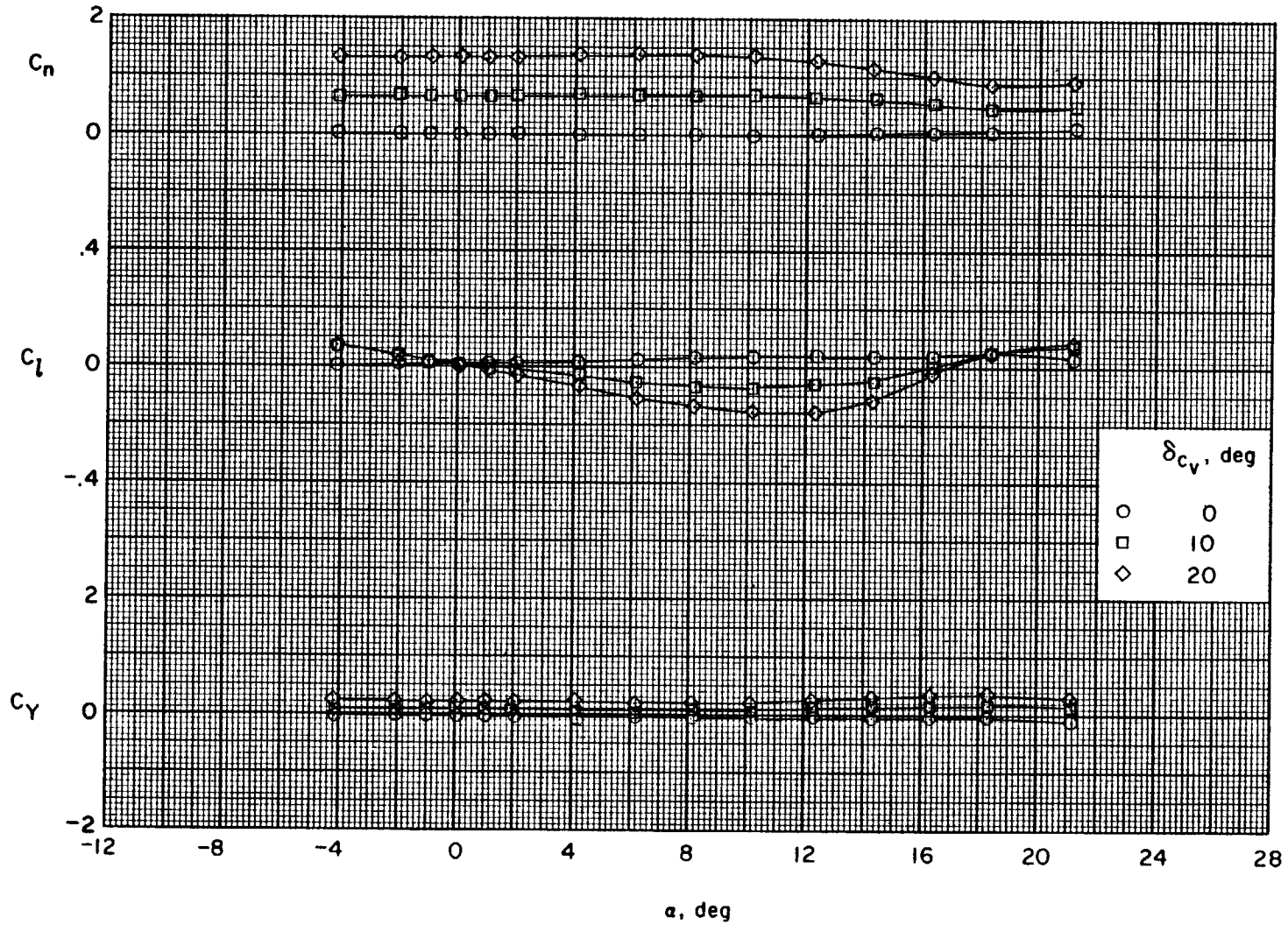

(e) M = 3.95.

Figure 12.- Continued.

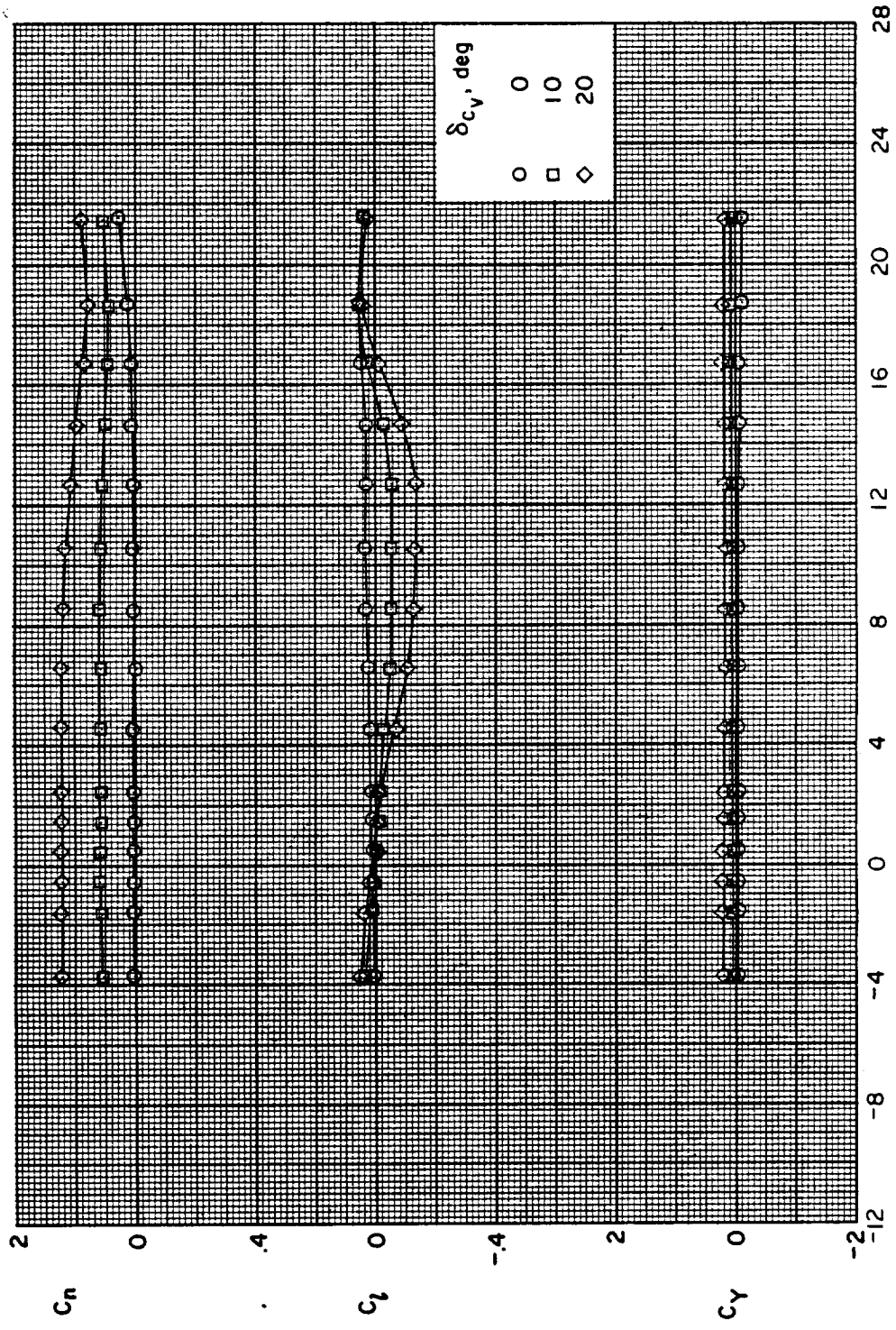

(f) M = 4.63.

Figure 12.- Concluded.